THE WORLD BANK
IBRD • IDA | WORLD BANK GROUP

ESMAP
Energy Sector Management Assistance Program

SOLAR RESOURCE AND PHOTOVOLTAIC POTENTIAL OF MYANMAR

May 2017

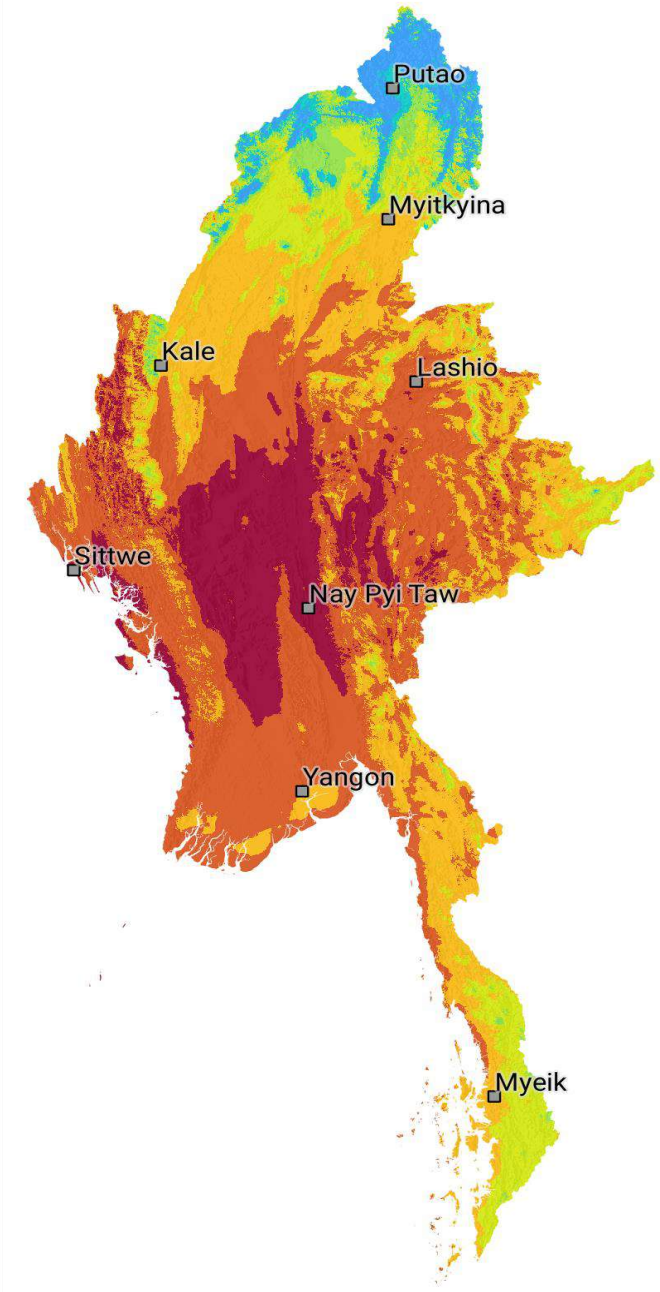

This report was prepared by Solargis, under contract to The World Bank.

It is one of several outputs from the global mapping activity "Global Solar Atlas" [Project ID: P161130]. This activity is funded and supported by the Energy Sector Management Assistance Program (ESMAP), a multi-donor trust fund administered by The World Bank, under a global initiative on Renewable Energy Resource Mapping. Further details on the initiative can be obtained from the ESMAP website.

This report is an interim output from the above-mentioned project. Users are strongly advised to exercise caution when utilizing the information and data contained, as this has not been subject to validation using ground measurement data or peer review.

To obtain additional maps and information on solar resources globally, please visit:

http://globalsolaratlas.info

World Bank Group, Global ESMAP Initiative

Renewable Energy Resource Mapping and Geospatial Planning – Myanmar

Project ID: P150328

Solar Resource and Photovoltaic Power Potential of Myanmar

May 2017

This report has been prepared by Marcel Suri, Tomas Cebecauer, Nada Suriova, Branislav Schnierer, Juraj Betak, Branislav Cief, Veronika Madlenakova, Artur Skoczek and Marek Caltik from Solargis

All maps in this report are prepared by Solargis

Solargis s.r.o., Pionierska 15, 831 02 Bratislava, Slovakia

Reference No. (Solargis): 170-02/2017

http://solargis.com

Solargis is ISO 9001:2008 certified company for quality management

Table of contents

Acronyms

AC	Alternating current
AERONET	The AERONET (AErosol RObotic NETwork) is a ground-based remote sensing network dedicated to measure atmospheric aerosol properties. It provides a longterm database of aerosol optical, microphysical and radiative parameters.
AOD	Aerosol Optical Depth at 670 nm. This is one of atmospheric parameters derived from MACC database and used in Solargis. It has important impact on accuracy of solar calculations in arid zones.
CFSR	Climate Forecast System Reanalysis. The meteorological model operated by the US service NOAA.
CFSv2	The Climate Forecast System Version 2. CFSv2 meteorological models operated by the US service NOAA (Operational extension of Climate Forecast System Reanalysis, CFSR).
CPV	Concentrated Photovoltaic systems, which uses optics such as lenses or curved mirrors to concentrate a large amount of sunlight onto a small area of photovoltaic cells to generate electricity.
CSP	Concentrated solar power systems, which use mirrors or lenses to concentrate a large amount of sunlight onto a small area, where it is converted to heat for heat engine connected to an electrical power generator.
DC	Direct current
DIF	Diffuse Horizontal Irradiation, if integrated solar energy is assumed. Diffuse Horizontal Irradiance, if solar power values are discussed.
DNI	Direct Normal Irradiation, if integrated solar energy is assumed. Direct Normal Irradiance, if solar power values are discussed.
ECMWF	European Centre for Medium-Range Weather Forecasts is independent intergovernmental organisation supported by 34 states, which provide operational medium- and extended-range forecasts and a computing facility for scientific research.
ESMAP	Energy Sector Management Assistance Program, a multi-donor trust fund administered by the World Bank
EUMETSAT	European Organisation for the Exploitation of Meteorological Satellites, intergovernmental organisation for establishing, maintaining and exploit European systems of operational meteorological satellites
GFS	Global Forecast System. The meteorological model operated by the US service NOAA.
GHI	Global Horizontal Irradiation, if integrated solar energy is assumed. Global Horizontal Irradiance, if solar power values are discussed.
GIS	Geographical Information System
GTI	Global Tilted (in-plane) Irradiation, if integrated solar energy is assumed. Global Tilted Irradiance, if solar power values are discussed.

KSI	Kolmogorov–Smirnov Index, a statistical index for comparing of functions or samples
MACC	Monitoring Atmospheric Composition and Climate – meteorological model operated by the European service ECMWF (European Centre for Medium-Range Weather Forecasts)
Meteosat IODC	Meteosat satellite operated by EUMETSAT organization. IODC: Indian Ocean Data Coverage
MERRA	Modern-Era Retrospective Analysis for Research and Applications, a NASA reanalysis for the satellite era using an Earth observing systems
MTSAT 2	Multifunctional Transport Satellite operated by Japan Meteorological Agency (JMA), also known as Himawari 7, positioned at Pacific position, longitude 145° East
Himawari 8	Geostationary weather satellite operated by the Japan Meteorological Agency (JMA), positioned at Pacific position
NASA	National Aeronautics and Space Administration organization
NOAA NCEP	National Oceanic and Atmospheric Administration, National Centre for Environmental Prediction
NOAA ISD	NOAA Integrated Surface Database with meteorological data measured by ground-based measurement stations
NOCT	The Nominal Operating Cell Temperature, is defined as the temperature reached by open circuited cells in a module under the defined conditions: Irradiance on cell surface = 800 W/m^2, Air Temperature = 20°C, Wind Velocity = 1 m/s and mounted with open back side.
PV	Photovoltaic
PVOUT	Photovoltaic electricity output calculated from solar resource and air temperature time series.
RSR	Rotating Shadowband Radiometer
SOLIS	Solar Irradiance Scheme, Solar clear-sky model for convert meteorological satellite images into radiation data
SRTM	Shuttle Radar Topography Mission, a service collecting topographic data of Earth's land surfaces
STC	Standard Test Conditions, used for module performance rating to ensure the same measurement conditions: irradiance of 1000 W/m^2, solar spectrum of AM 1.5 and module temperature at 25°C.
TEMP	Air Temperature at 2 metres
UV	Ultraviolet radiation

Glossary

AC power output of a PV power plant	Power output measured at the distribution grid at a connection point.
Aerosols	Small solid or liquid particles suspended in air, for example desert sand or soil particles, sea salts, burning biomass, pollen, industrial and traffic pollution.
All-sky irradiance	The amount of solar radiation reaching the Earth's surface is mainly determined by Earth-Sun geometry (the position of a point on the Earth's surface relative to the Sun which is determined by latitude, the time of year and the time of day) and the atmospheric conditions (the level of cloud cover and the optical transparency of atmosphere). All-sky irradiance is computed with all factors considered
Bias	Represents systematic deviation (over- or underestimation) and it is determined by systematic or seasonal issues in cloud identification algorithms, coarse resolution and regional imperfections of atmospheric data (aerosols, water vapour), terrain, sun position, satellite viewing angle, microclimate effects, high mountains, etc.
Clear-sky irradiance	The clear sky irradiance is calculated similarly to all-sky irradiance but without considering the impact of cloud cover.
Fixed-mounted modules	Photovoltaic modules assembled on fixed bearing structure in a defined tilt to the horizontal plane and oriented in fixed azimuth.
Frequency of data (30-minute, hourly, daily, monthly, yearly)	Period of aggregation of solar data that can be obtained from the Solargis database.
Installed DC capacity	Total sum of nominal power (label values) of all modules installed on photovoltaic power plant.
Longterm average	Average value of selected parameter (GHI, DNI, etc.) based on multiyear historical time series. Longterm averages provide a basic overview of solar resource availability and its seasonal variability.
P50 value	Best estimate or median value represents 50% probability of exceedance. For annual and monthly solar irradiation summaries, it is close to average, since multiyear distribution of solar radiation resembles normal distribution.
P90 value	Conservative estimate, assuming 90% probability of exceedance (with the 90% probability the value should be exceeded). When assuming normal distribution, the P90 value is also a lower boundary of the 80% probability of occurrence. P90 value can be calculated by subtracting uncertainty from the P50 value. In this report, we apply a simplified assumption of normal distribution of yearly values.
PV electricity production	AC power output of a PV power plant expressed as percentage of installed DC capacity.
Root Mean Square Deviation (RMSD)	Represents spread of deviations given by random discrepancies between measured and modelled data and is calculated according to this formula: $$RMSD = \sqrt{\frac{\sum_{k=1}^{n}\left(X^{k}{}_{measured} - X^{k}_{modeled}\right)^{2}}{n}}$$ On the modelling side, this could be low accuracy of cloud estimate (e.g. intermediate clouds), under/over estimation of atmospheric input data, terrain,

	microclimate and other effects, which are not captured by the model. Part of this discrepancy is natural - as satellite monitors large area, while sensor sees only micro area of approx. 1 sq. centimetre. On the measurement side, the discrepancy may be determined by accuracy/quality and errors of the instrument, pollution of the detector, misalignment, data loggers, insufficient quality control, etc.
Solar irradiance	Solar power (instantaneous energy) falling on a unit area per unit time [W/m^2]. Solar resource or solar radiation is used when considering both irradiance and irradiation.
Solar irradiation	Amount of solar energy falling on a unit area over a stated time interval [Wh/m^2 or kWh/m^2].
Spatial grid resolution	In digital cartography, the term applies to the minimum size of the grid cell or in the other words minimal size of the pixels in the digital map

Executive summary

This report presents results of the solar resource mapping and photovoltaic power potential evaluation, as a part of a technical assistance for the renewable energy development in Myanmar, implemented by the World Bank.

The study has two objectives:

- Improve the awareness and knowledge of resources for solar energy technologies by producing a comprehensive countrywide data set and maps based on satellite and meteorological modelling. This report evaluates key solar climate features, and geographic and time variability of solar power potential in the country. The outcomes are supported by explanation of the methodology and evaluation of the data uncertainty.
- Provide support information for installation of meteorological stations in Myanmar by identifying and evaluating the most feasible areas. The data used in this report are based on the satellite and meteorological models. Due to lack of accurate solar measurements, the data and the outcomes published in this study have higher uncertainty, compared to other regions. The regional uncertainty of models can be reduced in future by acquiring high quality measurements at several meteorological stations with specialised solar-measuring equipment.

Satellite-based and meteorological models are applied for computing solar resource and meteorological data that are used for production of high-resolution maps and for preparing aggregated data layers for Geographical Information Systems (GIS). A set of primary data parameters is discussed in the study. They are relevant for evaluation of energy yield and performance of the solar power plants, especially based on the use of photovoltaic technology:

- Global Horizontal Irradiation (GHI), Diffuse horizontal Irradiation (DIF), Global Tilted Irradiation (GTI) and Direct Normal Irradiation (DNI);
- Air temperature at 2 metres above ground;
- Photovoltaic power potential (PVOUT).

The deliverables are designed to support country-wide solar energy strategy, and for selection of sites, where solar power plants could be developed. This phase delivers data computed by Solargis model without any support from the local measurements.

The model outcomes are delivered in two data formats:

- Raster GIS data for the whole territory of the Republic of the Union of Myanmar, representing longterm monthly and yearly average values. This data layers are accompanied by geographical data layers in raster and vector format.
- Digital maps for high resolution poster printing and in medium resolution format

The report also provides an indicative analysis of regions and areas where deployment of solar measuring stations could take place. These stations would contribute to the validation of the models and reducing the data uncertainty. Once at least one year of measurements is available the data can be used for adaptation of solar and meteorological models and for detailed analysis of solar climate at representative sites.

This report addresses the following topics:

Chapter 1 provides inventory of existing studies related to solar energy and solar data in the country. Solar radiation basics and principles of photovoltaic power potential calculation are described in Chapter 2. Chapters 2.1 and 2.2 describe measuring and modelling approaches for developing reliable solar and meteorological data including information about the solar and meteorological data uncertainty. Chapter 2.3 explains the relevance of solar resource and meteorological information for deployment of solar power technologies. An emphasis is given to photovoltaic (PV) technology, which has high potential for developing utility-scale projects close to larger load centres. We consider also deployment of rooftop PV systems, off-grid, hybrid systems and mini-grids for electrification of small communities.

Chapter 3 analyses and evaluates the geographical, meteorological and resource potential of Myanmar for solar energy. Eight representative sites are selected to show regional differences in the country through tables and graphs. Chapter 3.1 introduces support geographical data that influence deployment strategies and performance of solar power plants. Chapters 3.2 to 3.5 summarize geographical differences and seasonal variability of solar resource in Myanmar. Chapter 3.6 presents PV power generation potential of the country. The theoretical specific PV electricity output is calculated from the most commonly used PV technology: fixed system with crystalline-silicon (c-Si) PV modules optimally tilted and oriented towards South. Chapter 3.7 delineates solar climate zones and characterizes them from the viewpoint of deployment of solar monitoring stations as well as PV power plants. Chapter 3.8 summarizes analytical information and brings conclusions.

In Chapter 4 the solar resource and meteorological conditions are evaluated in the context of deployment of solar meteorological stations, excluding areas that are not suitable for solar meteorological stations in Myanmar.

Chapter 5 summarizes the technical features of the delivered data products.

This report, supported by the GIS data and maps, serves as an input for knowledge-based decisions targeting development of solar power in Myanmar. The outcomes show very good potential for exploitation of solar resources in Myanmar, indicating good opportunities for deployment of all type of photovoltaic applications.

1 Introduction

This report is a result of the activity funded and supported by the Energy Sector Management Assistance Program (ESMAP), a multi-donor trust fund administered by The World Bank, under a global initiative on Renewable Energy Resource Mapping. The ESMAP initiative helps developing basic solar and meteorological data infrastructure, and knowledge, based on the best-available meteorological models and measurement practices. Indirect benefit is better understanding of geographical and temporal variability of solar resource and meteorological parameters relevant for solar power industry, in other words better understanding of the weather impact on the PV power generation and performance of PV power systems.

The outcomes of this activity are publicly available GIS data sources, maps, and interactive applications; all available at http://globalsolaratlas.info/.

1.1 Background

Solar electricity offers a unique opportunity to achieve long-term sustainability goals, such as development of modern economy, healthy and educated society, clean environment, and improvement of geopolitical stability. Solar power plants exploit local solar energy resources; they do not require heavy support infrastructure, they are scalable, and supply or improve electricity services. Important feature of solar electricity is that it is accessible also in remote locations, without access to electricity, thus providing development opportunities anywhere.

While solar resources are fuel to solar power plants, the local geographical and climate conditions determine the efficiency of their operation. Free fuel makes solar technology attractive; however effective investment and technical decisions require **detailed, accurate and validated solar and meteorological data**. Accurate data are also needed for the cost-effective operation of solar power plant. High quality solar resource and meteorological data can be obtained by satellite-based meteorological models and by instruments installed at the meteorological stations.

1.2 Inventory of previous solar resource projects

Several solar resource assessment initiatives are documented below, available as publications or online data resources. The works show growing interest in solar resource assessment and energy modelling in the region.

Solar energy potential and applications in Myanmar, Mandalay Technological University, Myanmar 2008

The publication by Thet Thet Han Yee and the team from the Mandalay Technological University presents monthly averaged measurements of GHI solar radiation for 11 stations in Myanmar [1]. The data is sourced by MEPE (Myanmar Electric Power Enterprise), further details of these measurements are not provided. It is underlined in the study that accurate data is important for design of solar power system. The publication also describes case studies in different of solar energy applications in Myanmar.

Energy utilization and the status of sustainable energy in the Union of Myanmar, Naresuan University, Thailand, 2011

The publication by Wint Wint Kyaw et al. from the Naresuan University, Thailand presents potential for renewable energy resources and power applications. Monthly averaged sunshine hours and GHI data for 5 stations in

Myanmar is developed [2]. Source and further details are not available. The publication also describes different PV installation in Myanmar known to that times (approx. 2011).

Satellite-derived solar resource maps for Myanmar, Silpakorn University, Thailand, 2012

This project was carried out under the collaboration on renewable energy and energy conservation between Department of Alternative Energy Development and Efficiency (DEDE), Thailand and Department of Meteorology and Hydrology together with Department of Energy Planning of Myanmar. Solar Energy Research Laboratory of Silpakorn University, Thailand, carried out mapping of the solar potential using a satellite-based solar radiation model. The model was developed by prof. Serm Janjai and the team at the Silpakorn University [3]. It processed data representing a period from 1998 to 2010. The outputs were validated at five solar monitoring stations in Myanmar, established for two years for the model validation. The outcome of the project, delivered in 2012, was monthly and yearly GHI solar radiation data layers calculated from the model for the entire country. The claimed mean bias for GHI was 3.8% and RMSD (Root Mean Square Deviation) of the monthly values was 9.6%.

SWERA GIS data and maps

Monthly average values of GHI and DNI solar parameters are available at SWERA web site, two sources are available, developed by separate projects:

- Data developed by NREL using their Climatological Solar Radiation (CSR) model. This model uses aggregated data on cloud cover, atmospheric water vapor and trace gases, and the volume of aerosols in the atmosphere to calculate the monthly average daily total insolation (sun and sky) falling on a horizontal surface (spatial resolution of grid data is approx. 40 km).

  http://en.openei.org/datasets/dataset/solar-monthly-and-annual-average-direct-normal-dni-global-horizontal-ghi-latitude-tilt-and-4

- Data provided by NASA Surface meteorology and Solar Energy (Release 6.0, Jan 2008). Available as monthly and annual averages representing a period from July 1983 to June 2005. Spatial resolution of the grid data layers is approx. 110 km.

  http://en.openei.org/datasets/dataset/solar-monthly-and-annual-average-global-horizontal-irradiance-gis-data-at-one-degree-resolution-of

Renewable energy developments and potential in the Greater Mekong Subregion, Asian Development Bank, 2015

In 2010, the Asian Development Bank (ADB) initiated the regional technical assistance project Promoting Renewable Energy, Clean Fuels, and Energy Efficiency in the Greater Mekong Subregion (GMS), to assist the five countries—Cambodia, the Lao People's Democratic Republic, Myanmar, Thailand, and Viet Nam—in improving their energy supply and security in an environmentally friendly and collaborative manner. Three reports, related to the Greater Mekong Subregion, were prepared: (i) Renewable Energy Developments and Potential, (ii) Energy Efficiency Developments and Potential Energy Savings, and (iii) Business Models to Realize the Potential of Renewable Energy and Energy Efficiency.

The first report provides estimates of the theoretical and technical potential of selected renewable energy sources (solar, wind, bioenergy) in each of the countries and together, with an outline of the policy and regulatory measures that have been introduced by the respective governments to develop this potential [4]. The technical potential of solar energy is analyzed, based on Solargis data, focusing on the estimated land area suitable for photovoltaic (PV) installations and the efficiency of the solar systems.

1.3 Evaluation of the existing data and studies and best practices

It has been communicated by all reviewed publications that though Myanmar has considerable potential in solar energy, it has not been tapped to a satisfactory matter. The limited technical and financial resources of the public and private sectors are major impediments to the development and use of renewable energies. While some projects were focusing on offgrid PV, and home- and community-based solar systems, large-scale solar PV development has not started.

The previously developed solar and meteorological data sets (See Chapter 1.2) do not fulfil the requirements for accuracy and reliability needed for large-scale commercial development. The main features that differentiate Solargis database from the above-mentioned data sets (NASA, SWERA, etc.):

- The models are based on new and advanced algorithms, validated at different climate zones
- Use of modern and systematically updated input data for the models: satellite, atmospheric and meteorological
- Database has global coverage at very high resolution
- Historical subhourly time series data is updated in real time
- Data can be used for project development but also for monitoring and forecasting

- Data is systematically validated and quality controlled
- There is customer support and supporting consultancy services

The new data set from Solargis focuses on a supply of data and services for development and financing of solar power plants, worldwide, and in Myanmar. The main objective is to systematically supply reliable, validated and high-resolution data to solar industry with low uncertainty and systematic quality control.

Production of accurate solar and meteorological data requires elaborated models, outputs of which cover extensive territories at high level of detail. The long record of historical data should be produced by such models for representative characterization of the solar climate that is critical in the phase of project development and energy yield assessment. The solar and meteorological models should also be able to update the data in real time to support monitoring and forecasting of solar power plants.

At the country level, modern solar measuring stations are used for accuracy enhancement of such models. They are also needed for developing understanding of the regional and local patterns of weather. This knowledge helps to reduce risks and to improve performance of solar systems. A combination of the model data with modern solar and meteorological measurements is used to support solar energy development in all stages of its lifecycle.

Solar meteorological stations are typically installed at the sites where large solar power plants are developed. Such stations stay on the site, over the project lifetime, and provide data for monitoring, performance evaluation and forecasting of solar power. For improved accuracy and reliability of the measurements, it is a good practice to combine local measurements with solar and meteorological models.

High accuracy solar resource and meteorological data are needed for development and operation of commercial solar power plants. Typically, detailed data, describing the local climate, is needed for a site of interest. Existing meteorological stations are geographically dispersed, and they typically do not operate high-accuracy solar sensors. In majority of cases, high accuracy solar measurements for a site of interest are not available. Therefore, a procedure how solar and meteorological data is used in a project development is following:

- In the first stage, for energy yield and performance assessment of the power plants, the data from solar and meteorological models are used. This data has higher uncertainty as it has not been validated by local measurements.
- When the site is secured and the project development starts, a solar meteorological station is installed. The high accuracy meteorological equipment is used to collect local data for an initial period of at least one year. Such measurements are than used for site adaptation of solar models, and for delivering higher accuracy data that is used for energy yield assessment, financial calculations and for optimising the technical design.
- After solar power plant starts the operation, the solar and meteorological measurements are used in combination with models for monitoring, performance evaluation and forecasting of solar power.

At large power plants, solar measurements are collected over their all lifetime. To summarize, the solar and meteorological data is used for the following tasks related to solar power generation:

1. Country-level evaluation and strategical assessment
2. Prospection, selection of candidate sites for future power plants, and prefeasibility analysis
3. Project evaluation, solar and energy yield assessment, technical design and financing
4. Monitoring and performance assessment of solar power plants and forecasting of solar power
5. Quality control of solar measurements.

This report addresses the first topic, from the list above.

1.4 Objectives

This report offers a country-level evaluation of geographical conditions, the solar resources, and photovoltaic power generation potential of Myanmar. The study also describes methods, and outcomes of solar resource mapping.

The analysis is based on the use of the Solargis model data. The solar model was only validated by measurements available in a wider region, with similar geographical conditions. Because of limited validation, one must expect higher uncertainty of the model outputs. To reduce this uncertainty, and to improve understanding of the solar climate at the regional and local scales, it is proposed to install several solar meteorological stations in the country, equipped by high accuracy instruments. This report evaluates suitable sites for deployment of this type of solar meteorological stations.

2 Solargis methods and data

2.1 Solar resource data

2.1.1 Introduction

Solar resource (physical term solar radiation) is fuel to solar energy systems. The solar radiation available for solar energy systems at the ground level depends on processes in the atmosphere. This leads to a high spatial and temporal variability of at the Earth's surface. The interactions of extra-terrestrial solar radiation with the Earth's atmosphere, surface and objects are divided into four groups:

1. Solar geometry, trajectory around the sun and Earth's rotation (declination, latitude, solar angle)
2. Atmospheric attenuation (scattering and absorption) by:
    2.1 Atmospheric gases (air molecules, ozone, NO_2, CO_2 and O_2)
    2.2 Solid and liquid particles (aerosols) and water vapour
    2.3 Clouds (condensed water or ice crystals)
3. Topography (elevation, surface inclination and orientation, horizon)
4. Shadows, reflections from surface or local obstacles (trees, buildings, etc.) and re-diffusion by atmosphere.

The atmosphere attenuates solar radiation selectively: some wavelengths are associated with high attenuation (e.g. UV) and others with a good transmission. Solar radiation called "short wavelength" (in practice, 300 to 4000 nm) is of main interest to solar power technology and is used as a reference. The component that is neither reflected nor scattered, and which directly reaches the surface, is called **direct radiation**; this is the component that produces shadows. Component scattered by the atmosphere, and which reaches the ground is called **diffuse radiation**. Small part of the radiation reflected by the surface and reaching an inclined plane is called the **reflected radiation**. These three components together create **global radiation**. A proportion of individual components at any time is given by Sun position and by the actual state of atmosphere – mainly occurrence of clouds, air pollution and humidity.

According to the generally adopted terminology, in solar radiation two terms are distinguished:

- **Solar irradiance** indicates power (instant energy) per second incident on a surface of 1 m^2 (unit: W/m^2).
- **Solar irradiation**, expressed in MJ/ m^2 or Wh/m^2 it indicates the amount of incident solar energy per unit area during a lapse of time (hour, day, month, etc.).

Often, the term *irradiance* is used by the authors of numerous publications in both cases, which can be sometimes confusing.

In **solar energy applications**, the following three solar resources are relevant:

- **Direct Normal** Irradiation/Irradiance (DNI): it is the direct solar radiation from the solar disk and the region closest to the sun (circumsolar disk of 5° centred on the sun). DNI is the component that is important to concentrating solar collectors used in Concentrating Solar Power (CSP) and high-performance cells in Concentrating Photovoltaic (CPV) technologies.
- **Global Horizontal** Irradiation/Irradiance (GHI): sum of direct and diffuse radiation received on a horizontal plane. GHI is a reference radiation for the comparison of climatic zones; it is also the essential parameter for calculation of radiation on a flat plate collector.
- **Global Tilted** Irradiation/Irradiance (GTI) or total radiation received on a surface with defined tilt and azimuth, fixed or sun-tracking. This is the sum of the scattered radiation, direct and reflected. A term

Plan of Array (POA) irradiation//irradiance is also used. In the case of photovoltaic (PV) applications, GTI can be occasionally affected by shading from surrounding terrain or objects, and GTI is then composed only from diffuse and reflected components. This happens usually for sun at low angles over the horizon.

Solar radiation data can be acquired by two complementary approaches:

1. **Ground-mounted sensors** are good in providing high frequency and accurate data (for well-maintained, high accuracy measuring equipment) for a specific location.
2. **Satellite-based models** provide data with lower frequency of measurement, but representing long history over lager areas. Satellite-models are not capable of producing instantaneous values at the same accuracy as ground sensors, but can provide robust aggregated values.

This Chapter summarizes approaches for measuring and computing these parameters, and the main sources of uncertainty. Methods for combination of data acquired by these two complementary approaches with the aim to get maximum from their benefits were developed. The most effective approach is to correlate multiyear satellite time series with data measured locally over short periods of time (at least one year) to reduce uncertainty and achieve more reliable long term estimates.

2.1.2 Solar radiation measurements

Global irradiance for horizontal and tilted plane is measured by (i) *pyranometers* using thermocouple junction or (ii) silicon *photodiode cells*. **Diffuse irradiance** is measured by the same sensors as global irradiance, except that the sun is obscured with a sun-tracking disk or rotating shadow band to block the direct component. **Direct Normal Irradiance** is commonly measured by *pyrheliometers*, where the instrument always aims directly at the sun using a continuously sun tracking mechanism.

A variety of instruments exists with different properties and achievable accuracy of measurements (Table 2.1). In the solar industry, the data accuracy requirements are high, therefore, where possible, it is recommended to measure solar radiation with the highest-accuracy instruments:

- **Secondary standard pyranometers** for Global Horizontal Irradiation (GHI) and (with shading ball/disc on a tracker) also for Diffuse Horizontal Irradiation (DIF)
- **First class pyrheliometer** for Direct Normal Irradiation (DNI).

This instrumentation is more expensive, and it is also more susceptible to soiling. Operation of solar instruments requires dedicated cleaning and maintenance, to guarantee data with low uncertainty.

Accuracy of Global Horizontal irradiance, measured with a thermopile **pyranometer**, is affected by two sources of error: the thermal imbalance problem and the cosine error of the sensor, resulting in a minimum uncertainty (for the most accurate sensor) of daily sums at about ±2%.

Direct Normal Irradiance, if measured by **pyrheliometers**, may be measured at daily uncertainty of about ±1% for a freshly calibrated high-accuracy pyrheliometer under ideal conditions. This uncertainty can more than double in case of rapid fluctuations of radiation, when using older instruments, or after prolonged exposure to challenging weather.

Table 2.1: Theoretically-achievable uncertainty of pyranometers at 95% confidence level

ISO 9060 class	Hourly totals	Daily totals
Secondary standard	±3%	±2%
First class	±8%	±5%
Second class	±20%	±10%

Global and diffuse components can be measured also by a *Rotating Shadowband Radiometer* (RSR) or by an integrated pyranometer such *Sunshine Pyranometer* (e.g. by SPN1). In such a case, DNI is calculated from global and diffuse irradiance.

Rotating Shadowband Radiometer (RSR) instruments can be installed as an alternative to the above-mentioned instruments, if measurements take place in a more challenging and remote environment with limited possibilities for cleaning and maintenance. However, if RSR is to be used, it is proposed to add one redundant measurement using a thermopile-type instrument for crosschecking the accuracy of RSR measurements. The photodiodes and RSR devices are also affected by cosine error and temperature. Empirical functions are used to correct the raw data, but theoretical daily uncertainty is around ±4% to ±5%. These instruments have narrower spectral sensitivity, thus operating these instruments in different environmental conditions from those, for which they were calibrated, may lead to increased uncertainty.

Choice of the best instruments does not alone guarantee good results. Rigorous on-site maintenance is crucial for sustainable quality of the longterm measuring campaign. Not only regular care of instruments is necessary, but also maintaining regular service documentation, changes in instrumentation, calibration, cleaning and variations of the instruments' behaviour. The radiometric response of the instruments also undergoes seasonal variability and longterm drift. Without careful maintenance, periodical check-up and calibration, the measured values can significantly differ from the "true" ones. **Uncertainty of measurements in outdoor conditions is always higher than the one declared in the technical specifications of the instrument** (Table 2.1). The uncertainty increases in extreme operating conditions, and in case of limited or insufficient maintenance.

Measuring solar radiation is sensitive to imperfections and errors, which results in visible and hidden anomalies in the output data. The errors may be introduced by measurement equipment, system setup or operation-related problems. Errors in data can severely affect derived data products and subsequent analyses; a thorough quality check is needed prior the data use.

2.1.3 Solargis satellite-based model

Numerical models using satellite and atmospheric data have become a standard for calculating solar resource time series and maps. The same models are also used for real-time data delivery for system monitoring and solar resource forecasting. Data from reliable operational solar models are routinely used by solar industry.

In this study, we applied a model developed and operated by the company Solargis. This model operationally calculates a high-resolution solar resource data and other meteorological parameters. Its geographical extent covers most of the land surface between latitudes 60° North and 55° South. A comprehensive overview of the Solargis model was made available in several publications [5, 6, 7, 8]. The related uncertainty and requirements for bankability are discussed in [9, 10].

In Solargis approach, solar irradiance is calculated in 5 steps:

1. Calculation of clear-sky irradiance, assuming all atmospheric effects except of clouds,
2. Calculation of cloud properties from the satellite data,
3. Integration of clear-sky irradiance and cloud effects and calculation of global horizontal irradiance (GHI)
4. Calculation of direct normal irradiance (DNI) from GHI and clear-sky irradiance.
5. Calculation of global tilted irradiance (GTI) from GHI and DNI.

Models used in individual calculation steps are parameterized by a set of inputs characterizing the cloud properties, state of the atmosphere and terrain conditions.

The **clear-sky irradiance** is calculated by the simplified SOLIS model [11]. This model allows fast calculation of clear-sky irradiance from the set of input parameters. Sun position is a deterministic parameter, and it is described by the algorithms with satisfactory accuracy. Stochastic variability of clear-sky atmospheric conditions is determined by changing concentrations of atmospheric constituents, namely aerosols, water

vapour and ozone. Global atmospheric data, representing these constituents, are routinely calculated by world atmospheric data centres:

- In Solargis, the new generation **aerosol data set** representing Atmospheric Optical Depth (AOD) is used. The core data set is from MACC-II/CAMS project (ECMWF) [12, 13]. An important feature of this data set is that it captures daily variability of aerosols and allows simulating more precisely the events with extreme atmospheric load of aerosol particles. Thus, it reduces uncertainty of instantaneous estimates of GHI and especially DNI, and it allows for improved statistical distribution of irradiance values [14, 15]. For years 1999 to 2002, data from the MERRA-2 model (NASA) [16] homogenized with MACC-II/CAMS model are used. The Solargis calculation accuracy of the clear-sky irradiance is especially sensitive to the information on aerosols.
- **Water vapour** is also highly variable in space and time, but it has lower impact on the values of solar radiation, compared to aerosols. The daily GFS and CFSR values (NOAA NCEP) are used in Solargis, thus representing the daily variability from 1999 to the present [17, 18, 19].
- **Ozone** absorbs solar radiation at wavelengths shorter than 0.3 μm, thus having negligible influence on the broadband solar radiation.

The **clouds** are the most influencing factor, modulating clear-sky irradiance. Effect of clouds is calculated from the satellite data in the form of cloud index (cloud transmittance). The cloud index is derived by relating irradiance recorded by the satellite in several spectral channels and surface albedo to the cloud optical properties. In this study, a data from the Meteosat IODC (Eumetsat) and MTSAT (JMA) satellites are used. In Solargis, the data from Meteosat IODC is available for a period from 1999 till the present time, data from MTSAT satellite is available from 2007 until early 2016; both systems deliver updated data at a time step of 30 minutes (Map 2.1). Continuation of MTSAT for the Pacific satellite mission is Himawari-8 (in operation since early 2016). Data from Himawari has not been included in this works. In Solargis, the modified calculation scheme by Cano has been adopted to retrieve cloud optical properties from the satellite data [20]. A number of improvements have been introduced to better cope with specific situations such as snow, ice, or high albedo areas (arid zones and deserts), and with complex terrain.

To calculate **Global Horizontal Irradiance** (GHI) for all atmospheric and cloud conditions, the clear-sky global horizontal irradiance is coupled with the cloud index.

From GHI, other solar irradiance components (direct, diffuse and reflected) are calculated. **Direct Normal Irradiance** (DNI) is calculated by the modified Dirindex model [21]. Diffuse horizontal irradiance is derived from GHI and DNI according to the following equation:

$$DIF = GHI - DNI * \cos Z \quad (1)$$

Where Z is the zenith angle between the solar position and the Earth's surface.

Calculation of **Global Tilted Irradiance (GTI)** from GHI deals with direct and diffuse components separately. While calculation of the direct component is straightforward, estimation of diffuse irradiance for a tilted surface is more complex, and is affected by limited information about shading effects and albedo of nearby objects. For converting diffuse horizontal irradiance for a tilted surface, the Perez diffuse transposition model is used [22]. The reflected component is also approximated considering that knowledge of local conditions is limited.

Model for simulation of **terrain** effects (elevation and shading) based on high-resolution elevation and horizon data is used in the standard Solargis methodology [23]. Model by Ruiz Arias is used to achieve enhanced spatial representation – from the resolution of satellite (several km) to the resolution of digital terrain model.

Solargis model version 2.1 has been used for computing the data. Table 2.2 summarizes technical parameters of the model inputs and of the primary outputs.

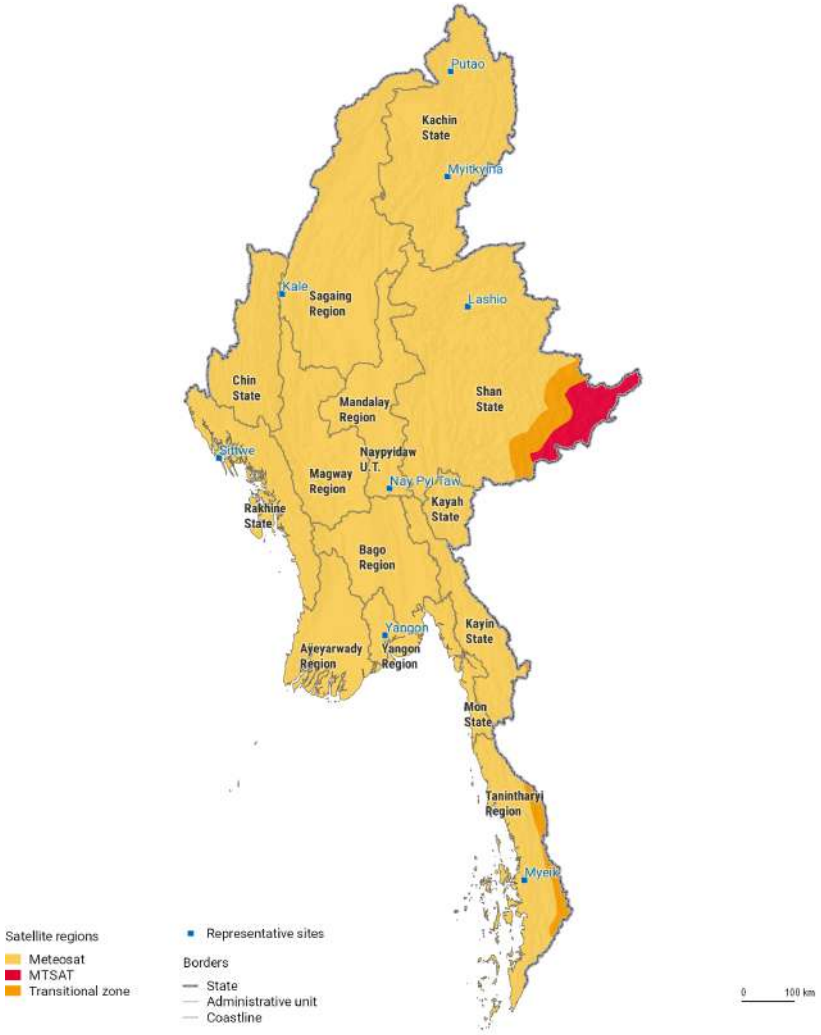

Map 2.1: Coverage of geostationary satellite data used in solar resource data calculation

Table 2.2: Input data used in the Solargis model and related GHI and DNI outputs for Myanmar

Inputs into the Solargis model	Source of input data	Time representation	Original time step	Approx. grid resolution
Cloud index	Meteosat IODC (EUMETSAT)	1999 to date	30 minutes	3.2 x 3.3 km
	MTSAT 2 satellite (JMA)	2007 to 2015	30 minutes	5.0 x 7.0 km
	Himawari 8 (JMA)*	2016 to date	10 minutes	2.8 x 3.9 km
Atmospheric optical depth (aerosols)	MERRA-2 (NASA)	1999 to 2002	1 hour	50 km
	MACC/CAMS (ECMWF)	2003 to date	3 hours	75 km and 125 km
Water vapour	CFSR/GFS (NOAA)	1999 to date	1 hour	35 and 55 km
Elevation and horizon	SRTM-3 (SRTM)	-	-	1 km
Solargis primary data outputs (GHI and DNI)	-	1999 (2007) to 2015**	30 minutes	1 km

* *Data from Himawari-8 satellite has not been used for this work.*

** *Solargis operational model provides the data updates in real time. The deliverables within this project cover complete calendar years from 1999 (Meteosat IODC) and 2007 (MTSAT) till 2015 (see Chapter 5.1)*

The achievable uncertainty of the solar irradiance derived from the satellite-based models depends on performance and limits of partial models as well as on the quality and the model inputs (mostly aerosols and satellite data). The modelling of solar irradiance in variable geographical conditions of Myanmar is challenging, and several features influencing the final data uncertainty should be considered:

1. **Aerosols**: there is a limited knowledge available on aerosols (pollution, burning biomass, forest fires etc.). Some of satellite based aerosol datasets are included in the AOD (Atmospheric Optical depth) data products used in the Solargis model, but local sources of pollution may not be accurately recorded in these data inputs.
2. **Persistent cloudy weather and monsoons**: for this type of weather conditions the accuracy of cloud properties identification (their effect on amount of irradiance at ground level) from the satellite data is in general lower.
3. Specific **satellite data** features: Myanmar is located in between of two geostationary satellite missions IODC (operated by EUMETSAT) and MTSAT/Himawari (operated by JMA). For booth satellite missions, the country is located at the edge of image scenes: the satellites observe the territory from relatively low viewing angle. In such regions, the identification of clouds has higher uncertainty. Moreover, data from older satellite platforms have lower positional accuracy (image may be slightly shifted). Even though the Solargis model uses advanced methods to correct image geometry, the identification of clouds has higher uncertainty in very contrast areas such as coastlines, due to residual positional inaccuracies of satellite images.
4. **High mountains** are very challenging for solar radiation modelling: Snow cover and presence of terrain shading makes the cloud identification erroneous as the clouds and snow have similar reflectivity in visible wavelengths. The use of satellite data acquired in the infrared spectrum helps in the cloud identification, but the resulting uncertainty is still higher.

2.1.4 Measured vs. satellite data – adaptation of solar model

For qualified solar resource assessment, it is important to understand characteristics of ground measurements and satellite-modelled data (Table 2.3). In general, top-quality and well-maintained instruments provide data with lower uncertainty than the satellite model. However, such data are rarely available for the required location and extrapolation of measured information from nearby station is limited only to short distances. Moreover, the period of measurements is usually too short to describe longterm weather conditions. On the other hand, the satellite data can provide long climatic history (17/9 years in Myanmar) for any location, but may not accurately represent the micro-climatic conditions of a specific site.

The ground measurements and satellite data complement each other; it is beneficial to correlate them and to adapt the satellite model for the specific site. Site-adapted satellite model data provide long history time series with lower uncertainty. The **model adaptation** has two steps:

1. Identification of systematic differences between hourly satellite data and local measurements for the period when both data sets overlap;
2. Development of a correction method that is applied for the whole period represented by the satellite time series.

The improvements of such site-adapted data depend on the quality and accuracy of measured and satellite data. In the most favourable cases, the resulting uncertainty is still slightly higher than uncertainty of ground measurements. In general, site adaptation of satellite data by local measurements will result in lower uncertainty under the following conditions:

- At least one year of ground-measured data is available (preferably two years or more) to cover all seasons;
- The solar measuring station is equipped with more than one instrument, allowing redundancy checks for GHI, DNI and DIF values;
- Ground measurements are of high quality, which should be traceable in the cleaning, maintenance and

calibration logs.

- High quality satellite data are used - with good representation of irradiance variability, extreme situations and with consistent longterm quality.
- Advanced site-adaptation methods are used, capable to address specific sources of satellite-ground data differences (e.g. correction of aerosols, reduction of cloud identification problems). Besides reduced uncertainty of longterm estimate (lower bias), the model adaptation method should also improve random deviations (lower RMSD) and should provide more representative (sub) hourly values (lower KSI).

Table 2.3: Comparing solar data from solar measuring stations and from satellite models

	Data from solar measuring stations	**Data from satellite-based models**
Availability/ accessibility	Available only for limited number of sites. Most often, data cover only recent years.	Solargis data is available for any location within latitudes 60N and 55S. Data cover long period; in Myanmar for this study, 17 and 9 years (depending on the satellite region).
Original spatial resolution	Data represent the microclimate of a site.	Satellite models represent area with complex spatial resolution: clouds are mapped at a grid cell of approx. 3.2 x 7.0 km, aerosols at 50 x 50 km and 125 x 125 km and water vapour at 34 x 34 km. Terrain can be modelled at spatial resolution of up to 90 metres. Methods for enhancement of spatial resolution are often used.
Original time resolution	Seconds to minutes	30 minutes in Southeast Asia
Quality	Data need to go through rigorous quality control, gap filling and cross-comparison.	Quality control of the input data is necessary. Outputs are regularly validated. Under normal operation, the data have only few gaps, which are filled by intelligent algorithms.
Stability	Instruments need regular cleaning and control. Instruments, measuring practices, maintenance and calibration may change over time. Thus, regular calibration is needed. Longterm stability is typically a challenge.	If data are geometrically and radiometrically pre-processed, a complete history of data can be calculated with one single set of algorithms. Data computed by an operational satellite model may change slightly over time, as the model and its input data evolve. Thus, regular reanalysis and temporal harmonization of inputs is used in state-of-the-art models.
Uncertainty	Uncertainty is related to the accuracy of the instruments, maintenance and operation of the equipment, measurement practices, and quality control.	Uncertainty is given by the characteristics of the model, resolution and accuracy of the input data. Uncertainty of models is higher than high quality local measurements. The data may not exactly represent the local microclimate, but are usually stable and may show systematic deviation, which can be reduced by good quality local measurements (site-adaptation of the model).

The **site-adaptation of the model** data is typically performed for locations where large-scale solar power plants are planned. During the project development phase a meteorological station with high-accuracy instruments is installed on the site and operated for at least one year, to get good understanding of local conditions. Local measurements are then used for site-adaptation of satellite model. The site-adapted long-term data are crucial for local solar resource evaluation and for accurate simulation of performance of various solar energy technologies with low uncertainty.

The ground measurements can be correlated with satellite data also at a regional level – within so called **regional model adaptation**, focused on broader territory rather than a single site. In the case of regional adaptation, the method aims to identify and reduce regional systematic deviations of the model, typically driven by insufficient characterization of aerosols or specific cloud patterns. The regional adaptation requires

measurements from several stations, which allows distinguishing the systematic model issues relevant to a large region, from the features related to a microclimate. The result of regional adaptation is improved solar resource database in the regional context with overall reduction of systematic errors.

2.1.5 Validation of solar radiation model data and uncertainty

Accuracy of Solargis data has been compared with high-quality solar measurements at 220+ meteorological stations, distributed worldwide. Map 2.2 and Table 2.4 show selected validation sites in the broader region, fulfilling the minimum requirements of measured data quality. Tables 2.5 to 2.6 show the Solargis model quality indicators for solar primary parameters: DNI and GHI.

Table 2.4: Selected validation sites in the region

Site name	Country	Latitude [°]	Longitude [°]	Elevation [m]	Source
Kanpur	India	26.5127	80.2319	123	SOLRADNET
Pantnagar*	India	29.0458	79.5208	241	SOLRADNET
Silpakorn	Thailand	13.8188	100.0408	72	SOLARFLUX
USM Penang*	Malaysia	5.358	100.302	51	SOLARFLUX
Bukit Kototabang	Indonesia	-0.2019	100.3181	864	GAW
Palangkaraya*	Indonesia	-2.228	113.946	27	SOLARFLUX
El Nido airport	Philippines	11.205	119.413	4	SOLARFLUX
Ishigakijima	Japan	24.3367	124.1633	11	BSRN
Cocos (Keeling) Islands	Australia	-12.1892	96.8344	3	BSRN

** **Note:** Less than one year of measurements*

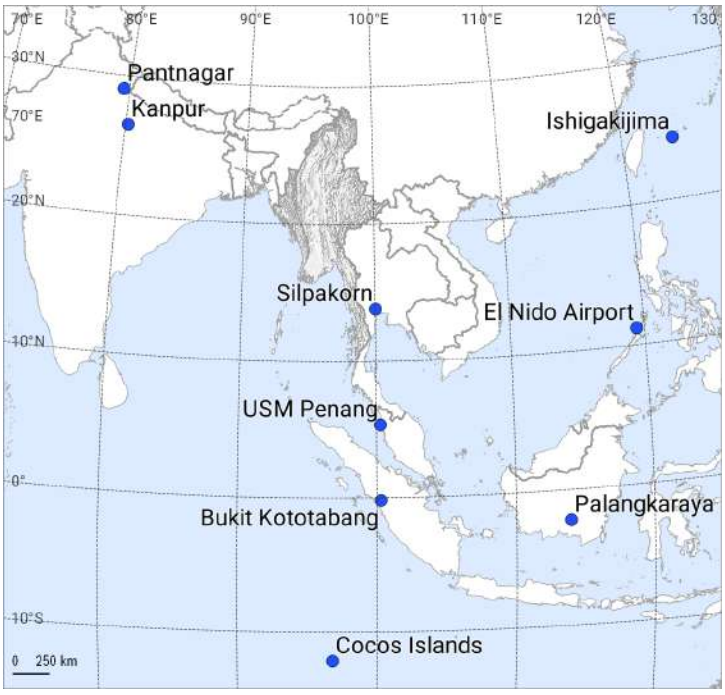

Map 2.2: Solar radiation validation sites

Comparison of the validation statistics, computed for the solar meteorological sites in the region, shows overall stability of the Solargis model and of the underlying input data. At the local level, slightly increased bias was identified, which may be an effect of the specific local conditions (e.g. anthropogenic pollution), limited accuracy of model and its input data as well as properties of ground measurements (short period of available data, lower accuracy of instruments).

Table 2.5: Global Horizontal Irradiance – quality indicators of the database in the region

Global Horizontal Irradiance, GHI	Bias		Root Mean Square Deviation, RMSD		
	[W/m^2]	[%]	Hourly [%]	Daily [%]	Monthly [%]
Kanpur	-9	-2.0	15.1	8.2	2.6
Pantnagar*	-5	-1.2	17.4	11.4	2.5
Silpakorn	-9	-1.9	23.6	12.2	5.0
USM Penang*	-11	-2.8	29.4	10.8	3.0
Bukit Kototabang	2	0.6	31.6	14.8	2.5
Palangkaraya*	-20	-4.6	21.7	9.8	8.0
El Nido airport	-13	-3.1	26.4	10.7	5.7
Ishigakijima	-5	-1.3	24.2	14.3	2.3
Cocos (Keeling) Islands	-18	-3.6	20.7	10.9	4.2

Table 2.6: Direct Normal Irradiance – quality indicators of the database in the region

Direct Normal Irradiance, DNI	Bias		Root Mean Square Deviation, RMSD		
	[W/m^2]	[%]	Hourly [%]	Daily [%]	Monthly [%]
Bukit Kototabang	19	8.9	72.6	42.1	11.0
Ishigakijima	2	0.7	43.7	25.7	4.9
Cocos (Keeling) Islands	-13	-3.1	43.6	22.0	5.7

None of the analysed ground measurement sites (Tables 2.5 to 2.6) is located in Myanmar. Based on this analysis, we have only partial knowledge of the **uncertainty of yearly solar radiation of the Solargis data** in Myanmar. The estimate is based on the data from surrounding regions. This approach is still valid as the performance of the Solargis model is stable over territories with the same geographical conditions, which was confirmed worldwide. In Myanmar, we recognise three main regions with slightly different expected uncertainty (Table 2.7 and Map 2.3).

Table 2.7: Uncertainty of long-term yearly estimates for GHI, GTI and DNI values in Myanmar

	Global Horizontal Irradiation (GHI)	Global Tilted Irradiation (GTI)	Direct Normal Irradiation (DNI)
Central lowlands (plains) and hilly land	<±5.5%	< ±6.5%	< ±14%
Mountains	±6 to 10%	±7 to 11%	±14 to 20%
Coastal zone	±6 to 8%	±7 to 9%	±12 to 18%

In the independent data comparison exercise, run for Europe and North Africa, Solargis has been identified as the best performing satellite-based solar resource database [24].

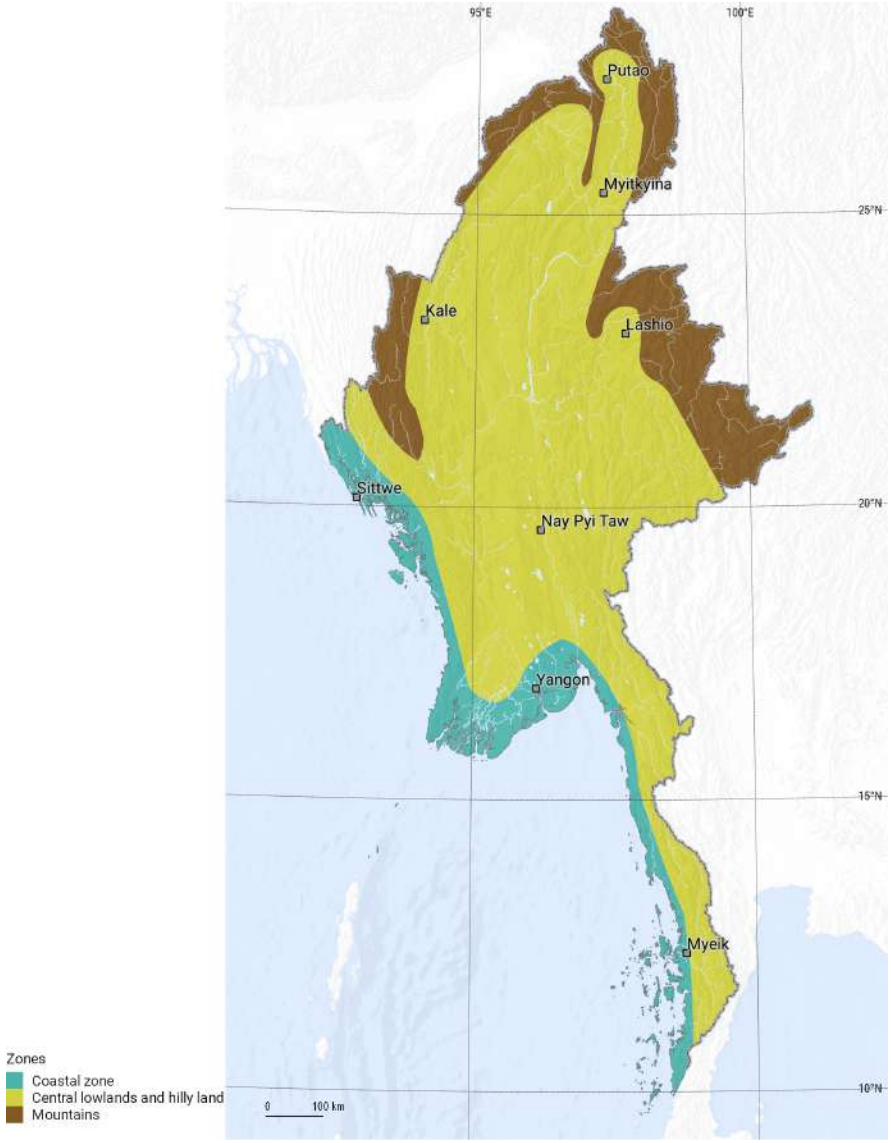

Map 2.3: Regions of solar resource uncertainty in Myanmar
Source: SRTM-3

2.2 Meteorological data

2.2.1 Measured vs. modelled data – features and uncertainty

Meteorological parameters are an important part of solar energy project assessment, as they determine the operating conditions and effectiveness of operation of solar power plants. The most important meteorological parameter for the operation of photovoltaic power plants is air temperature, which directly impacts power production (energy yield is decreasing when temperature is increasing). Meteorological data can be collected by two approaches: (1) by measuring at the meteorological sites, and (2) computing by the meteorological models.

The requirements for the meteorological data for solar energy projects are:

- Long and continuous record of data should be available, preferably covering the same period as satellite-based solar resource data,

- Data should reliably represent the local climate,
- Data should be accurate, quality-controlled and without gaps.

The best option would be to have continuous measurements from high-accuracy sensors installed at **meteorological stations**. However, except for sites where long-term meteorological observations are operated as part of national meteorological service or some other observation network, this option is typically not available. Even if some measurements are available, often the time series is incomplete or not reliable.

Most often, the only alternative is to derive historical meteorological data from the **meteorological models**. Several models are available; a good option is to use Climate Forecast System Reanalysis (CFSR) and its operational extension the Climate Forecast System Version 2 (CFSv2) models (source NOAA, NCEP, USA) covering long period of time with continuous data [18, 19]. The outputs of these models are used in Solargis.

The ground measurements play an important role in the assessment of local climate conditions as they determine the efficiency of photovoltaic power production. The role of the measurements in solar energy development has two aspects:

- Measurements are used for validation and accuracy enhancement of data derived from the solar and meteorological models;
- The high frequency measurements (typically one-minute data) are used for improved understanding of the microclimate of the site, especially for capturing the extremes.

Data inputs and method

In this delivery, the air temperature is derived from the meteorological models: CFSR and CFSv2 (Table 2.8). The original spatial resolution of the models is enhanced to 1 km for air temperature by spatial disaggregation and use of the Digital Elevation Model SRTM-3.

Important note: the numerical weather model has lower spatial and temporal resolution compared to the solar resource data. **Local microclimate of the site may deviate from the values derived from the numerical models.**

Table 2.8: Original source of Solargis meteorological data for Myanmar: models CFSR and CFSv2.

	Climate Forecast System Reanalysis (CFSR)	Climate Forecast System (CFSv2)
Period	1999 to 2010	2011 to date*
Original spatial resolution	30 x 35 km	20 x 22 km
Original time resolution	1 hour	1 hour

** **Note:** Solargis generates data updates from CFSv2 model in real time. The deliverables within this project cover complete calendar years from 1999 (compatible with Meteosat IODC region) and 2007 (compatible with MTSAT satellite region) till 2015.*

Data from the two sources described above have their advantages and disadvantages (Table 2.9). Air temperature retrieved from the meteorological models has lower spatial and temporal resolution, when compared to on-site meteorological measurements, and the models have lower accuracy. Thus, modelled parameters may characterize only regional climate patterns rather than local microclimate; especially extreme values may be smoothed and not well represented.

Table 2.9: Comparing data from meteorological stations and weather models

	Meteorological station data	Data from meteorological models
Availability/ accessibility	Available only for selected sites. Data may cover various periods of time	Data is available for any location Data cover long period of time (decades)
Original spatial resolution	Local measurement representing microclimate with all local weather occurrences	Regional simulation, representing regional weather patterns with relatively coarse grid resolution. Therefore, the local values may be smoothed, especially extreme values.
Original time resolution	From 1 minute to 1 hour	1 hour
Quality	Data need to go through rigorous quality control, gap filling and cross-comparison.	Only basic quality control is needed. No gaps Relatively stable outputs if data processing systematically controlled.
Stability	Sensors, measuring practices, maintenance and calibration may change over time. To achieve long-term stability is often a challenge.	In case of reanalysis, long history of data is calculated with one single stable model. Data for operational forecast model may slightly change over time, as the model development evolves.
Uncertainty	Uncertainty is related to the quality and maintenance of sensors and measurement practices, usually sufficient for solar energy applications.	Uncertainty is given by the resolution and accuracy of the model. Uncertainty of meteorological models is higher than high quality local measurements. The data may not exactly represent the local microclimate, but are usually sufficient for solar energy applications.

2.2.2 Validation of air temperature data and uncertainty

The validation was carried out to compare the modelled data with the measurements, available at selected meteorological stations in Myanmar. These measurements are available through NOAA ISD network (Table 2.10 and Map 2.4). In general, the data from the meteorological models represent larger area, and it may not be capable to represent accurately the local microclimate, especially in mountains of Myanmar.

Table 2.10: Meteorological stations and time periods considered in the model validation

Meteorological station	Data source	Validation period	Latitude* [°]	Longitude* [°]	Elevation* [m a.s.l.]
Putao	NOAA ISD	01/2008 – 12/2015	27.333	97.417	409
Myitkyina	NOAA ISD	01/2008 – 12/2015	25.367	97.400	147
Homalin	NOAA ISD	01/2008 – 12/2015	24.867	94.917	131
Lashio	NOAA ISD	01/2008 – 12/2015	22.933	97.750	749
Nyaung	NOAA ISD	01/2008 – 12/2015	21.200	94.917	55
Taunggyi	NOAA ISD	01/2008 – 12/2015	20.783	97.050	1436
Kengtung	NOAA ISD	01/2008 – 12/2015	21.300	99.617	828
Sittwe	NOAA ISD	01/2008 – 12/2015	20.133	92.873	8
Yangon	NOAA ISD	01/2008 – 12/2015	16.907	96.133	33
Victoria Point	NOAA ISD	01/2008 – 12/2015	9.967	98.583	47

** **Note**: the position of meteorological stations from the ISD network may be less accurate*

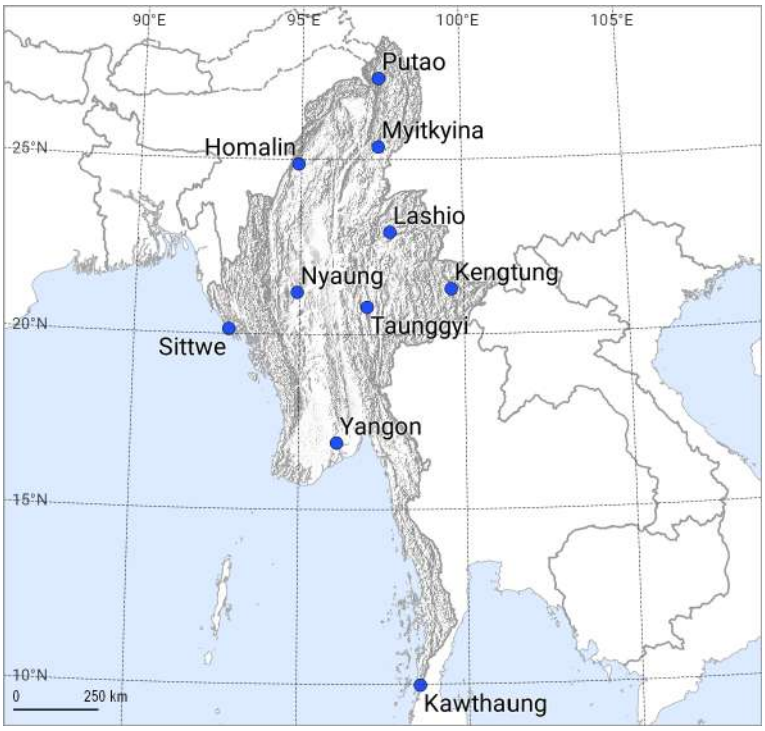

Map 2.4: Position of meteorological stations considered in the validation of air temperature

Air temperature is derived from both meteorological models and recalculated to the spatial resolution of 1 km by post-processing and disaggregation (Table 2.11). Considering the spatial and time interpolation, for hourly values the deviation of the model to the ground observations can occasionally reach several degrees Celsius.

For aggregated values, the modelled air temperature in Myanmar fits quite well the measured data, representing both seasonal and daily patterns with only 1 out of 10 stations having bias higher than ±1.5ºC, and 3 out of 10 having bias higher than ±1.0ºC. Average hourly RMSD for all 10 station stays below 5.0ºC what indicates that instantaneous temperature values have much higher uncertainty compared to long-term averages. The uncertainty of the estimate for air temperature is summarized in Table 2.12.

Table 2.11: Air temperature at 2 m: accuracy indicators of the model outputs [ºC].

Meteorological station	CFSR and CFSv2 models			
	Bias	RMSD hourly	RMSD daily	RMSD monthly
Putao	-0.9	5.0	3.2	1.1
Myitkyina	-0.6	4.3	2.0	1.0
Homalin	-0.6	4.3	2.6	1.3
Lashio	-0.4	4.9	2.6	1.3
Nyaung	-0.4	3.6	2.2	1.2
Taunggyi	-1.3	3.5	2.2	1.7
Kengtung	-2.6	4.7	3.2	2.7
Sittwe	-0.3	2.0	1.3	0.5
Yangon	-0.3	2.1	1.4	0.9
Victoria Point	-1.2	2.7	1.9	1.3

Table 2.12: Expected uncertainty of model air temperature in Myanmar.

	Unit	Annual	Monthly	Hourly
Air temperature at 2 m	°C	±1.5	±2.0	±4.5

2.3 Simulation of photovoltaic power potential

Solar radiation is the most important parameter for PV power simulation, as it is fuel for solar power plants. The intensity of global irradiance received by tilted surface of PV modules (GTI) is calculated from two primary parameters stored in the Solargis database, and delivered in this project:

- Global Horizontal Irradiance (GHI)
- Direct Normal Irradiance (DNI)

There are two main types of solar energy technologies: photovoltaic (PV) and concentrating solar power (CSP). There is no reasonable potential for CSP in Myanmar, and therefore **this report focuses only on evaluation of the photovoltaic technology**.

Photovoltaics exploits global horizontal irradiance or global tilted irradiance, i.e. the sum of direct and diffuse components, see equation (1) in Chapter 2.1.3. To simulate power production from a PV system, global irradiance received by a flat surface of PV modules must be correctly calculated. Due to clouds, PV power generation reacts to changes of solar radiation in the matter of seconds or minutes (depending on the size of a module field), thus intermittency (short-term variability) of the PV power production is to be considered. Similarly, the effect of seasonal variability is to be considered as well.

PV technology will presumably dominate in solar energy applications in Myanmar. It is one of attractive options for small-scale provision of electricity, particularly in remote areas [25]. Available units are ranging from small solar home systems, through local mini-grid systems (hybrid systems, where PV is support for diesel generators) to ground-mounted grid connected systems [26]. For PV systems applications, several technical options are available and have been briefly described below.

Two types of mounting of PV modules can be considered:

- Build in an open space, where PV modules are ground-mounted in a fixed position or on sun-trackers
- Mounted on roofs or façades of buildings,

Three types of a PV system can be considered for Myanmar:

- Grid-connected PV power plants
- Mini-grid PV systems
- Off-grid PV systems

Most utility scale PV power plants are built on **open space** and have **PV modules mounted at a fixed position** with optimum inclination (tilt). Fixed mounting structures offer a simple and efficient choice for implementing the PV power plants. A well-designed structure is robust and ensures long-life performance even during harsh weather conditions at low maintenance costs. **Sun-tracking systems** are the other alternative. Solar trackers adjust the orientation of the PV modules during a day to a more favourable position in relation to the sun, so the PV modules collect more solar radiation.

Roof or façade mounted PV systems are typically small to medium size, i.e. ranging from hundreds of watts to hundreds of kilowatts. Modules can be mounted on roofs (flat or tilted), façades or can be directly integrated as part of a building structure. PV modules in these systems are often installed in a suboptimal position (deviating from the optimum angle), and this results in a lower performance ratio. PV modules, which are mounted at low tilt, are affected by higher surface pollution due to less effective natural cleaning. Another reduction of PV power output is often determined by nearby shading structures. Trees, masts, neighbouring buildings, roof structures or self-shading of crystalline silicon modules especially have some influence on reduced PV system performance.

The main characteristics of **grid-connected systems** is their geographic dispersion and connection into a distribution grid. Direct connection into grid also means that the inverter must provide all protections required by regulations (voltage, frequency, isolation check, etc.). For comparison, a utility scale power plant has its own protection equipment, separated from the inverter and assembled typically on the high-voltage side. Inverters can reach higher efficiencies and are required to have anti-islanding protection, which means that they work only if grid voltage is present (due to safety reasons). Other connection options, combined with batteries, are also used.

Mini-grid PV systems provide small isolated distribution grid for local consumers, usually located in remote areas. Typical size of installed PV systems is tens to hundreds of kWp. Mini-grid may be adapted to meet requirements of local needs, sometimes with several types of electricity generators (hybrid systems) and battery storage. This type of electrification gives prospects for development to remote and rural communities, because it is often the sole economically viable option for supply of electricity.

Off-grid PV systems are small systems, not connected into distribution grid. They are usually equipped with energy storage (classic lead acid or modern-type batteries) and/or connected to diesel generators. Batteries are maintained through charge controllers for protection against overcharging or deep discharge. Depending on size and functionality of the off-grid PV system, it can work with AC (together with inverter) or DC voltage source.

In this study, the PV power potential is studied for **a system with fixed-mounted PV modules**, considered here as the mainstream technology. Installed capacity of a PV power plant is usually determined by the available space and options to maintain the stability of the power grid.

2.3.1 Principles of PV energy simulation

PV energy simulation results, presented in Chapter 3.6, are based on software developed by Solargis. This Chapter summarizes key elements of the simulation chain.

Table 2.13: Specification of Solargis database used in the PV calculation in this study

Data inputs for PV simulation	Global tilted irradiation (GTI) for optimum angle (range of 12° to 30° in Myanmar) towards South, derived from GHI and DNI; air temperature at 2 m (TEMP).
Spatial grid resolution (approximate)	1 km (30 arc-sec)
Time resolution	30-minute
Geographical extent (this study)	Republic of the Union of Myanmar
Period covered by data (this study)	01/1999 to 12/2015 (in very East only 01/2007 to 12/2015) see Map 2.1

The PV software has implemented scientifically proven methods [27 to 34] and uses sub-hourly Solargis time series of solar radiation and air temperature data on the input (Table 2.13). Data and model quality are checked using field tests and ground measurements.

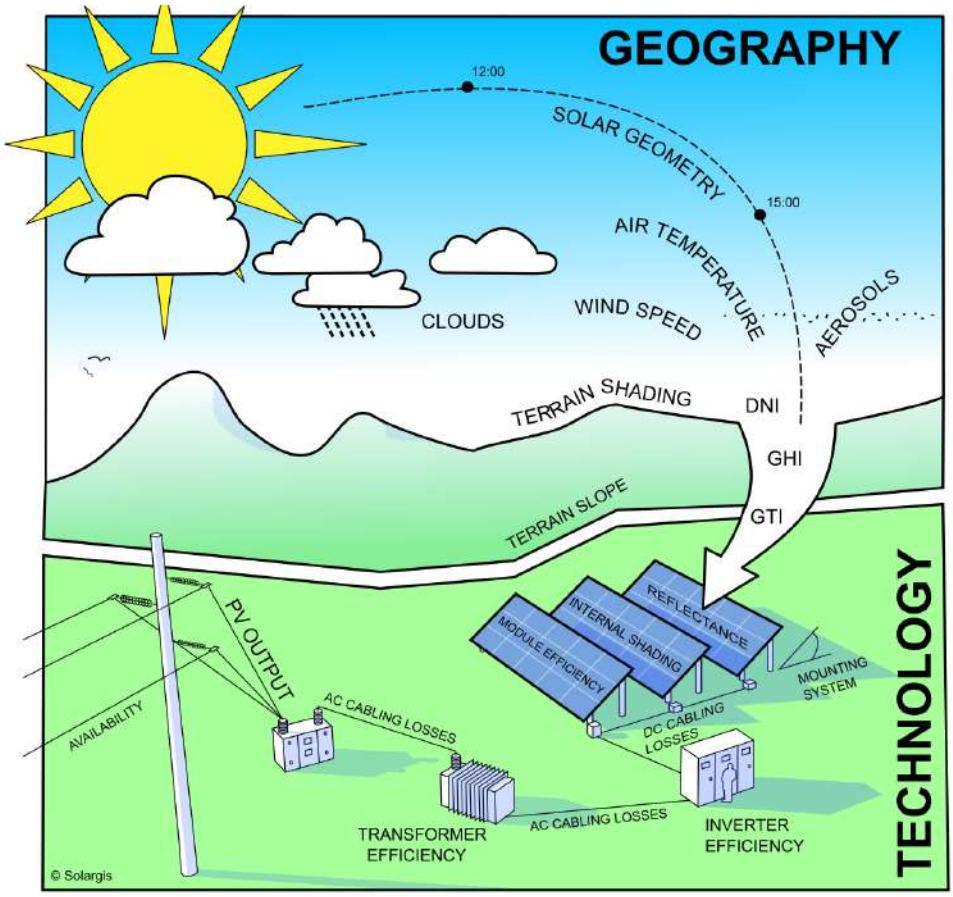

Figure 2.1: Simplified Solargis PV simulation chain

In PV energy simulation procedure, there are several energy losses occurring in the individual steps of energy conversion (Figure 2.1):

1. **Losses due to terrain shading** caused by far horizon**.** Shading of local features such as nearby building, structures or vegetation is not considered in the calculation,
2. Energy conversion in PV modules is reduced by **losses due to angular reflectivity**, which depend on relative position of the sun and plane of the module and **temperature Losses,** caused by performance of PV modules working outside of STC conditions defined in datasheets,
3. DC output of PV array is further reduced by **losses due to dirt, snow** (in high mountains) or **soiling** depending mainly on the environmental factors and module cleaning**, losses by inter-row shading** caused by preceding rows of modules and **mismatch** and **DC cabling losses**, which are given by slight differences between nominal power of each module and small losses on cable connections,
4. DC to AC energy conversion is performed by inverter. Efficiency of this conversion step is reduced by **inverter losses**, given by inverter efficiency function. Further factors, reducing AC energy output, are **losses in AC cabling** and **transformer losses** (apply only for large–scale open space systems),
5. **Availability.** This empirical parameter quantifies electricity losses incurred by shutdown of a PV power plant due to maintenance or failures, including issues in the power grid. Availability of well operated PV system is approximately 99%.

According to experience in many countries, the crystalline silicon PV modules show low performance reduction over time due to aging. The rate of the performance degradation is higher at the beginning of the exposure, and then stabilizes at a lower level. Initial degradation may be close to value of 0.8% for the first year and 0.5% or less for the next years [31]. Degradation of conversion efficiency of PV modules is not considered in this study.

Results of calculation of PV power potential for Myanmar are shown in Chapter 3.6.

2.3.2 Technical configuration of a reference PV system

Photovoltaic power production has been calculated using numerical models developed and implemented in-house by Solargis. As introduced in Chapter 2.1, 30-minute **time series of solar radiation and air temperature**, representing last 17 (9) years, are used as an input to the simulation. The models are developed based on the advanced algorithms, expert knowledge and recommendations given in [33], and tested using monitoring results from existing PV power plants. Table 2.15 summarizes losses and related uncertainty throughout the PV computing chain.

In this study, the reference configuration for the PV potential calculation is a PV system with crystalline-silicon (c-Si) modules mounted in a fixed position on a table facing South and inclined at an angle close to optimum, i.e. at the angle at which the yearly sum of global tilted irradiation received by PV modules is maximized (a range between 12° and 30° depends on a geographical region). The fixed-mounting of PV modules is very common and provides a robust solution with a minimum maintenance effort. Geographic differences in potential PV production are shown at eight selected sites (Chapter 3.1).

Map 3.16 shows theoretical potential power production of a PV system installed with a typical technology configuration, for large-scale open space PV power plants. The technical parameters are described in Table 2.14.

Table 2.14: Reference configuration - photovoltaic power plant with fixed-mounted PV modules

Feature	Description
Nominal capacity	Configuration represents a typical PV power plant of 1 MW-peak or higher. All calculations are scaled to 1 kWp, so that they can be easily multiplied for any installed capacity.
Modules	Crystalline silicon modules with positive power tolerance. NOCT 46°C and temperature coefficient of the Pmax -0.45 %/K
Inverters	Central inverter with Euro efficiency 97.5%
Mounting of PV modules	Fixed mounting structures facing South with optimum tilt (the range from 12° to 30°). Relative row spacing 2.5 (ratio of absolute spacing and table width)
Transformer	Medium voltage power transformer

The results presented in Chapter 3.6 do not consider performance degradation of PV modules due to aging. They also lack a necessary detail; these results cannot be used for financial assumptions of any particular project. Detailed assessment of energy yield of a specific power plant is within a scope of site-specific bankable expert study.

PV electricity potential is calculated based on a set of assumptions shown in Tables 2.14 and 2.15. These assumptions are approximate, and they will differ in the real projects. As can be seen uncertainty of solar resource is the highest element of energy simulation.

Table 2.15: Yearly energy losses and related uncertainty in PV power simulation

Simulation step		Losses [%]	Uncertainty [± %]	Notes
1	Global Tilted Irradiation (model estimate with terrain shading)	N/A	6.5 to 11.0	Annual Global Irradiation falling on the surface of PV modules
2	Module surface angular reflectivity (numerical model)	-2.6 to -3.1	1.0	Medium polluted surface of PV modules is considered
	Temperature losses (numerical model)	-0.8 to -12.3	3.5	Depends on the temperature and irradiance. NOCT of 46°C is considered
3	Polluted surface of modules (empirical estimate)	-3.0	1.5	Losses due to dirt, dust, soiling, snow and bird droppings
	Module inter-row shading (model estimate)	-0.1 to -0.5	0.5	Partial shading of strings by modules from the preceding rows
	Mismatch between modules (empirical estimate)	-0.5	0.5	Well-sorted modules and lower mismatch are considered.
	DC cable losses (empirical estimate)	-2.0	1.5	This value can be calculated from the electrical design
4	Conversion in the inverter (value from the technical data sheet)	-2.5	0.5	Given by the Euro efficiency of the inverter, which is considered at 97.5%
	AC cable losses (empirical estimate)	-0.5	0.5	Standard AC connection is assumed
	Transformer losses (empirical estimate)	-1.0	0.5	Standard transformer is assumed
5	Availability	0.0	0.0	A theoretical value of 100% technical availability is considered
	Range of cumulative losses and indicative uncertainty	**-12.2 to -23.2**	**7.8 to 11.8**	These values are indicative and do not consider project specific features and performance degradation of a PV system over its lifetime

3 Solar resource and PV potential of Myanmar

3.1 Geography

This report analyses solar and meteorological data for Myanmar that determine photovoltaic power production and influence its performance efficiency. We analyse also other geographical factors that influence development and operation of solar photovoltaic power plants.

Myanmar is located in South Asia between latitudes 10° and 29° North and longitudes 92° and 101° East. We demonstrate the variability of solar potential in two forms:

- At the **country level** in the form of maps
- In the form of graphs and tables for **eight sites** that represent the variability of solar power production in regions where its deployment is relevant and the most likely.

The position of selected sites coincides with position of airports (with exception of Myeik) in regional centres, and it is summarised in Table 3.1 and Map 3.1. All the data in tables and graphs, shown in this Chapter 3, relate to these eight sites.

Table 3.1: Position of eight selected sites in Myanmar

ID	Site name	State	Latitude [°]	Longitude [°]	Elevation [metres a.s.l.]
1	Putao airport	Kachin	27.32555	97.42588	461
2	Myitkyina airport	Kachin	25.38203	97.35404	140
3	Kale airport	Sagaing	23.18905	94.05200	128
4	Lashio airport	Shan	22.97417	97.75324	773
5	Sittwe airport	Rakhine	20.13505	92.87303	3
6	Nay Pyi Taw airport	Naypyidaw Union	19.61741	96.21054	88
7	Yangon airport	Yangon	16.90346	96.13399	28
8	Myeik	Taninthayi	12.37086	98.77224	7

Geographic information and maps bring additional value to the solar data. Geographical characteristics of the country from regional to local scale may represent technical and environmental prerequisites, but also constraints for solar energy development.

In this report, we collected the following data that have some relevance to solar energy:

- Terrain: physical limitation for development (Maps 3.2 and 3.3);
- Land cover: defines primary areas used for human economic activities and settlements (Map 3.4),
- Main road network: defining accessibility of sites for location of power plants (Map 3.5)
- Protected areas limit size of the power station and intensity of land use for the related infrastructure (Map 3.6)
- Population density (Map 3.7).
- Days of rainfall (precipitation) and air temperature have impact on efficiency (performance ratio) of the PV installations (Maps 3.8 and 3.9)

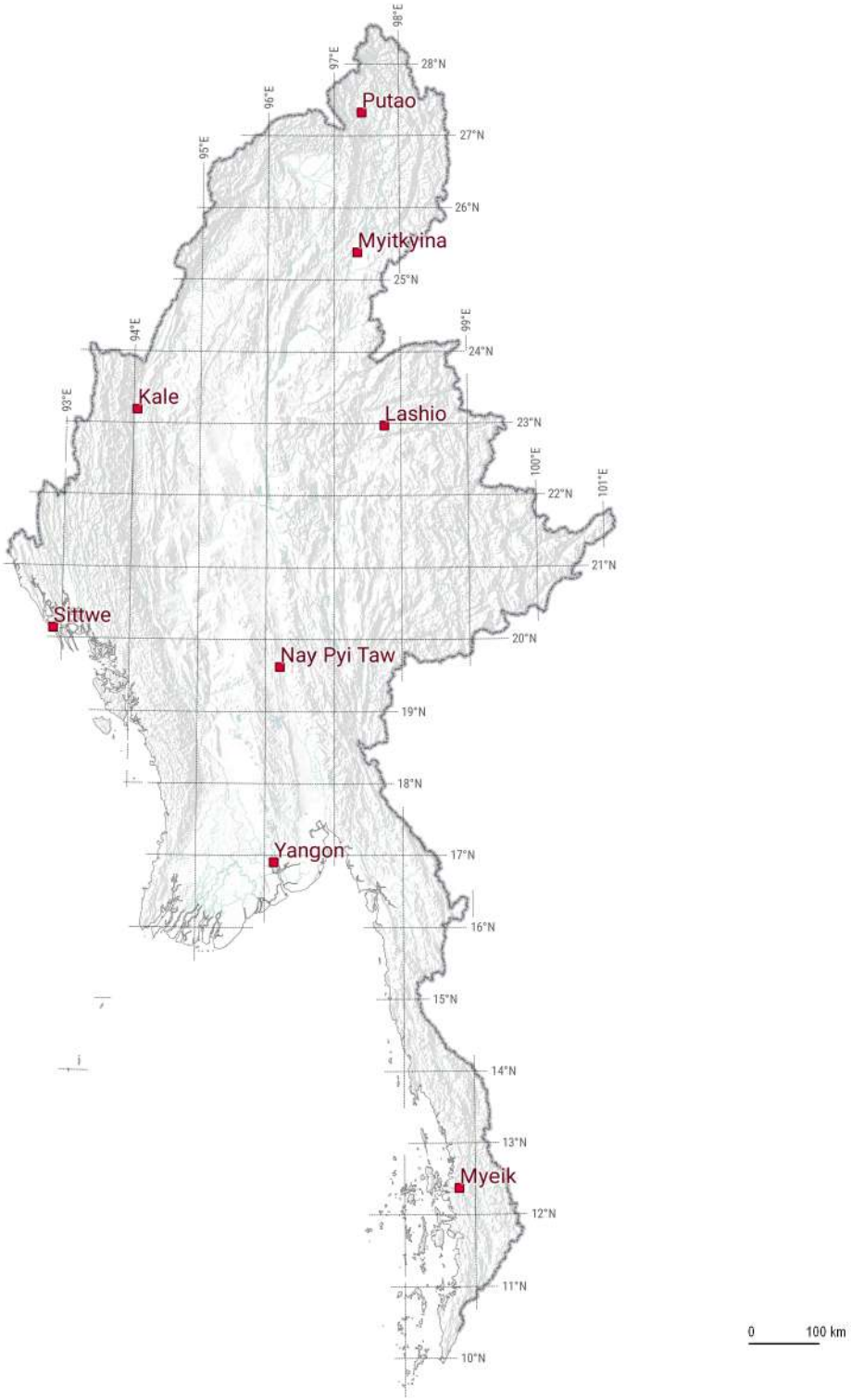

Map 3.1: Position of eight selected sites in Myanmar.

Eight sites are selected to show variability of Myanmar from the perspective of solar power production.

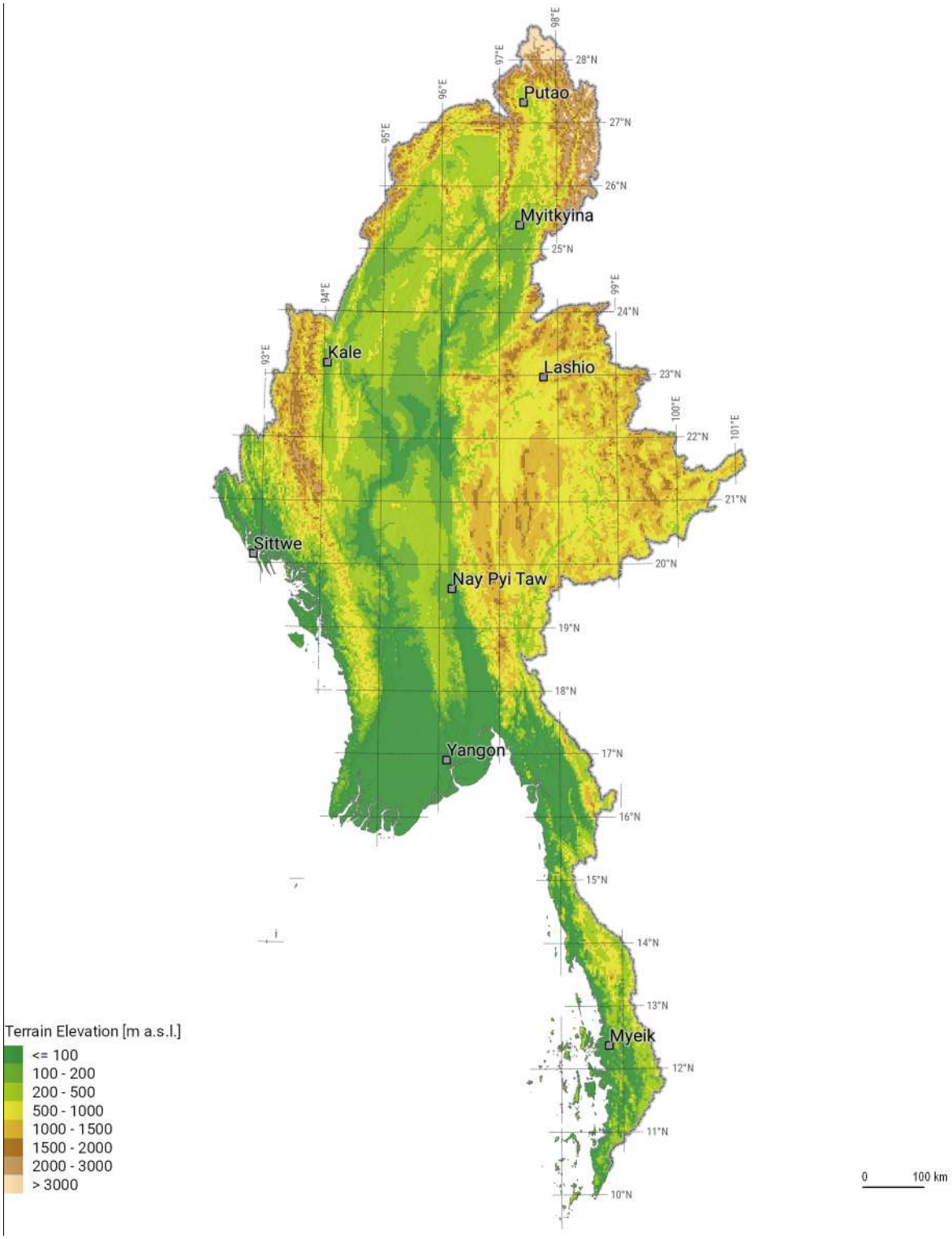

Map 3.2: Terrain elevation above sea level.
Source: SRTM-3

From the geographical viewpoint, Myanmar is a diverse country, spreading from tropical lowlands in south and central part, through highlands on the West but mostly in the eastern part of the country ranging from the elevation of 700 to 3000 m up to more than 5800 m high peaks in the North on the border with China (Map 3.2).

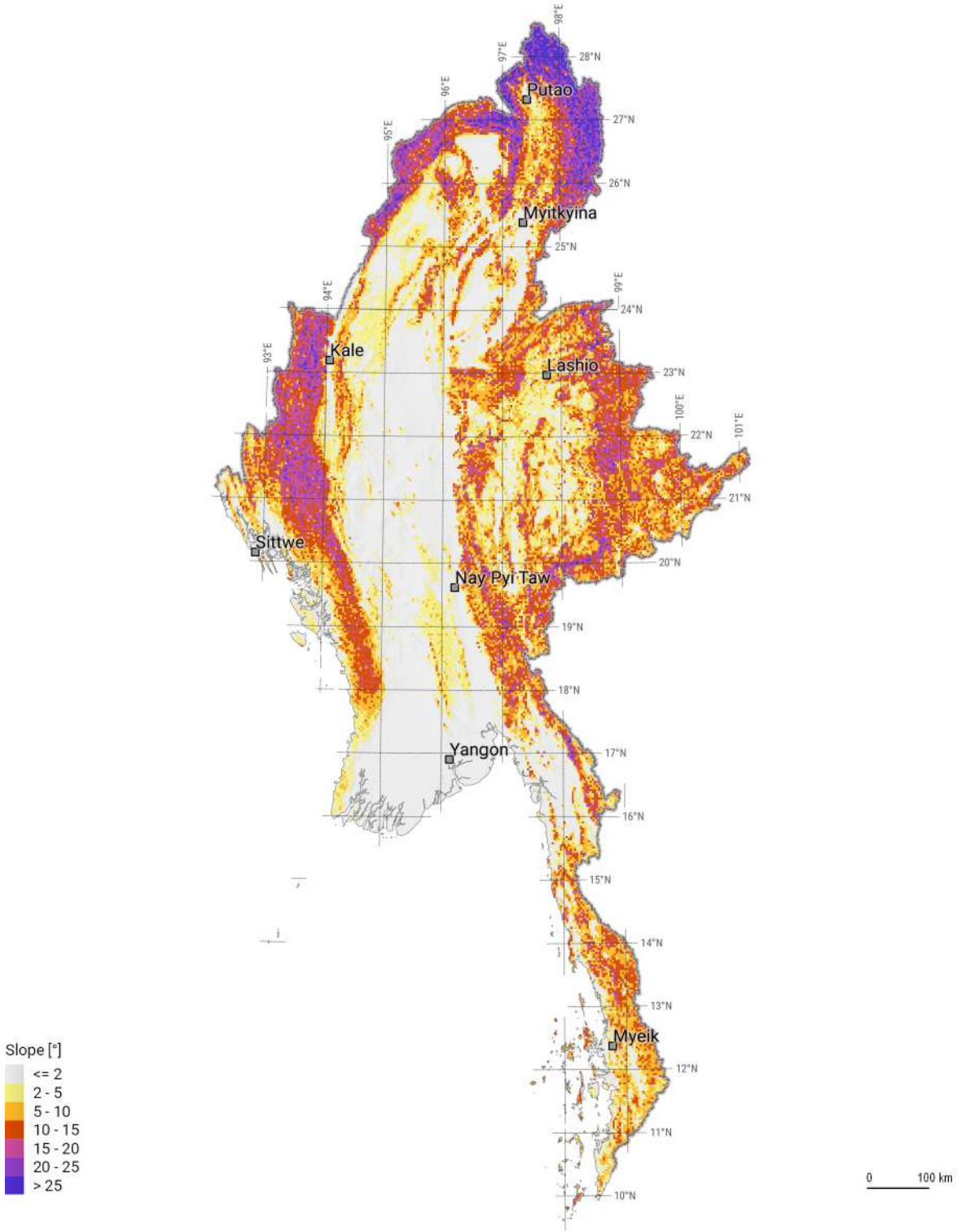

Map 3.3: Terrain slope.
Source: SRTM-3 and Solargis

Major part of the country has terrain with the slopes less than 5 degrees (Map 3.3); this territory does not pose physical limits to locating larger solar power installations. To some degree, the terrain may by a limiting factor for locating larger solar power facilities where the slope is above approx. 10 degrees. Small solar power installations (residential, off-grid stand-alone or mini-grids) in Myanmar can be installed anywhere; they play

crucial role for development especially in remote communities. The land cover map (Map 3.4) shows that the most of settlements and economic activities (industry, agriculture and transport) – that require access to electrical power – are developed in central lowland and adjacent hills. Settlements are dispersed in highlands and remote areas as well.

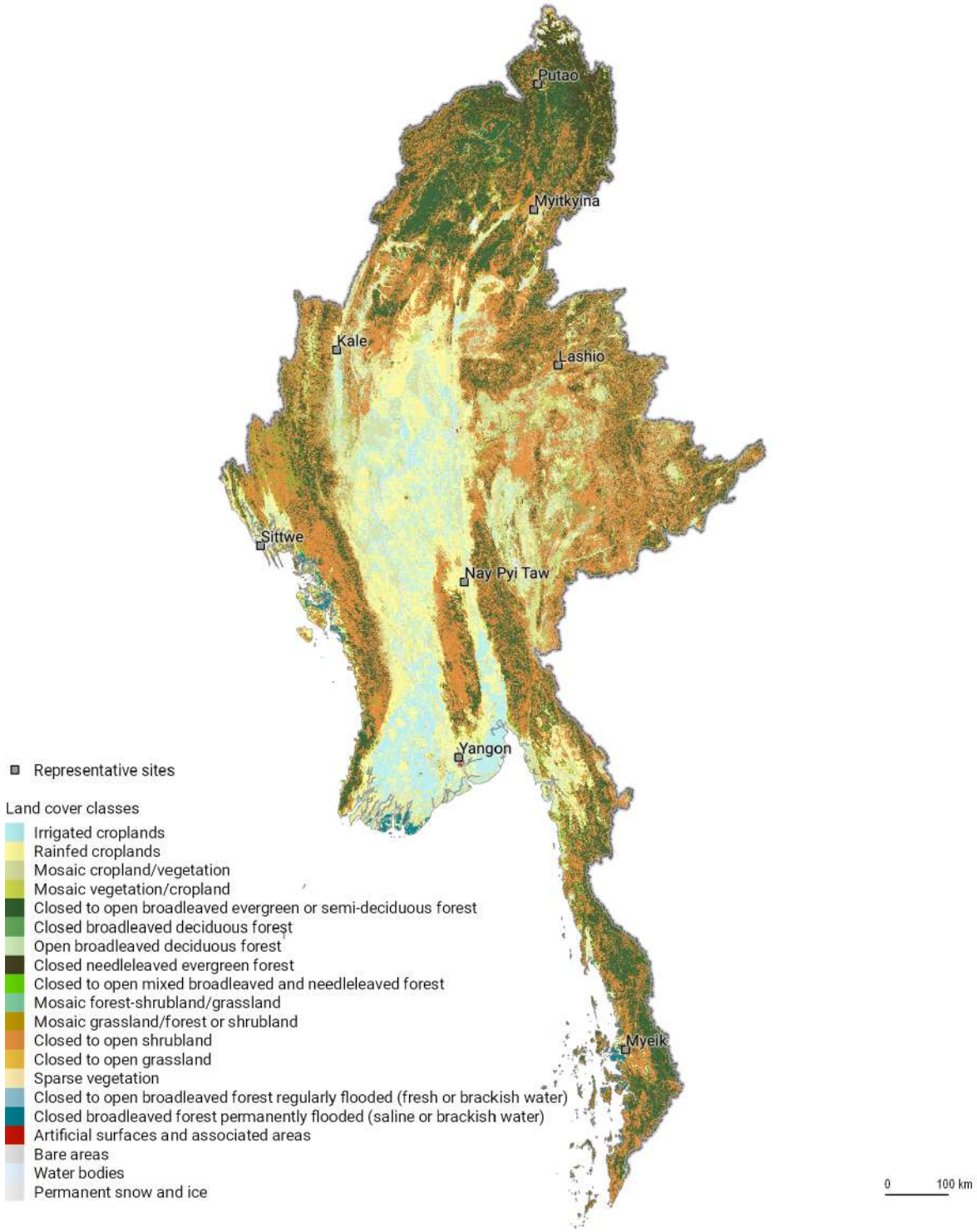

Map 3.4: Land cover.
Source: GlobCover 2009 © ESA 2010 and UCLouvain

Map 3.5: Roads and cities.
Source: OpenStreetMap.org contributors; administrative boundaries by Cartography Unit, GSDPM (World Bank Group)

Urbanisation and transport infrastructure is mostly developed in the central region, where also electricity demand is the highest (Map 3.5).

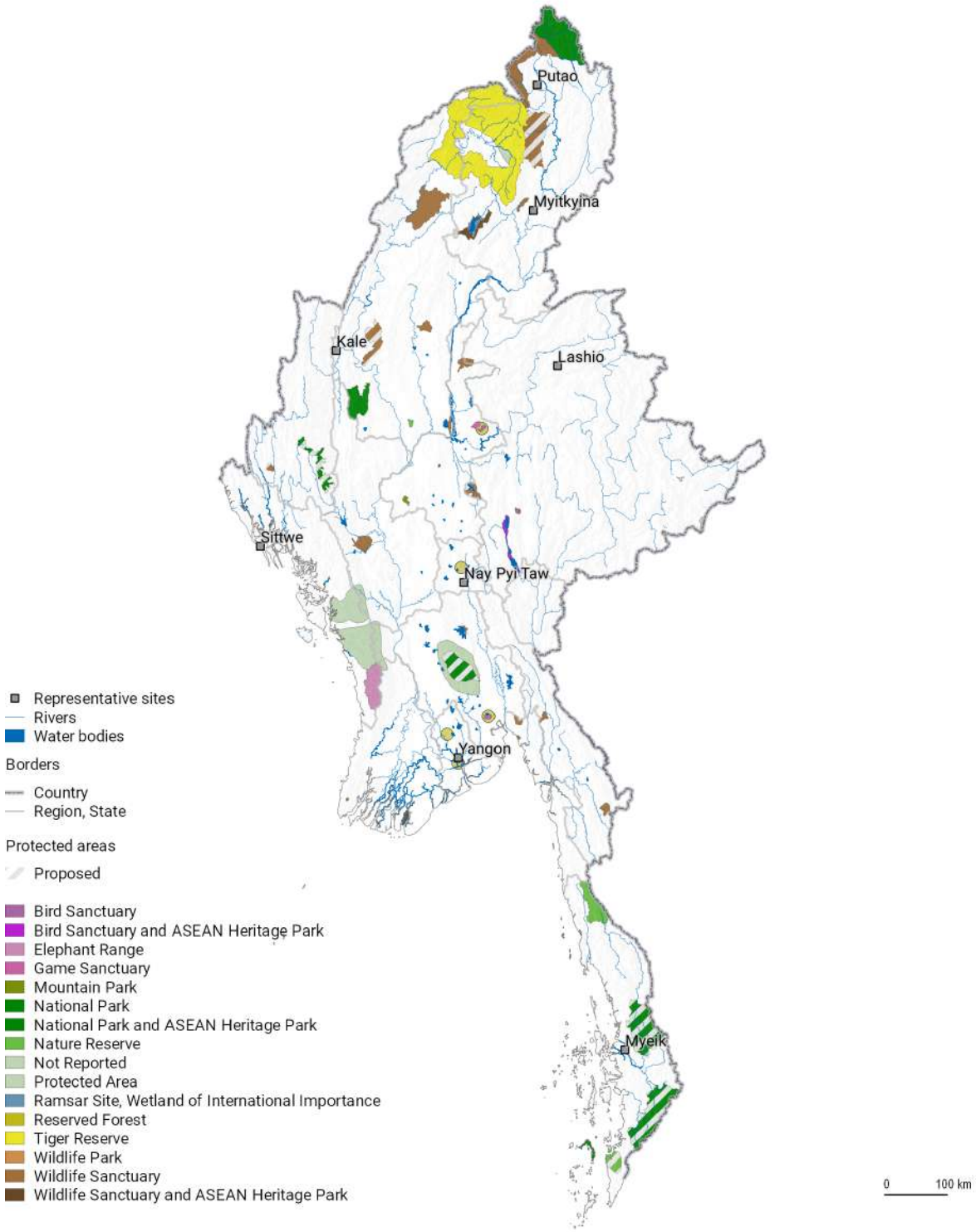

Map 3.6: Nature protection areas
Source: OpenStreetMap.org contributors, adapted by Solargis

Nature protection areas represent limitation for deployment of large scale solar power plants. However having just a local impact, it is not difficult to manage planning with the knowledge of these constrains.

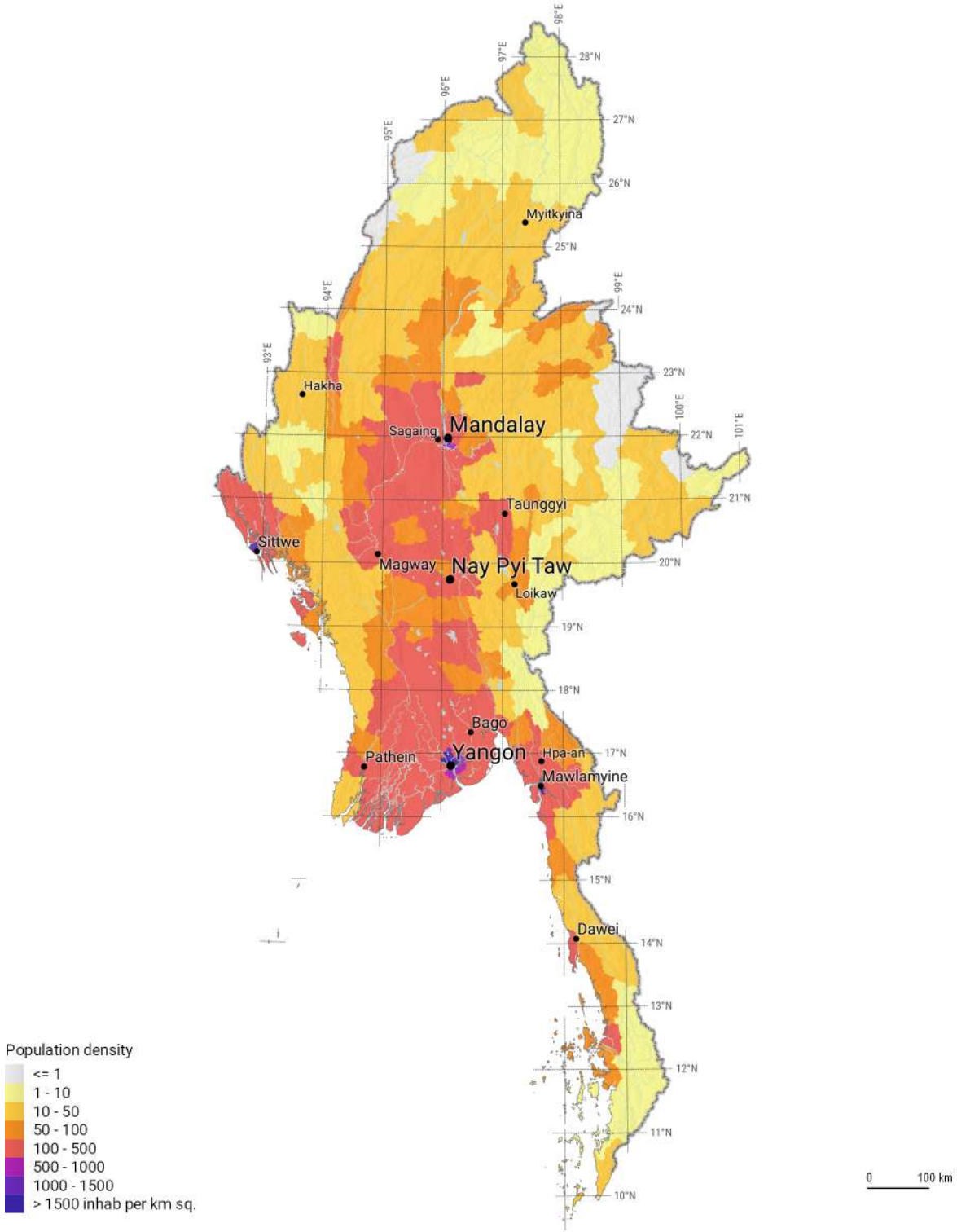

Map 3.7: Population density.
Source: Gridded Population of the World (GPW) v.4

The most densely populated areas coincide with the regions most suitable for solar investment.

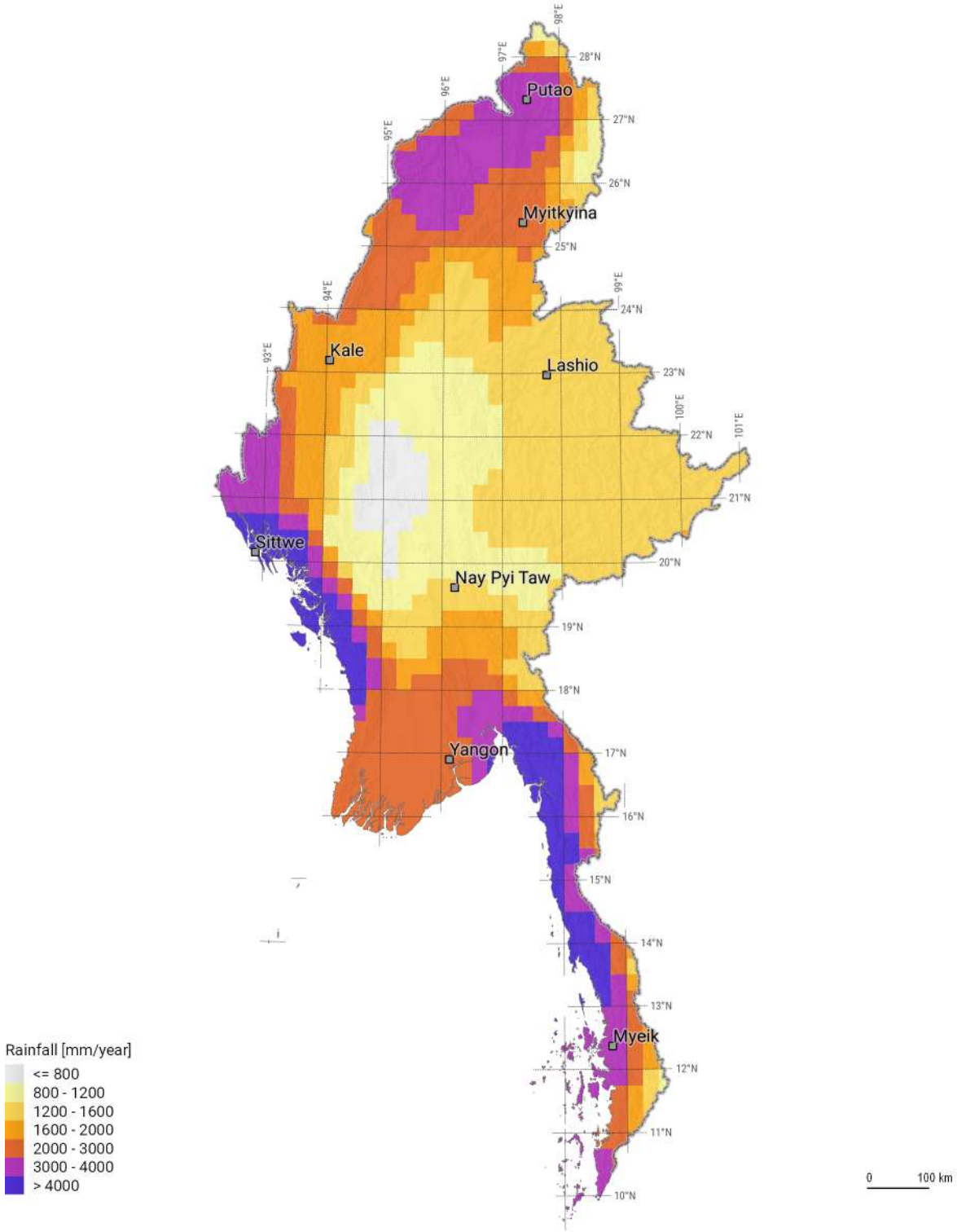

Map 3.8: Long-term yearly average of rainfall (sum of precipitation).
Source: Global Precipitation Climatology Centre (DWD)

More rain helps to keep surface of PV modules clean. Yet precipitation can should be considered also as a potential risk - in regions with occurrence of seasons with heavy rains.

3.2 Air temperature

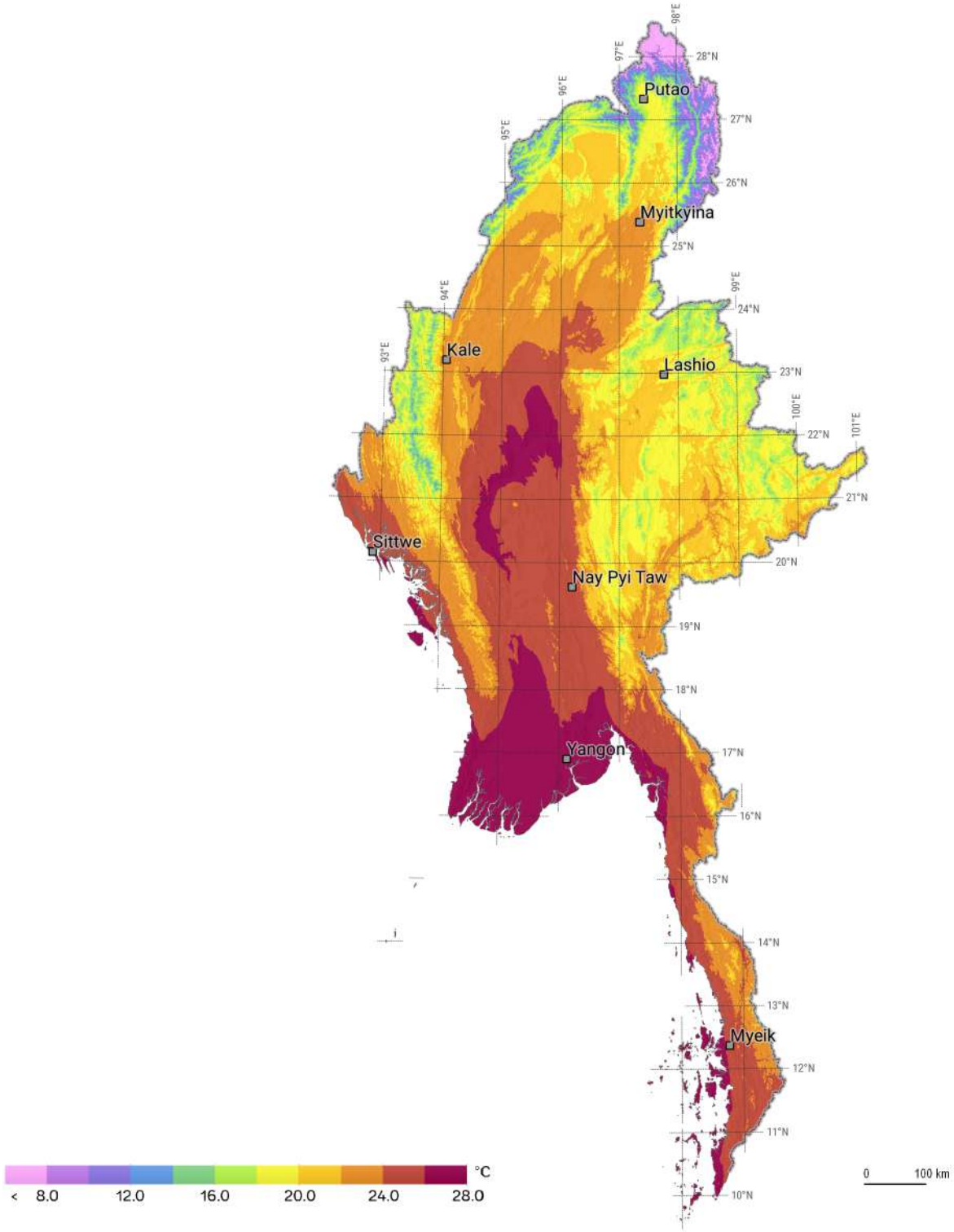

Map 3.9: Long-term yearly average of air temperature at 2 metres.
Source: Models CFSR and CFSv2, NOAA, post-processed by Solargis

Air temperature determines the operating environment and performance efficiency of the solar power systems. Air temperature is used as one of inputs in the energy simulation models. Map 3.9 shows yearly average.

The longterm averages of air temperature are derived from the CFSR and CFSv2 meteorological models (see Chapter 2.2) by Solargis post-processing.

In case of PV power plants, air temperature has a primary influence on the power conversion efficiency in the PV modules, and it also influences other components (inverters, transformers, etc.). Increasing air temperature reduces power conversion efficiency of a PV power plant.

Table 3.2: Monthly averages and average minima and maxima of air-temperature at 2 m at 8 sites

Month	Temperature [°C]															
	Putao		Myitkyina		Kale		Lashio		Sittwe		Nay Pyi Taw		Yangon		Myeik	
	Average	Min Max	Average	Min Max	Average	Min Max	Average	Min Max	Average	Min Max	Average	Min Max	Average	Min Max	Average	Min Max
January	**12.0**	6.7 20.3	**16.0**	9.6 25.9	**15.8**	8.9 24.8	**13.9**	6.9 23.7	**22.3**	18.8 25.8	**20.6**	12.9 30.2	**24.7**	18.1 32.0	**25.5**	20.0 33.6
February	**14.0**	8.5 22.0	**19.1**	12.0 29.2	**19.7**	12.4 28.8	**16.6**	8.1 27.1	**23.8**	20.1 27.3	**23.1**	14.1 33.4	**26.9**	19.0 35.1	**26.0**	20.3 34.3
March	**17.1**	11.6 24.8	**23.3**	16.1 33.4	**24.8**	17.1 33.9	**21.2**	12.8 31.3	**26.0**	22.6 29.1	**26.7**	17.9 36.8	**29.3**	21.3 37.9	**26.5**	21.5 34.2
April	**19.7**	14.9 26.9	**26.4**	19.9 36.0	**28.2**	21.4 37.0	**24.6**	17.0 33.4	**28.1**	25.5 30.6	**29.9**	22.4 38.9	**31.5**	25.2 39.4	**27.4**	23.1 34.0
May	**22.4**	17.7 29.3	**26.8**	21.6 34.1	**28.0**	22.5 35.3	**24.2**	18.8 31.3	**28.7**	26.9 30.4	**27.9**	23.6 33.9	**28.9**	25.7 33.5	**26.3**	23.8 30.6
June	**23.5**	20.1 29.1	**26.6**	23.2 31.8	**27.1**	23.3 32.5	**23.8**	20.0 29.4	**27.9**	26.9 29.1	**26.0**	23.4 30.3	**27.1**	25.0 30.1	**25.6**	23.8 28.4
July	**23.9**	20.4 29.3	**26.1**	23.0 30.9	**26.4**	23.0 31.2	**23.2**	19.7 28.2	**27.4**	26.5 28.4	**25.6**	23.1 29.8	**26.7**	24.6 29.7	**25.1**	23.5 27.6
August	**24.3**	20.2 30.7	**26.6**	22.8 32.1	**26.1**	22.6 31.0	**23.0**	19.3 28.1	**27.2**	26.2 28.3	**25.5**	23.0 29.8	**26.4**	24.4 29.5	**25.0**	23.5 27.6
September	**23.1**	19.1 29.9	**26.1**	22.0 32.5	**25.3**	21.8 30.6	**22.5**	18.2 28.4	**27.4**	26.0 28.9	**25.7**	22.6 30.6	**26.1**	23.8 29.5	**25.2**	23.2 28.5
October	**20.1**	15.7 27.4	**23.3**	19.0 30.2	**23.0**	18.9 28.7	**20.5**	15.9 27.1	**27.4**	25.4 29.5	**25.4**	21.2 32.3	**26.4**	23.3 30.6	**25.6**	22.8 30.8
November	**16.2**	10.9 24.4	**19.5**	13.9 28.0	**18.9**	13.3 26.3	**17.0**	11.4 24.9	**25.3**	22.7 28.2	**23.5**	17.9 31.3	**25.5**	21.2 31.0	**25.9**	22.0 32.7
December	**13.0**	7.7 21.4	**16.5**	10.7 25.7	**15.8**	9.6 23.9	**14.4**	8.5 22.8	**23.0**	20.0 26.2	**20.9**	14.4 29.6	**24.1**	18.8 30.7	**25.6**	20.6 33.2
YEAR	**19.1**		**23.0**		**23.3**		**20.4**		**26.2**		**25.1**		**27.0**		**25.8**	

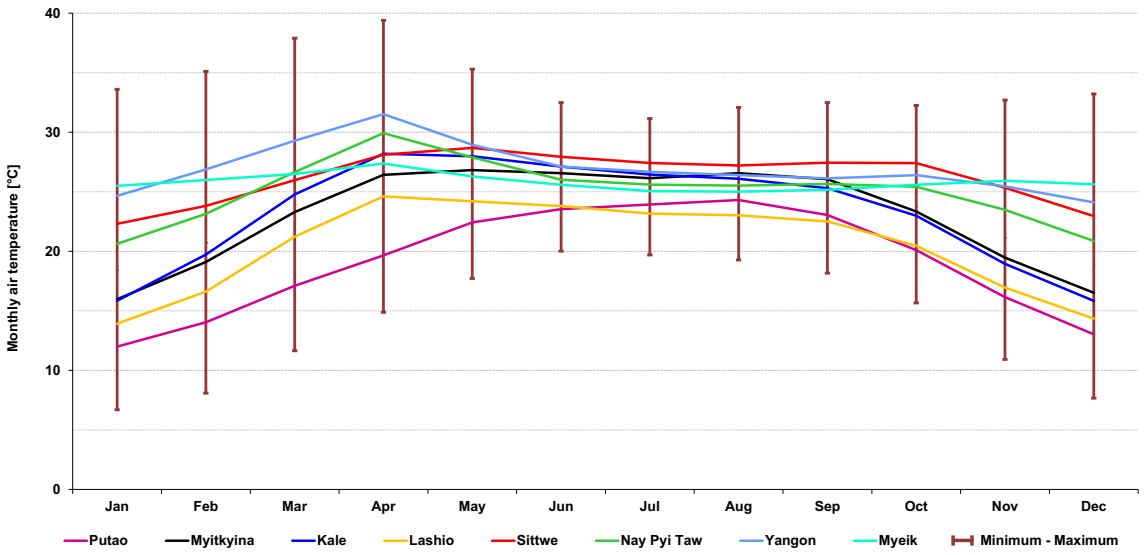

Figure 3.1: Monthly averages, minima and maxima of air-temperature at 2 m for selected sites.

Table 3.2 shows monthly characteristics of air temperature at eight selected sites; they represent statistics calculated over 24-hour diurnal cycle. Minimum and maximum air temperatures are calculated as average of minimum and maximum values of temperature during each day (assuming full diurnal cycle - 24 hours) of the given month.

Monthly averages of minimum and maximum daily values show their typical daily amplitude in each month (Figure 3.1). See Chapter 2.2 discussing the uncertainty of the air temperature model estimates.

3.3 Global Horizontal Irradiation

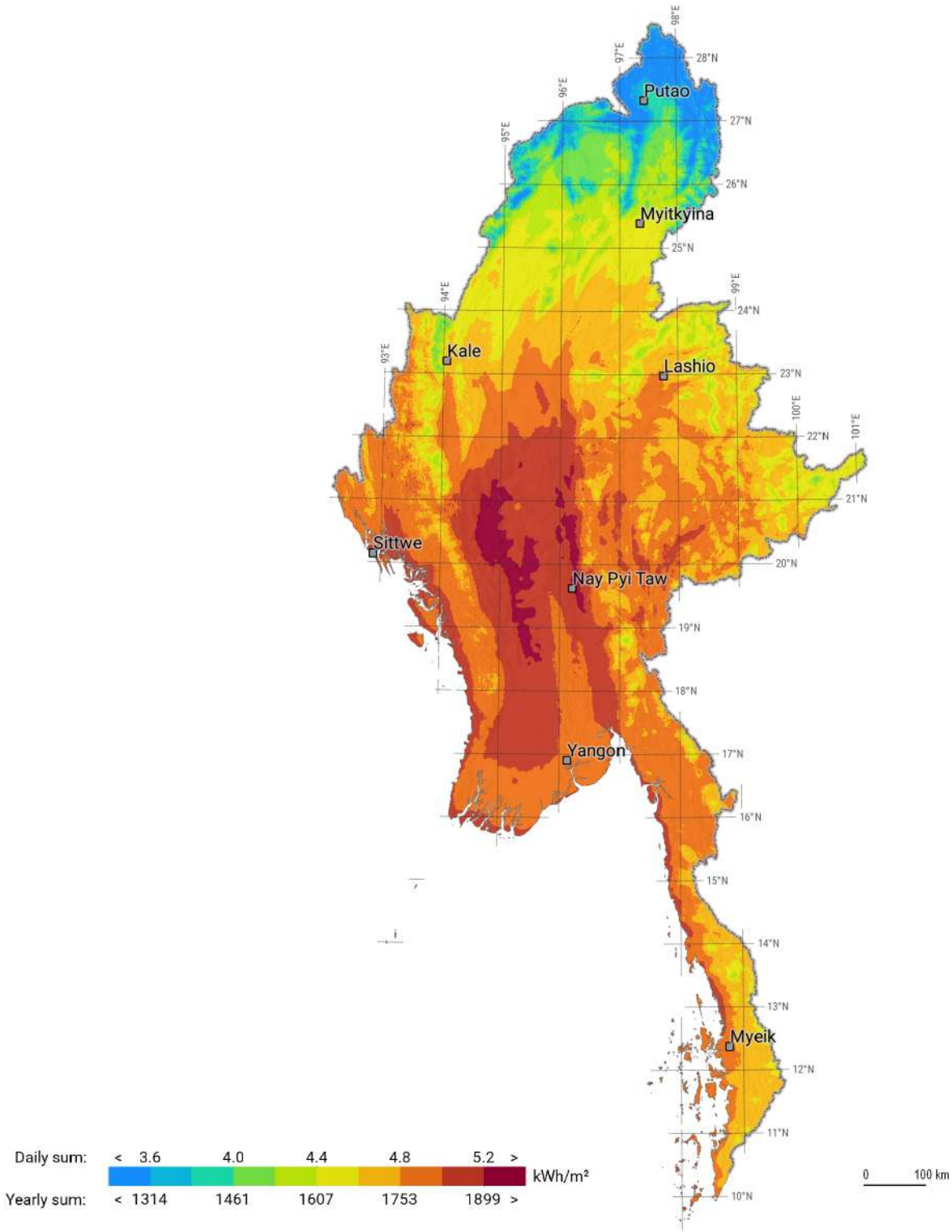

Map 3.10: Global Horizontal Irradiation – long term average of daily and yearly totals.
Source: Solargis

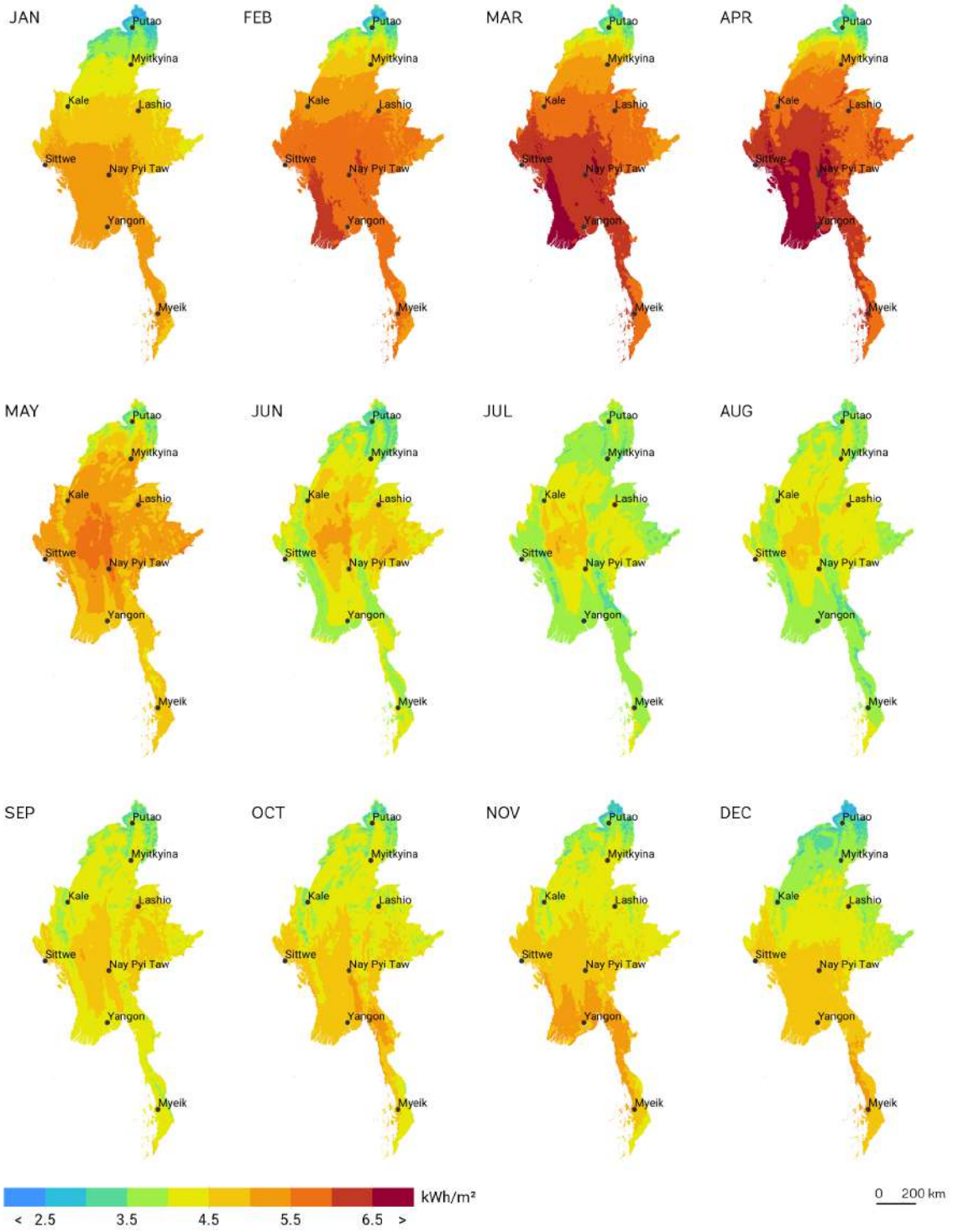

Map 3.11: Global Horizontal Irradiation – long-term monthly averages of daily totals.
Source: Solargis

Global Horizontal Irradiation (GHI) is used as a reference value for comparing geographical conditions related to PV electricity systems, as it eliminates the possible variations, given by the choice of components and the PV system design. The highest GHI is identified in the central, lowland area of the country, where average daily totals reach yearly total of 1900 kWh/m^2 (average daily total up to 5.2 kWh/m^2) or higher (Map 3.10). Further north, GHI values falls between 1400 and 1600 kWh/m^2 (average daily total from 3.8 kWh/m^2 up to 4.4 kWh/m^2).

Minimum GHI values in northernmost part of the country are lower than 1300 kWh/m^2 (average daily total approx. 3.6 kWh/m^2), yet the solar resource in these areas is still sufficiently high.

Table 3.3: Daily averages and average minima and maxima of Global Horizontal Irradiation at 8 sites

Month	Global Horizontal Irradiation [kWh/m^2]																Variability between sites [%]
	Putao		Myitkyina		Kale		Lashio		Sittwe		Nay Pyi Taw		Yangon		Myeik		
	Average	Min Max	Average	Min Max	Average	Min Max	Average	Min Max	Average	Min Max	Average	Min Max	Average	Min Max	Average	Min Max	
January	**3.47**	2.79 4.29	**4.25**	3.75 4.71	**4.53**	4.17 4.91	**4.72**	4.23 5.13	**5.06**	4.63 5.34	**5.18**	4.68 5.52	**5.16**	4.84 5.47	**5.22**	4.56 5.74	**12.9**
February	**3.84**	2.62 4.96	**4.91**	4.32 5.41	**5.33**	4.65 5.82	**5.52**	4.80 6.09	**5.79**	5.46 6.17	**5.90**	5.48 6.35	**5.94**	5.49 6.25	**5.71**	5.26 6.19	**13.1**
March	**3.91**	2.40 4.74	**5.08**	4.18 5.97	**5.56**	4.69 6.16	**5.69**	5.03 6.32	**6.33**	5.71 6.78	**6.28**	5.80 6.78	**6.41**	5.48 6.99	**6.06**	4.83 6.77	**14.9**
April	**3.64**	2.88 4.93	**5.43**	4.57 6.07	**5.77**	4.88 6.33	**5.74**	5.07 6.22	**6.66**	6.29 7.08	**6.44**	5.53 7.18	**6.52**	5.39 7.34	**6.22**	4.78 6.94	**16.8**
May	**4.10**	3.39 5.18	**5.10**	4.25 6.03	**5.26**	4.15 6.08	**5.17**	4.42 6.01	**5.49**	4.27 6.40	**5.67**	5.03 6.25	**4.76**	4.10 5.53	**4.68**	3.90 5.90	**10.0**
June	**3.64**	3.03 4.60	**4.19**	3.57 4.73	**4.65**	4.00 5.49	**4.82**	4.33 5.61	**4.05**	3.01 5.08	**4.82**	4.15 5.36	**4.00**	3.69 4.61	**4.02**	3.36 4.95	**10.3**
July	**3.72**	3.09 4.55	**3.87**	3.28 4.60	**4.47**	3.51 5.01	**4.33**	3.68 5.04	**3.86**	3.17 4.62	**4.42**	3.83 5.25	**3.83**	3.34 4.44	**3.95**	3.30 4.54	**7.4**
August	**3.86**	3.10 4.96	**4.23**	3.72 5.13	**4.33**	3.87 5.05	**4.50**	4.02 4.99	**4.19**	3.25 5.00	**4.38**	3.86 4.86	**3.81**	3.21 4.22	**3.86**	3.02 4.64	**6.5**
September	**3.96**	3.10 4.86	**4.37**	3.71 4.86	**4.37**	3.94 4.89	**4.55**	3.72 5.14	**4.68**	3.90 5.14	**4.88**	4.46 5.36	**4.20**	3.82 4.60	**4.27**	3.48 5.11	**6.6**
October	**4.08**	3.44 4.93	**4.34**	3.76 4.70	**4.41**	3.94 4.96	**4.34**	3.35 5.17	**4.89**	4.14 5.57	**5.00**	4.35 5.64	**4.44**	4.00 4.97	**4.71**	4.25 5.53	**6.9**
November	**3.86**	3.25 4.48	**4.36**	3.85 4.95	**4.33**	3.56 5.04	**4.42**	3.67 5.19	**4.92**	4.08 5.47	**4.92**	3.99 5.68	**4.91**	4.23 5.62	**4.95**	4.49 5.49	**8.8**
December	**3.44**	3.10 3.92	**3.96**	3.43 4.35	**3.99**	3.42 4.38	**4.12**	3.47 4.60	**4.59**	3.97 4.92	**4.75**	3.97 5.21	**4.88**	4.35 5.26	**4.98**	4.26 5.46	**12.5**
YEAR	**3.79**	**3.61** **4.04**	**4.50**	**4.36** **4.69**	**4.75**	**4.62** **5.06**	**4.82**	**4.67** **5.09**	**5.04**	**4.92** **5.30**	**5.21**	**4.99** **5.48**	**4.90**	**4.69** **5.11**	**4.88**	**4.70** **5.18**	**9.2**

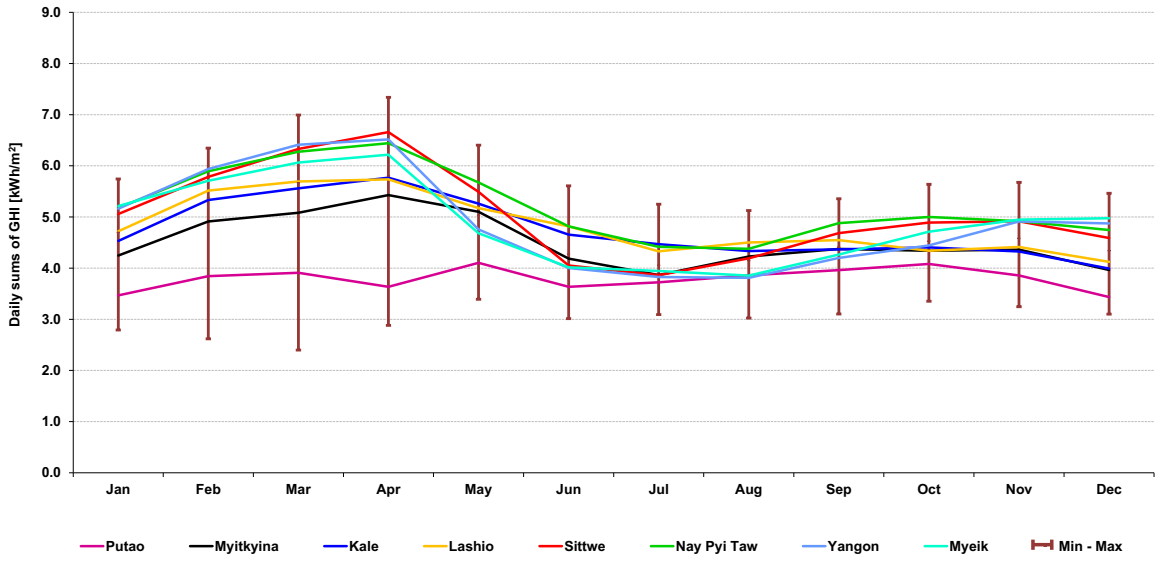

Figure 3.2: Long-term monthly averages, minima and maxima of Global Horizontal Irradiation.

Table 3.3 shows long-term average, and average minima and maxima of daily totals of Global Horizontal Irradiation (GHI) for a period 1999 to 2015 for eight selected sites.

Figure 3.2 compares monthly averages of daily values of Global horizontal irradiation (GHI). Most stable weather, but with lower GHI values is from June to December. Highest GHI daily sums (but also with higher variability) are seen during dry period from February to May. Similar pattern of GHI for almost all representative sites (except Putao) indicates that all sites will experience similar performance of PV power systems, with

variability between sites, given by local microclimate. Putao site is the least influenced by the dry and monsoon season, probably due to its position in northern mountains in comparison to other sites.

Weather changes in cycles and has also stochastic nature. Therefore, annual solar radiation in each year can deviate from the longterm average in the range of few percent. Figure 3.3 shows interannual variability, i.e. the magnitude of the year-by-year GHI change.

The interannual variability is calculated from the unbiased standard deviation of GHI over 17 years, considering a simplified assumption of normal distribution of the annual sums. Almost all sites (except Putao and Myeik) show similar varying patterns of GHI over the recorded period. Also, the extremes for those sites (minimum and maximum) or values close to the extremes are reached almost in the same years. Putao and Myeik sites show slightly different characteristics. The most stable GHI (the smallest interannual variability) is observed in Sittwe, Kale, Yangon and Nay Pyi Taw. The sites with highest interannual variability are Putao and Myeik.

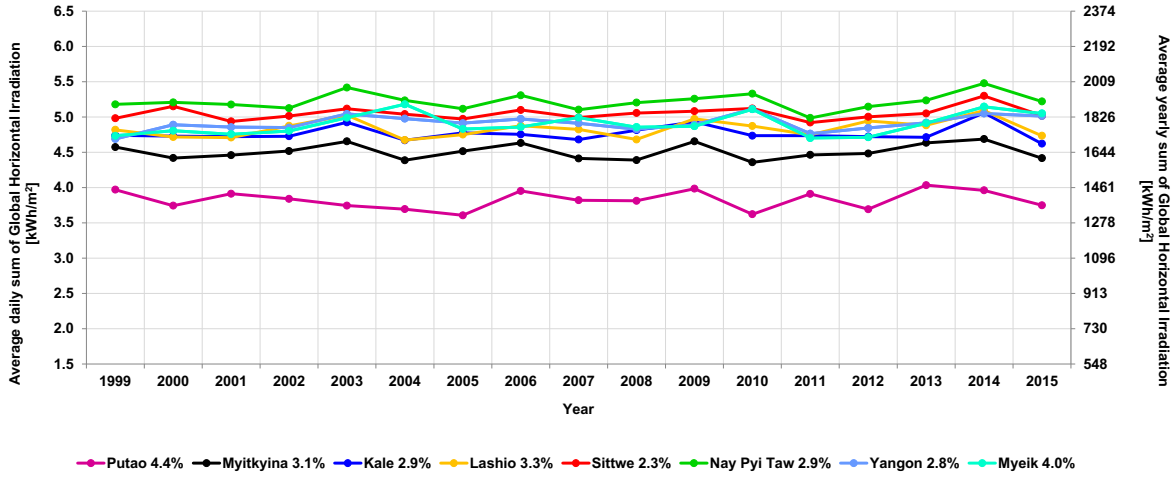

Figure 3.3: Interannual variability of Global Horizontal Irradiation for selected sites.

Map 3.12 delineates ratio of diffuse to global horizontal irradiation. This ratio is important for the performance of PV systems.

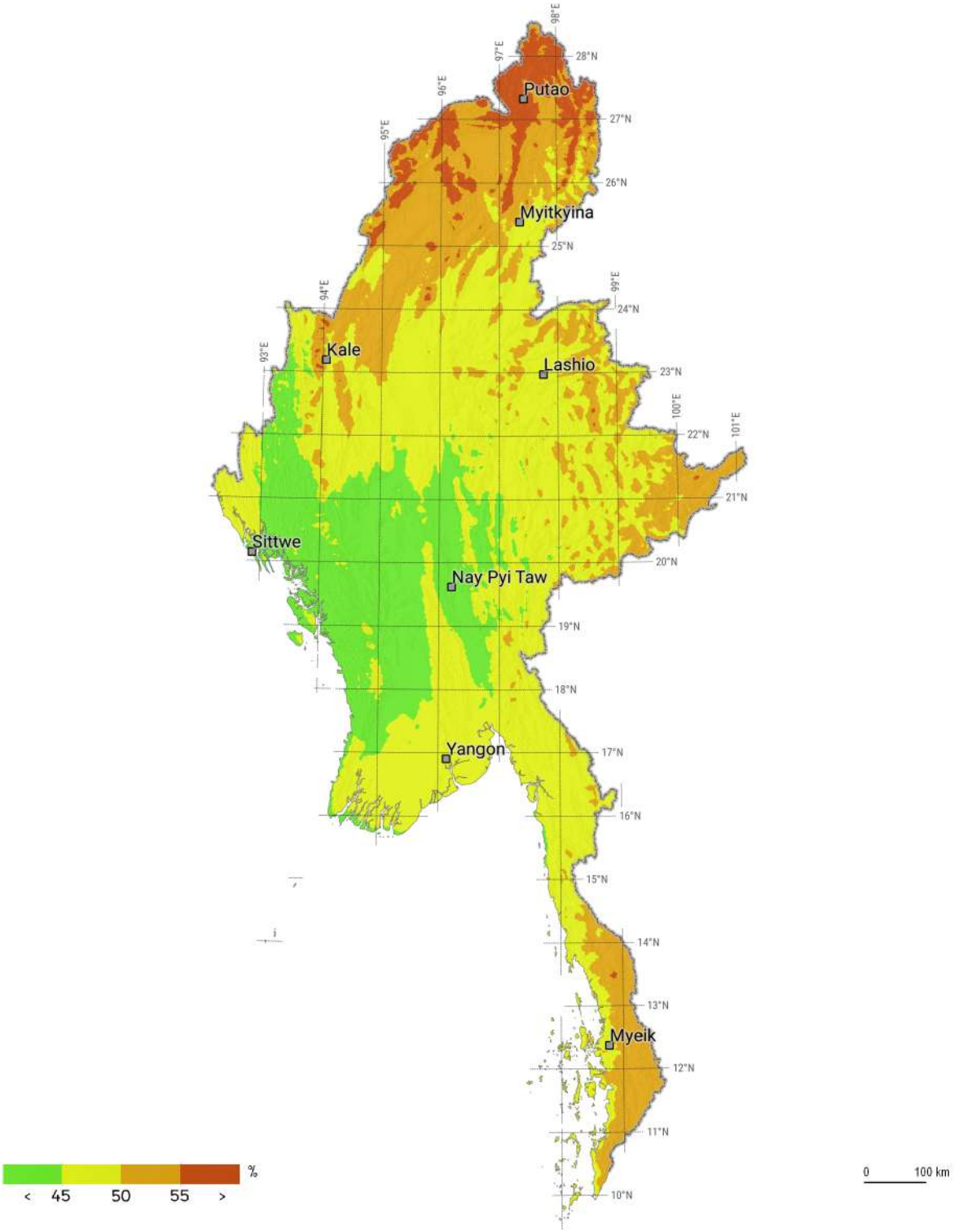

Map 3.12: Long-term average for ratio of diffuse and global irradiation (DIF/GHI).
Source: Solargis

3.4 Direct Normal Irradiation

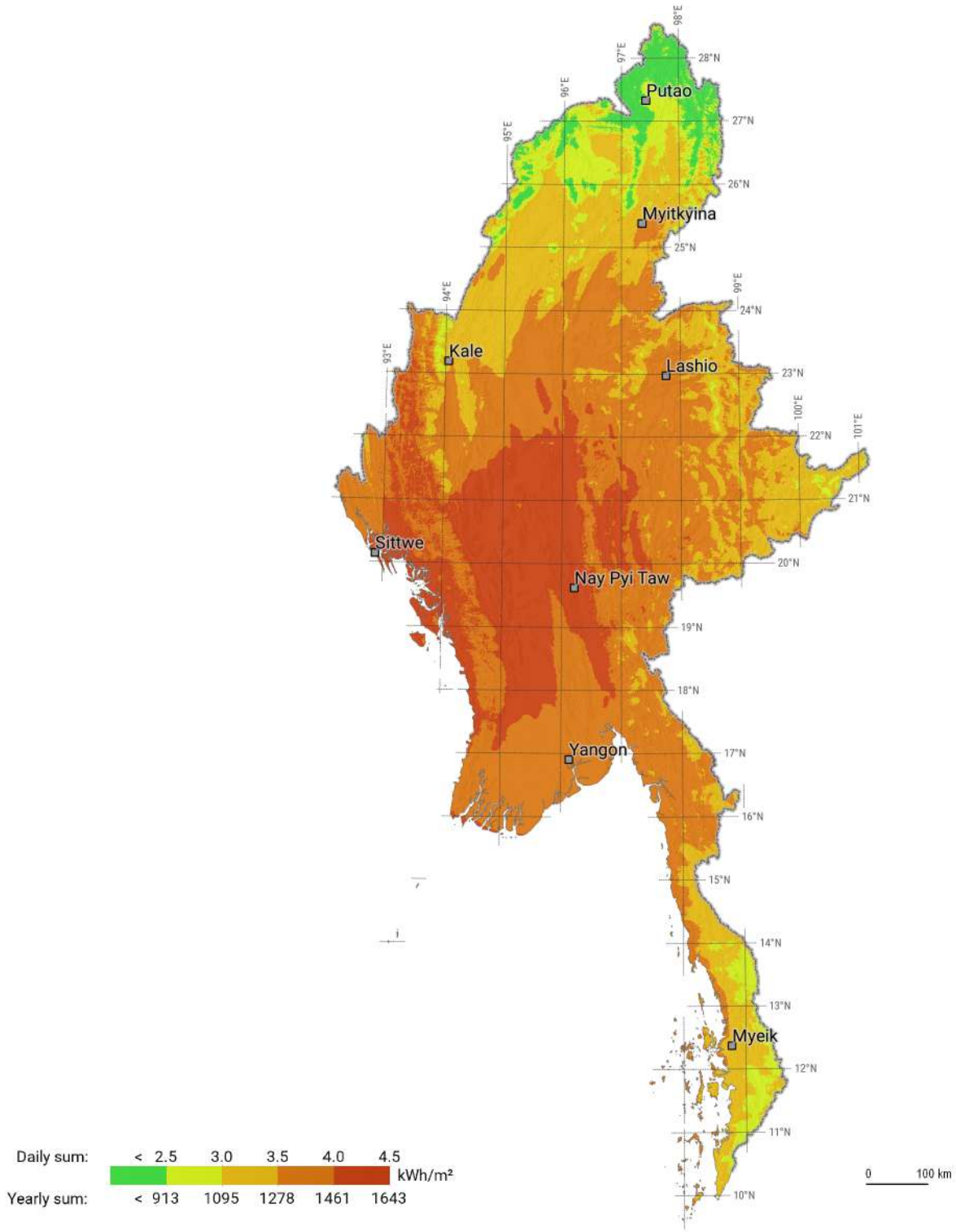

Map 3.13: Direct Normal Irradiation - longterm average of daily and yearly totals.
Source: Solargis

Direct Normal Irradiation (DNI) is one of the primary solar resource parameters, needed for computation of Global Tilted Irradiation (GTI, Chapter 3.5).

Table 3.4 and Figure 3.4 show long-term average daily totals and average daily minimum and maximum of DNI for eight selected sites, assuming a period 1999 to 2015. The highest DNI is found in the Nay Pyi Taw and Sittwe sites, the lowest in Putao.

Table 3.4: Daily averages and average minima and maxima of Direct Normal Irradiation at 8 sites

Month	Direct Normal Irradiation [kWh/m²]																Variability between sites [%]
	Putao		Myitkyina		Kale		Lashio		Sittwe		Nay Pyi Taw		Yangon		Myeik		
	Average	Min Max	Average	Min Max	Average	Min Max	Average	Min Max	Average	Min Max	Average	Min Max	Average	Min Max	Average	Min Max	
January	**3.79**	2.15 5.85	**5.35**	3.97 6.88	**5.42**	4.14 6.69	**6.21**	4.99 7.42	**5.98**	4.70 7.40	**6.68**	5.68 7.98	**5.66**	4.58 6.71	**4.60**	3.58 5.72	**16.8**
February	**3.29**	1.71 5.33	**5.08**	4.02 6.34	**5.63**	4.43 6.43	**6.23**	5.04 7.17	**6.05**	5.05 7.03	**6.43**	4.54 7.61	**5.95**	4.34 6.99	**4.58**	3.36 5.83	**19.5**
March	**2.12**	0.76 3.24	**3.42**	2.42 5.17	**3.92**	3.03 5.08	**4.12**	3.24 5.10	**5.24**	3.95 6.17	**5.05**	4.00 6.62	**5.35**	4.08 6.63	**4.51**	2.63 6.07	**25.7**
April	**1.58**	0.99 2.72	**3.12**	2.32 3.85	**3.60**	2.68 4.49	**3.45**	2.72 4.23	**4.86**	4.26 5.67	**4.56**	3.50 5.71	**5.06**	3.67 6.51	**4.74**	2.96 6.31	**30.4**
May	**1.67**	0.94 2.66	**2.75**	1.79 3.65	**2.90**	1.70 3.69	**2.80**	1.99 3.93	**3.30**	1.98 4.20	**3.54**	2.66 4.22	**2.55**	1.52 3.89	**2.81**	1.61 4.65	**19.8**
June	**1.16**	0.57 2.55	**1.80**	1.16 2.91	**2.08**	1.57 2.80	**2.22**	1.69 3.31	**1.85**	0.92 3.44	**2.42**	1.42 3.11	**1.58**	1.09 2.56	**1.91**	1.21 3.07	**20.7**
July	**1.27**	0.76 2.18	**1.47**	0.94 2.21	**1.95**	1.28 2.75	**1.86**	1.33 2.64	**1.64**	0.87 2.58	**1.97**	1.28 3.06	**1.37**	0.99 2.15	**1.79**	1.02 2.48	**16.2**
August	**1.55**	0.88 2.76	**1.92**	1.30 2.84	**1.97**	1.53 2.78	**2.07**	1.57 2.71	**2.00**	1.07 2.93	**2.01**	1.27 2.61	**1.44**	0.96 1.83	**1.66**	0.94 2.44	**13.2**
September	**2.18**	1.35 3.61	**2.73**	2.02 3.57	**2.44**	1.89 3.08	**2.63**	1.91 3.55	**3.00**	1.79 3.53	**2.86**	2.36 3.48	**2.08**	1.60 2.61	**2.25**	1.30 3.34	**13.4**
October	**3.58**	2.36 5.18	**3.97**	2.90 4.89	**3.60**	2.78 4.86	**3.41**	1.92 5.20	**4.33**	3.02 5.54	**4.06**	2.94 5.38	**2.85**	2.32 3.58	**2.96**	2.22 4.12	**14.4**
November	**4.46**	2.78 6.07	**5.52**	3.98 7.30	**4.76**	3.33 6.61	**5.04**	3.70 7.45	**5.67**	4.06 7.33	**5.74**	3.41 8.22	**4.93**	3.27 6.97	**4.03**	2.84 5.20	**12.1**
December	**4.17**	3.16 5.53	**5.29**	3.67 6.56	**4.57**	3.25 5.62	**5.13**	3.54 6.33	**5.47**	4.53 6.19	**6.13**	4.93 7.85	**5.42**	4.64 6.63	**4.53**	3.28 5.53	**12.5**
YEAR	**2.57**	**2.34** **2.98**	**3.53**	**3.23** **3.99**	**3.56**	**3.43** **4.11**	**3.75**	**3.51** **4.26**	**4.10**	**3.83** **4.50**	**4.28**	**3.96** **4.83**	**3.67**	**3.43** **4.09**	**3.36**	**3.00** **3.79**	**14.4**

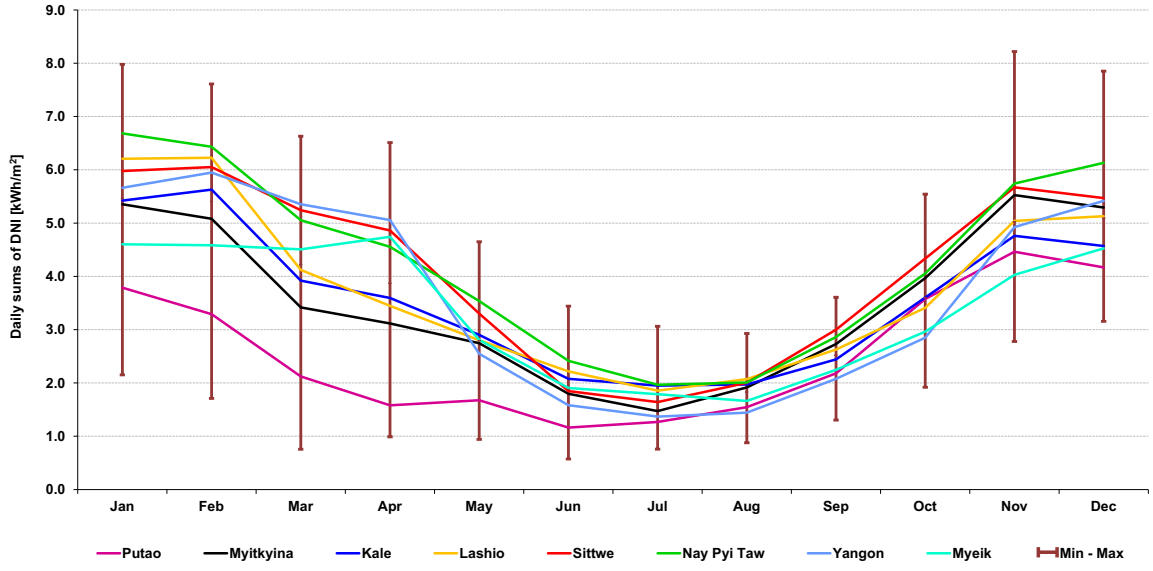

Figure 3.4: Daily averages of Direct Normal Irradiation at selected sites.

In all sites, DNI shows similar pattern with maximum in dry season from November to April. Minimum DNI values are observed during monsoon season in May to September, where DNI is lower by about 40% to 70%. During this season also the lowest variability (given by minimum and maximum range of values) occurs, probably due to

constant and high occurrence of clouds and aerosols (fog, smoke). The highest variability is recorded for a season from November to April.

The highest values are found in Magwe and Bago regions. Generally, central part of the country has higher DNI potential; lower values in the south and north are influenced by higher presence of aerosols and clouds in the atmosphere.

Interannual variability of DNI for selected sites (Figure 3.5) is calculated from the unbiased standard deviation of yearly DNI over 17 years and it is based on a simplified assumption of normal distribution of the yearly sums. Every site has its own variability pattern, only few events were so strong that influenced almost all sites (except Putao), for example high values in years 2003 or 2014. The most stable DNI (the smallest interannual variability) is observed in Sittwe and Yangon, the most unstable DNI is recorded at Myeik and the lowest DNI in Putao.

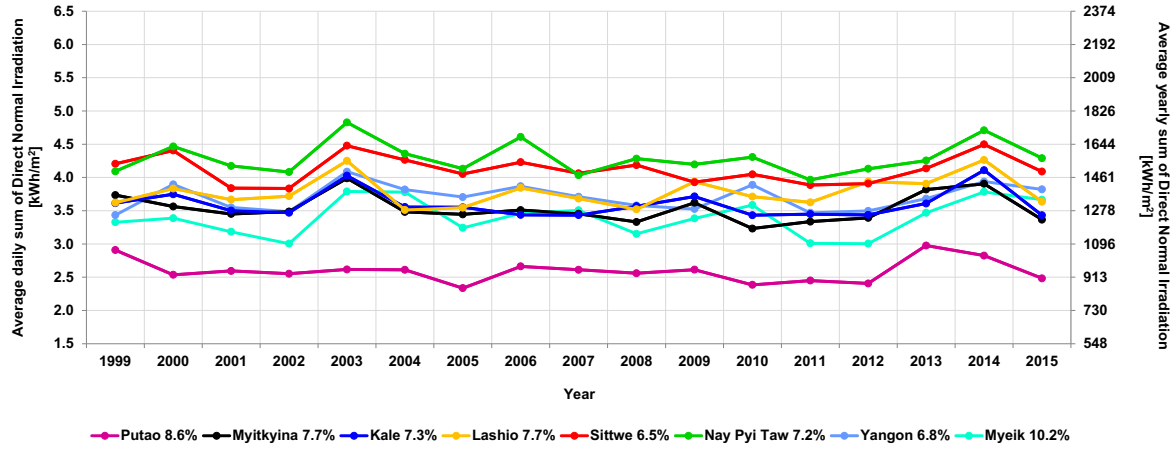

Figure 3.5: Interannual variability of Direct Normal Irradiation at representative sites

Daily totals in any single year can be displayed for a better visual presentation of DNI in relation to GHI. Figure 3.6 shows daily totals for year 2015 in Nay Pyi Taw. Blue pattern, representing GHI sums is transparent to make visible lower values of DNI pattern (yellow).

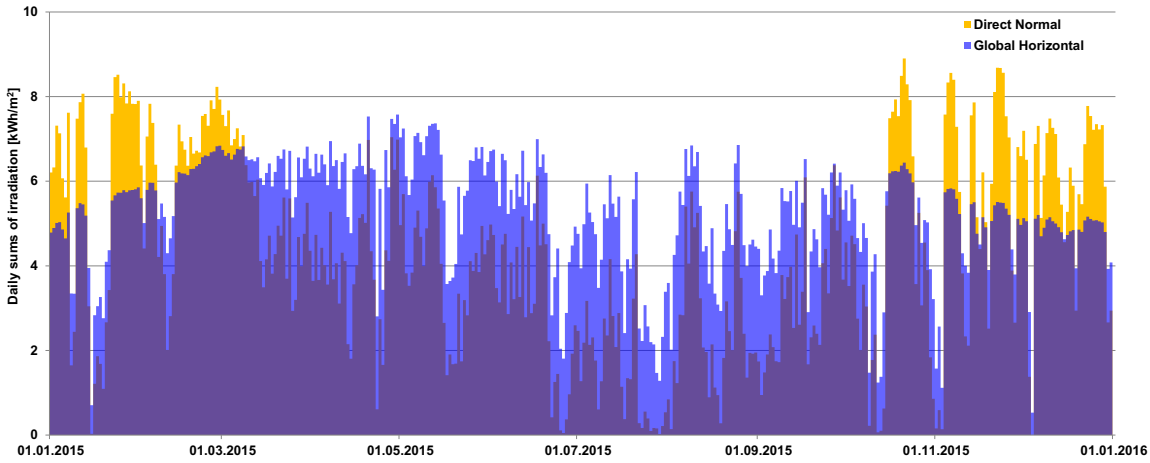

Figure 3.6: Daily totals of GHI and DNI in Nay Pyi Taw, year 2015

Source: Solargis

3.5 Global Tilted Irradiation

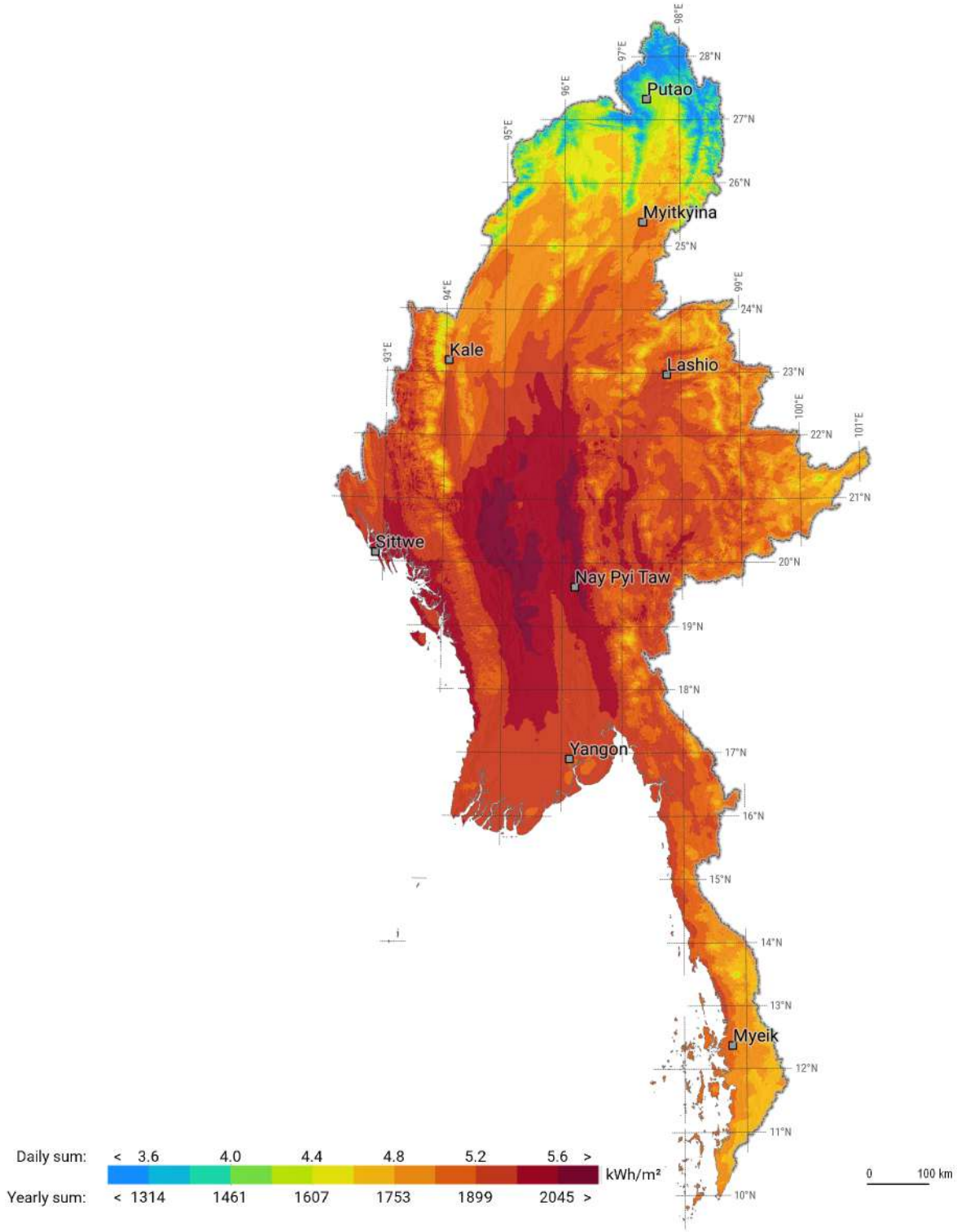

Map 3.14: Global Tilted Irradiation at optimum angle – longterm average of daily and yearly totals.
Source: Solargis

Global Tilted Irradiation (GTI) is the key source of energy for flat-plate photovoltaic (PV) technologies (Chapter 3.6). The regional trend of GTI received by PV modules tilted at optimum angle (GTI) is similar to DNI (Map 3.14). PV modules tilted at optimum inclination show increase of average yearly GTI totals to about 1900 kWh/m^2 (daily totals about 5.2 kWh/m^2) and more, especially in the central territories with lowlands.

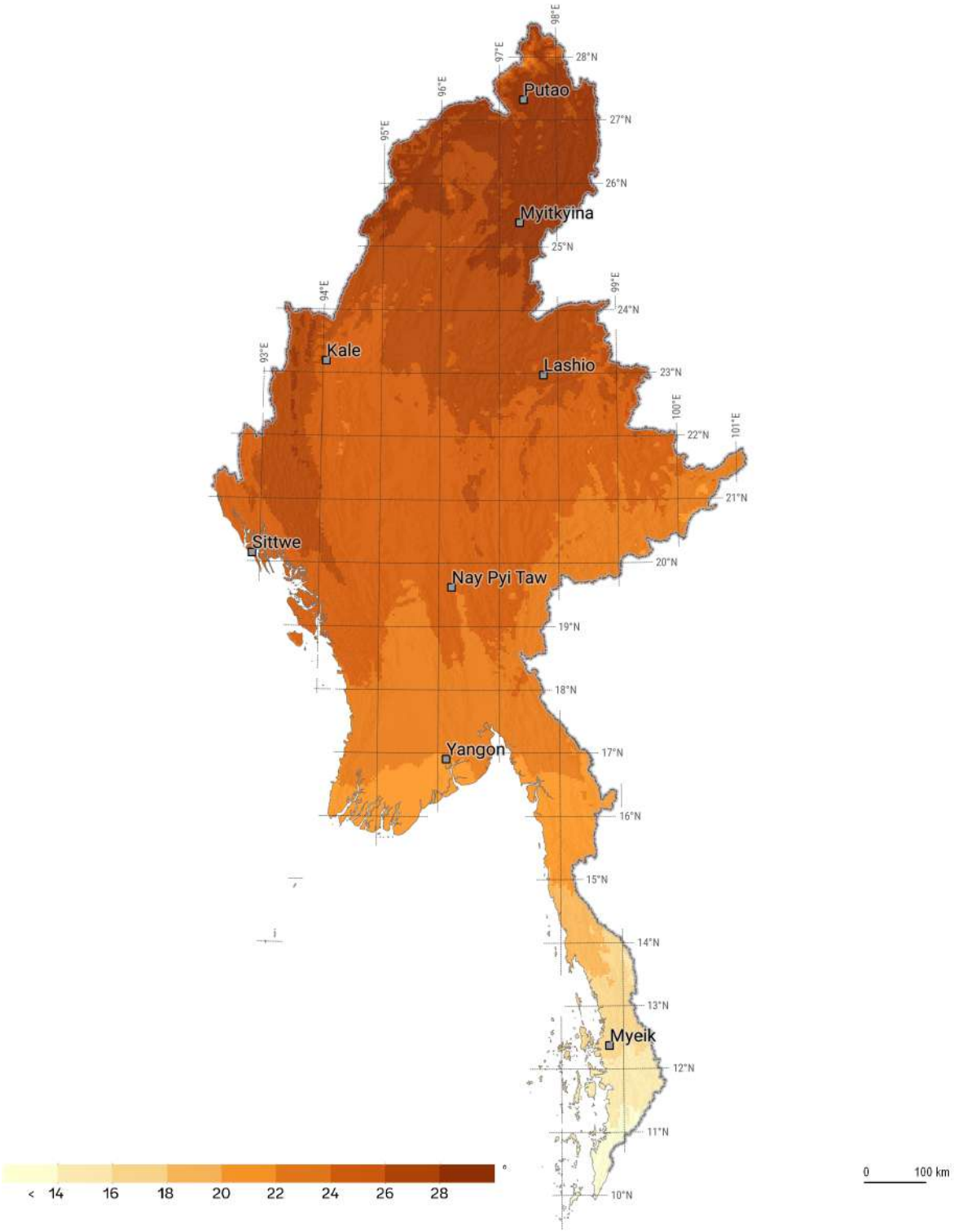

Map 3.15: Optimum tilt of PV modules to maximize yearly PV power production.
Source: Solargis

The main parameter influencing optimum tilt in Myanmar is latitude, which spans between 10° and 29° North (Map 3.15). For this region, optimum tilt is southwards between 12° and 30° (increasing from South to North). The optimum tilt is determined also by ratio between diffuse and global horizontal irradiation, which reduces the effect of latitude in the North and augments it in the central area.

Table 3.5 shows long-term averages of daily total of Global Tilted Irradiation (GTI) for selected sites. It is assumed that solar radiation is received by PV modules surface inclined at the optimum tilt.

Table 3.5: Daily averages and average minima and maxima of Global Tilted Irradiation at 8 sites

Month	Global Tilted Irradiation [kWh/m^2]																Variability between sites [%]
	Putao		Myitkyina		Kale		Lashio		Sittwe		Nay Pyi Taw		Yangon		Myeik		
	Average	Min Max	Average	Min Max	Average	Min Max	Average	Min Max	Average	Min Max	Average	Min Max	Average	Min Max	Average	Min Max	
January	**4.70**	3.53 6.15	**5.87**	5.05 6.72	**6.00**	5.36 6.66	**6.39**	5.57 7.07	**6.53**	5.82 7.07	**6.75**	6.01 7.32	**6.35**	5.90 6.79	**5.97**	5.15 6.66	**12.2**
February	**4.70**	3.05 6.35	**6.13**	5.24 6.89	**6.52**	5.51 7.12	**6.82**	5.77 7.56	**6.91**	6.42 7.39	**7.05**	6.36 7.61	**6.86**	6.21 7.26	**6.25**	5.69 6.80	**13.8**
March	**4.20**	2.45 5.18	**5.53**	4.49 6.65	**6.02**	5.01 6.75	**6.15**	5.41 6.91	**6.81**	6.12 7.34	**6.72**	6.23 7.34	**6.78**	5.76 7.44	**6.26**	4.96 7.00	**16.2**
April	**3.57**	2.80 4.87	**5.38**	4.45 6.03	**5.72**	4.77 6.28	**5.65**	4.98 6.13	**6.54**	6.13 6.94	**6.31**	5.45 7.02	**6.35**	5.26 7.14	**6.05**	4.67 6.75	**19.0**
May	**3.80**	3.13 4.81	**4.71**	3.92 5.58	**4.89**	3.86 5.64	**4.75**	4.07 5.50	**5.04**	3.95 5.87	**5.20**	4.63 5.72	**4.39**	3.80 5.09	**4.37**	3.66 5.48	**10.4**
June	**3.28**	2.73 4.10	**3.75**	3.21 4.18	**4.22**	3.62 4.96	**4.32**	3.87 5.01	**3.65**	2.73 4.50	**4.32**	3.77 4.79	**3.64**	3.38 4.15	**3.70**	3.12 4.52	**10.9**
July	**3.40**	2.81 4.16	**3.52**	2.98 4.18	**4.10**	3.22 4.56	**3.93**	3.34 4.57	**3.52**	2.91 4.17	**4.03**	3.49 4.74	**3.52**	3.10 4.05	**3.67**	3.10 4.20	**8.1**
August	**3.69**	2.93 4.78	**4.04**	3.54 4.93	**4.16**	3.70 4.83	**4.28**	3.82 4.77	**3.98**	3.07 4.76	**4.16**	3.69 4.62	**3.62**	3.07 4.04	**3.69**	2.91 4.46	**5.1**
September	**4.12**	3.16 5.15	**4.56**	3.82 5.10	**4.51**	4.06 5.06	**4.68**	3.82 5.34	**4.80**	3.94 5.28	**4.99**	4.55 5.50	**4.23**	3.83 4.65	**4.27**	3.46 5.16	**6.5**
October	**4.82**	3.92 5.99	**5.10**	4.32 5.66	**5.04**	4.42 5.76	**4.93**	3.66 6.10	**5.55**	4.60 6.39	**5.62**	4.80 6.44	**4.81**	4.30 5.42	**4.98**	4.47 5.90	**6.4**
November	**5.18**	4.08 6.27	**5.89**	5.07 6.89	**5.53**	4.41 6.64	**5.69**	4.59 6.96	**6.19**	4.98 7.05	**6.18**	4.78 7.36	**5.88**	4.90 6.88	**5.55**	4.95 6.24	**6.8**
December	**4.85**	4.27 5.79	**5.65**	4.65 6.39	**5.32**	4.40 5.97	**5.61**	4.60 6.41	**6.03**	5.18 6.54	**6.30**	5.19 7.10	**6.10**	5.40 6.72	**5.77**	4.85 6.40	**9.1**
YEAR	**4.19**	**3.95** **4.49**	**5.00**	**4.85** **5.25**	**5.16**	**5.00** **5.52**	**5.26**	**5.11** **5.59**	**5.45**	**5.30** **5.74**	**5.63**	**5.39** **5.93**	**5.20**	**4.99** **5.40**	**5.04**	**4.86** **5.37**	**9.8**

Figure 3.7 compares long-term daily averages in selected sites. High GTI, is seen from October to May, and it has higher variability. Lower and stable values of GTI are observed during the monsoon season for all sites. Highest gains are expected from January to April. Variability of GTI between sites is similar through the whole year, except for Putao site. This may relate to a different climate of this site compared to other sites.

Surface inclined at optimum tilt receives more yearly global irradiation compared to the horizontal surface (Figure 3.8). Gains are site-dependent and are pronounced in dry season. The highest gain is recorded in December for all sites: in the range from approximately 16% in Myeik up to 42% in Myitkyina. On the other side, in the monsoon season, with highest sun position, the horizontal surface receives more global irradiation (about 8% to 10%) compared to the optimally tilted surface. This is seen for a period from April to August. As the energy gain in the other months is higher, the overall yearly gains of global irradiation for optimally tilted surface remains higher compared to the horizontal surface.

Detailed comparison of daily GTI and GHI values for Nay Pyi Taw is shown in Table 3.6 and Figure 3.9.

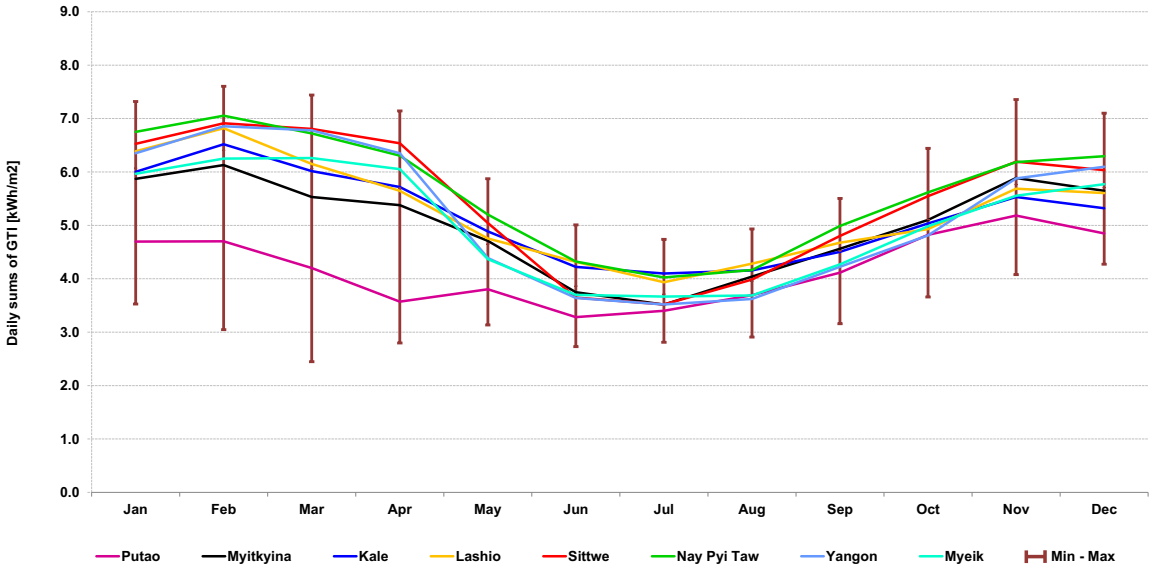

Figure 3.7: Global Tilted Irradiation – long term daily averages, minima and maxima.

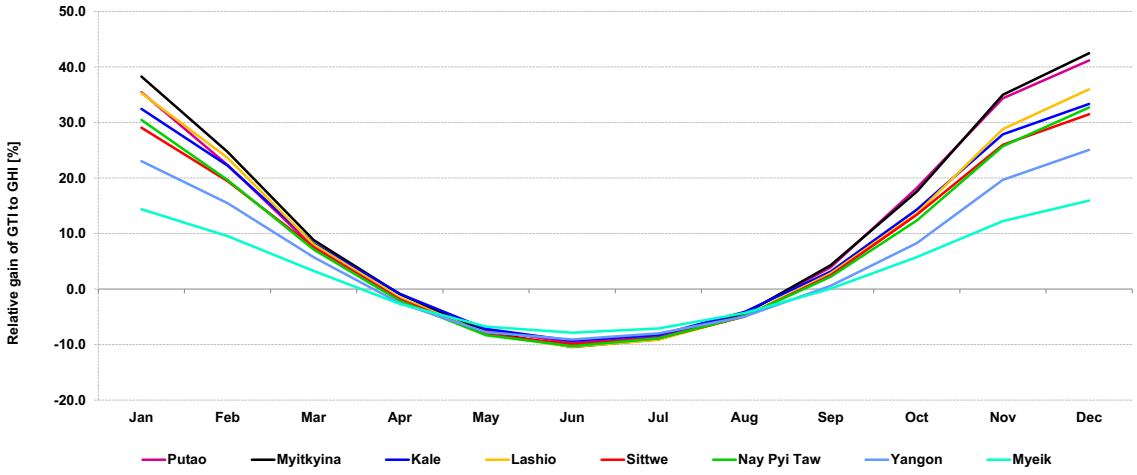

Figure 3.8: Monthly relative gain of GTI relative to GHI at selected sites.

Table 3.6: Relative gain of daily GTI to GHI in Nay Pyi Taw

Nay Pyi Taw	Average daily sum of irradiation [kWh/m^2]												Year
	Jan	Feb	Mar	Apr	May	Jun	Jul	Aug	Sep	Oct	Nov	Dec	
Global Horizontal	5.18	5.90	6.28	6.44	5.67	4.82	4.42	4.38	4.88	5.00	4.92	4.75	5.21
Global Tilted	6.75	7.05	6.72	6.31	5.20	4.32	4.03	4.16	4.99	5.62	6.18	6.30	5.63
Global Tilted vs. Horizontal [%]	**30**	**20**	**7**	**-2**	**-8**	**-10**	**-9**	**-5**	**2**	**12**	**26**	**33**	**8**

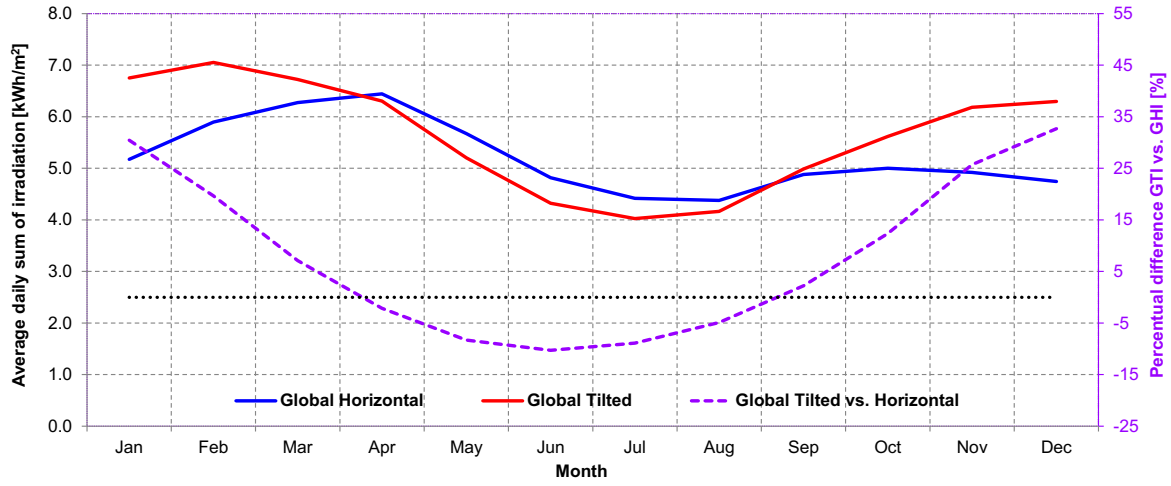

Figure 3.9: GHI and GTI monthly averages and relative gain of GTI to GHI in Nay Pyi Taw

For better visual presentation of gain for tilted surfaces in comparison to horizontal ones, daily totals in Nay Pyi Taw for year 2015 are shown in Figure 3.10. Blue pattern, representing GHI totals, is transparent to make visible lower values of red, GTI pattern, during monsoon season. The GTI gains in dry season are clearly visible in comparison with monsoon season, what shows benefits of tilted installations.

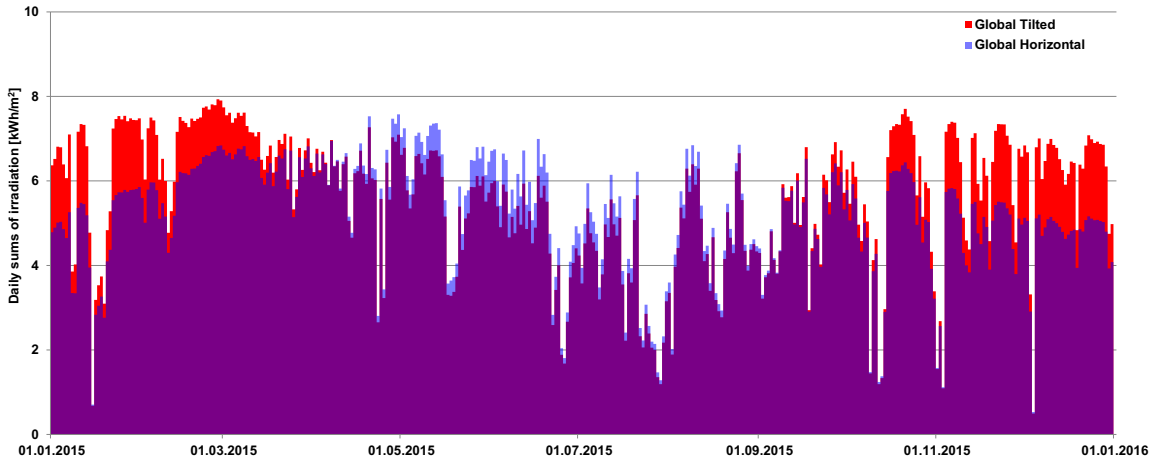

Figure 3.10: Daily values of GHI and GTI for Nay Pyi Taw, year 2015

3.6 Photovoltaic power potential

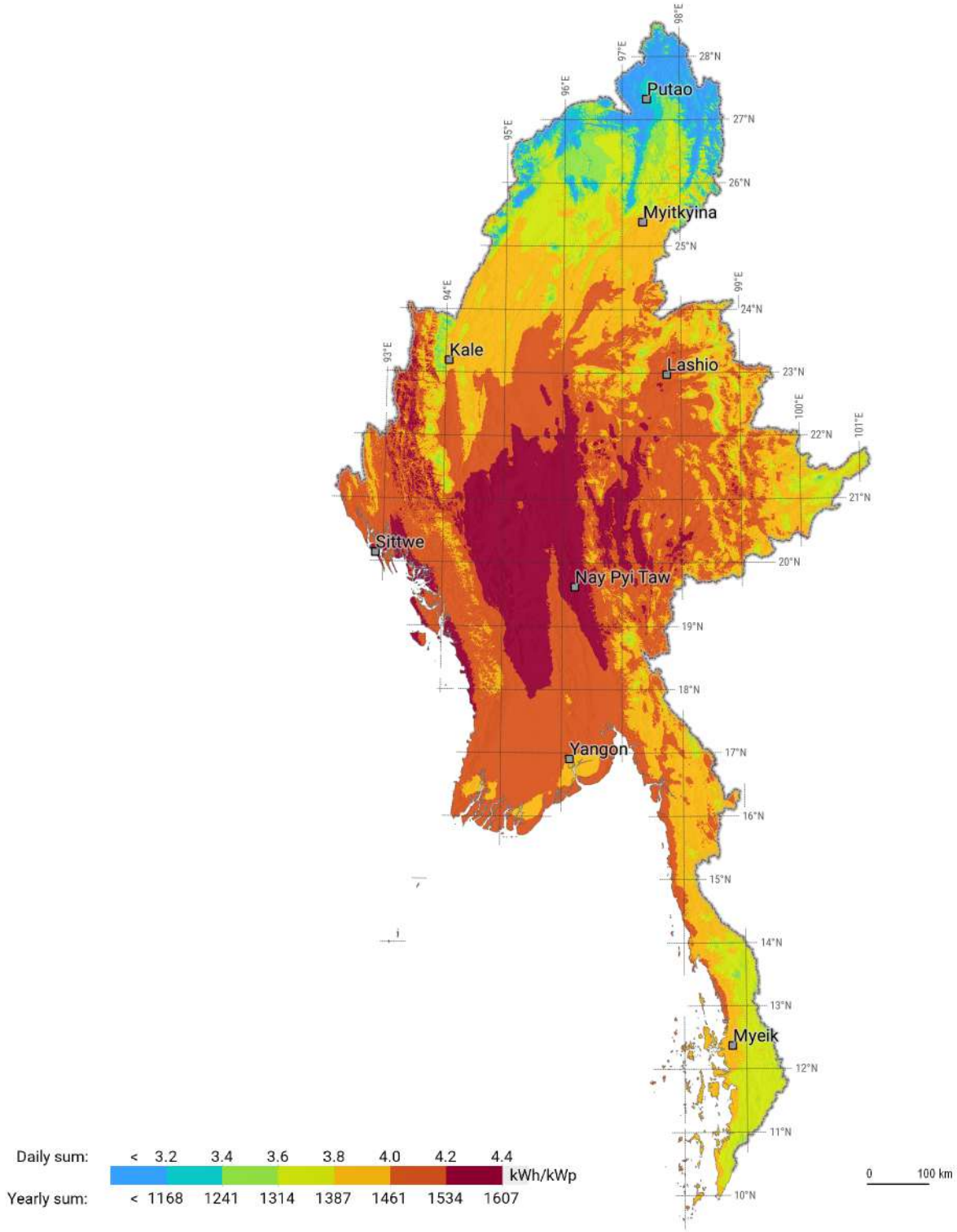

Map 3.16: PV electricity output from n open space fixed-mounted PV system with PV modules mounted at an optimum tilt and a nominal peak power of 1 kWp. Longterm averages of daily and yearly totals.

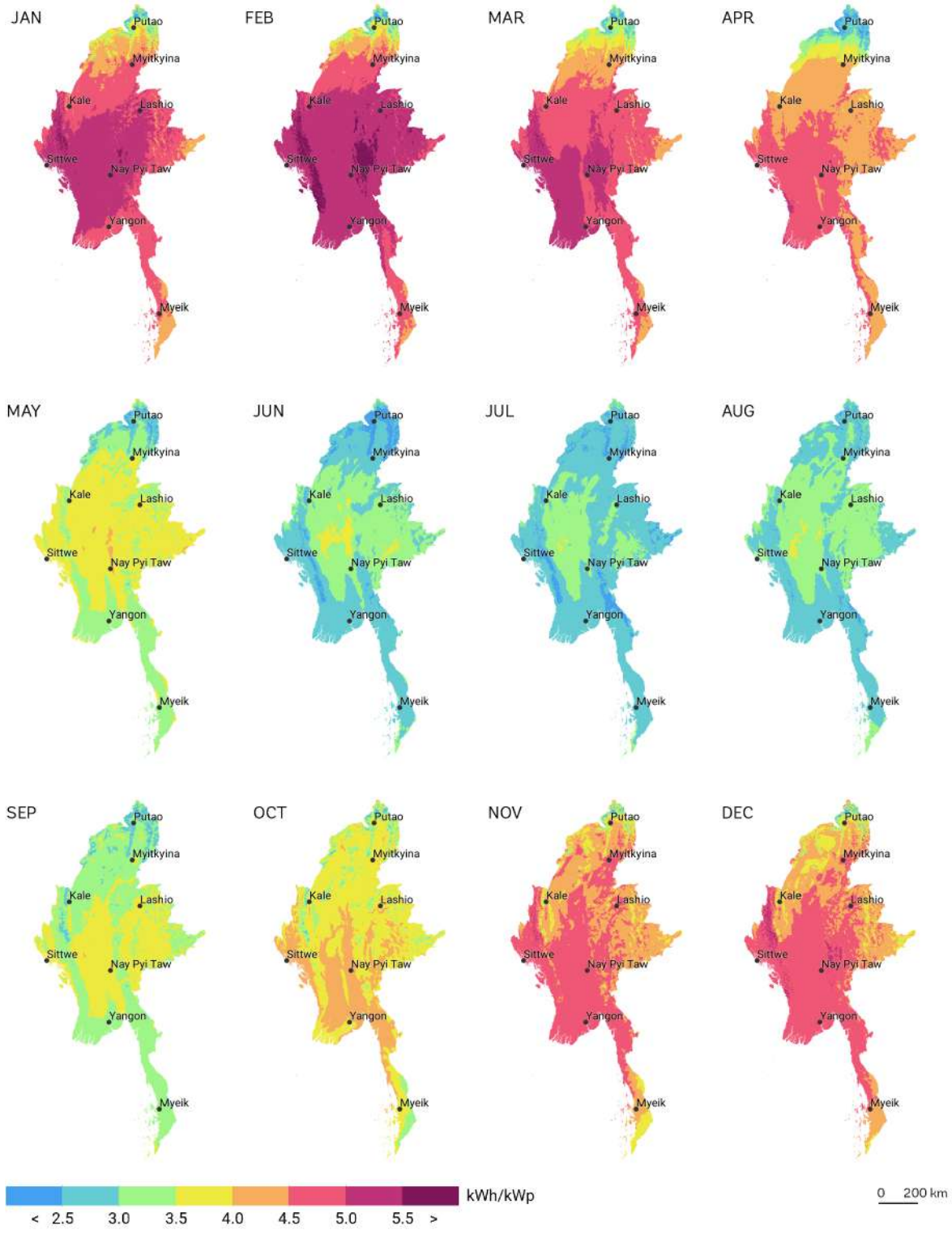

Map 3.17: PV power generation potential for an open-space fixed-mounted PV system. Longterm monthly averages of daily totals. Source: Solargis

Map 3.16 shows the average daily total of specific PV electricity output (considering a typical open-space PV system with a nominal peak power of 1 kW), i.e. the values are in kWh/kWp. Calculating PV output for 1 kWp of installed power makes it simple to scale the PV power production depending on the size of a power plant. Besides the technology choice, the electricity production depends on a geographical position of the power plant.

In Myanmar, the average yearly total of specific PV power production from a reference system (Table 2.14) varies between 1150 kWh/kWp (equals to average daily total of about 3.2 kWh/kWp) and 1600 kWh/kWp (about 4.4 kWh/kWp daily) with high values in the central region. In mountains, the power production is lower by up to 20% (or even more, due to terrain shading). Areas with high PV electricity production potential were previously identified also as areas with high GTI and DNI and lower DIF values.

Electricity production of a PV power plant depends on the site location, and it follows a combined pattern of global tilted irradiation and air temperature. High PV power production is identified at Nay Pyi Taw and Sittwe sites. The lowest specific PV production is in Putao, which may be a result of microclimate with highest annual DIF/GHI ratio compared to other sites (over 56%, Tab. 3.7). This means that the Putao site has more clouds, and aerosols. Difference in PV power production between sites with highest and lowest production is 24%: Nay Pyi Taw (4.32 kWh/kWp) and Putao (3.30 kWh/kWp).

Map 3.17 shows monthly production from a PV power system, and Figure 3.11 shows the values for eight sites. Season of relatively high PV yield is long enough for an effective operation of a PV system. As shown in Chapter 3.5, it is recommended to install modules at an optimum tilt rather than on horizontal surface. Besides higher yield, a benefit of tilted modules is improved self-cleaning of the surface pollution by rain.

Table 3.7: Annual performance parameters of a PV system with modules fixed at optimum angle

	Putao	Myitkyina	Kale	Lashio	Sittwe	Nay Pyi Taw	Yangon	Myeik
PVOUT Average daily total [kWh/kWp]	3.30	3.89	4.00	4.14	4.24	4.32	3.98	3.87
PVOUT Yearly total [kWh/kWp]	1206	1418	1458	1509	1545	1575	1450	1413
Optimum angle	30°	29°	26°	27°	25°	25°	22°	17°
Annual ratio of DIF/GHI	56.3%	49.2%	48.9%	48.1%	44.2%	43.4%	47.6%	49.4%
System PR	78.8%	77.6%	77.4%	78.6%	77.6%	76.6%	76.4%	76.8%

PVOUT - PV electricity yield for fixed-mounted modules at optimum angle; DIF/GHI – Ratio of diffuse/global horizontal irradiation; PR - Performance ratio for fixed-mounted PV

This also shows potential of sites in PV electricity generation. Sites in central lowlands (with highest photovoltaic production potential) are suitable for development of medium-size or large-scale grid connected PV power projects. Newly developed systems may be connected into existing high or medium voltage lines in these areas [35] and the energy produced during daytime will improve electricity balance in the distribution grid. On the opposite side, regions in mountains can benefit from lower air temperature. In conditions of grid unavailability, local micro-grids or small solar systems will work with higher efficiencies. These parts of country still have very good potential for PV electricity generation (see Putao or Lashio in Table 3.8).

Rural and remote populations can benefit from off-grid applications, such as small solar systems or mini-grids, especially in mountainous and border areas.

Monthly power production profiles are very similar for almost all sites (except Putao). High production can be reached in dry season (November to April), mostly in period from January to March. In all selected sites, reduced production is seen during the monsoon season with lower irradiation and higher air temperature.

Table 3.8: Average daily sums of PV electricity output from an open-space fixed PV system with a nominal peak power of 1 kW [kWh/kWp]

Site	Average daily sum of electricity production [kWh/kWp]												Year
	Jan	Feb	Mar	Apr	May	Jun	Jul	Aug	Sep	Oct	Nov	Dec	
Putao	3.83	3.80	3.34	2.78	2.93	2.52	2.61	2.82	3.18	3.77	4.13	3.94	3.30
Myitkyina	4.69	4.81	4.25	4.08	3.58	2.86	2.70	3.09	3.49	3.95	4.64	4.52	3.89
Kale	4.78	5.07	4.58	4.29	3.69	3.22	3.15	3.19	3.47	3.91	4.37	4.27	4.00
Lashio	5.12	5.36	4.75	4.31	3.67	3.37	3.08	3.35	3.67	3.89	4.55	4.54	4.14
Sittwe	5.15	5.38	5.24	5.01	3.87	2.80	2.71	3.09	3.72	4.28	4.83	4.77	4.24
Nay Pyi Taw	5.22	5.35	5.02	4.67	3.96	3.36	3.13	3.24	3.88	4.32	4.78	4.91	4.32
Yangon	4.89	5.18	5.03	4.70	3.33	2.80	2.72	2.80	3.28	3.73	4.56	4.74	3.98
Myeik	4.56	4.75	4.75	4.59	3.37	2.87	2.85	2.87	3.33	3.86	4.27	4.43	3.87

Table 3.9 and Figure 3.12 show monthly and yearly performance ratios (PR) for a reference installation at the selected sites. Yearly PR is found in a range between 76.4% (Yangon) and 78.8% (Putao). The Putao site is very specific: while it has lowest solar radiation (GHI, DNI), a PV system will work there with best performance ratio compare to the other sites, due to the lowest air temperature. Monthly PR variation falls in the range ±1.1% (Myeik) to ±2.6% (Putao and Kale); depending on the local climate, especially on air temperature. For most of the sites, performance ratio is higher from November to March, when PV output of the modules is less influenced by high air temperature. Myeik is the opposite case, where better PR is reached during the monsoon season.

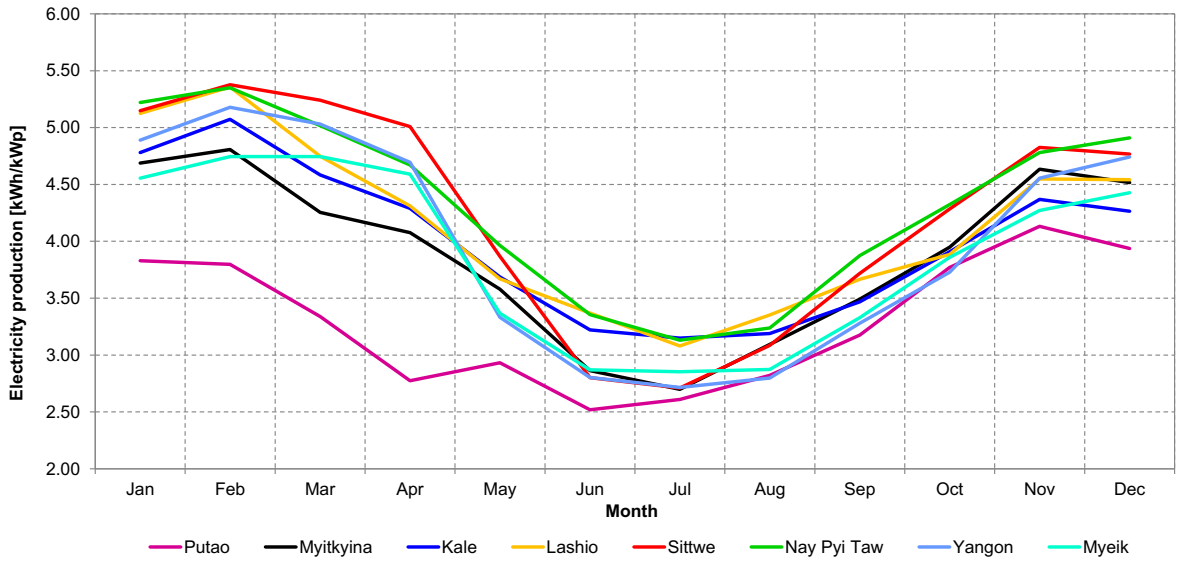

Figure 3.11: Monthly averages of daily totals of power production from the fixed tilted PV systems with a nominal peak power of 1 kW at eight sites [kWh/kWp]

Impact of air temperature on the performance of PV power plants is seen when comparing monthly temperature profiles in Figure 3.1 with monthly PR profiles in Figure 3.12. Sites Yangon or Nay Pyi Taw with visible temperature peak in April, has visible PR drop in the same month. Myeik, the site with stable air temperature through the whole year, has also stable performance ratio during the year. Other sites have very similar pattern, where the lower PR values, between May and September, are corresponding to warmer season, with PV output reduced by higher air temperature.

Table 3.9: Monthly and annual Performance Ratio of a free-standing PV system with fixed modules

Site	Monthly Performance Ratio [%]												Year
	Jan	Feb	Mar	Apr	May	Jun	Jul	Aug	Sep	Oct	Nov	Dec	
Putao	81.6	80.8	79.4	77.7	77.1	76.7	76.8	76.4	77.2	78.2	79.7	81.2	78.8
Myitkyina	79.9	78.4	76.9	75.8	76.0	76.4	76.8	76.6	76.5	77.4	78.7	80.0	77.6
Kale	79.6	77.8	76.2	75.0	75.5	76.3	76.8	76.8	77.0	77.6	79.0	80.2	77.4
Lashio	80.2	78.6	77.2	76.3	77.2	78.0	78.3	78.3	78.4	78.8	80.0	81.0	78.6
Sittwe	78.9	77.8	77.0	76.6	76.7	76.8	77.0	77.4	77.4	77.2	77.9	79.0	77.6
Nay Pyi Taw	77.3	75.9	74.6	74.1	76.2	77.6	77.8	77.8	77.7	76.9	77.3	78.0	76.6
Yangon	77.0	75.5	74.2	73.9	76.0	77.0	77.1	77.3	77.6	77.5	77.5	77.8	76.4
Myeik	76.4	75.9	75.8	75.8	77.1	77.6	77.8	77.9	77.9	77.4	76.9	76.7	76.8

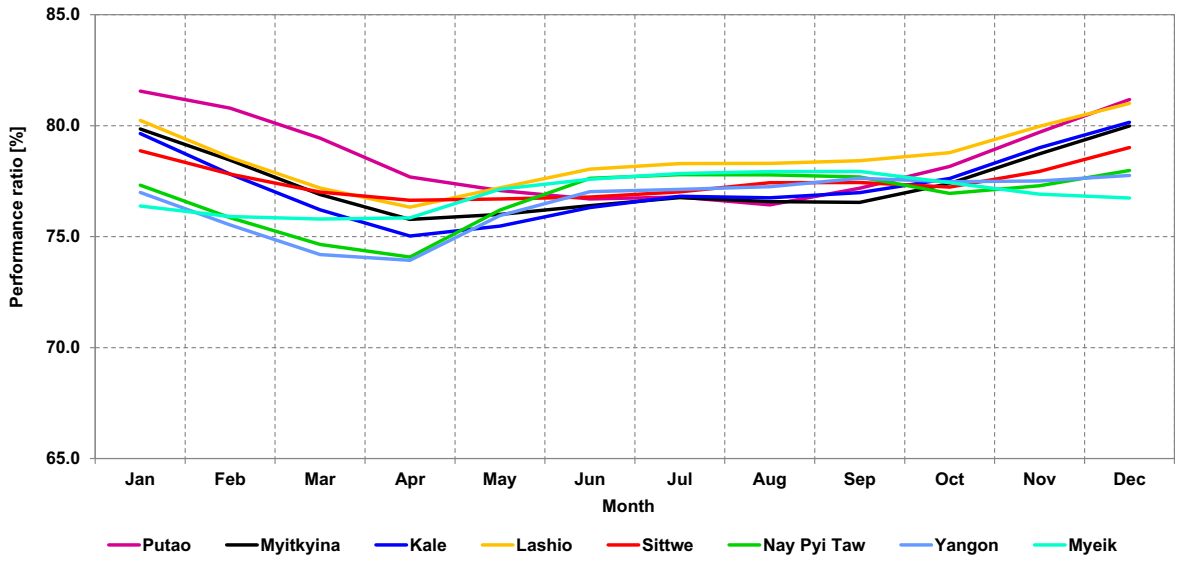

Figure 3.12: Monthly performance ratio of a PV system at selected sites.
Fixed mounted modules at optimum tilt are considered

3.7 Solar climate

The power production and performance efficiency of photovoltaic systems is primarily driven by **global horizontal irradiance** (Map 3.11). GHI determines absolute values of energy production of a PV system, and variability patterns of PV power production (interannual, seasonal, daily and very short-term variability). In general, the higher GHI, the higher PV energy is expected. Patterns of power generation are also determined by the ratio of diffuse to global radiation (Map 3.12). This simplified assumption is modulated by **air temperature** (Map 3.9), as it affects operation efficiency of a PV system. In general, high-temperature reduces performance efficiency of the PV system and low temperature makes power conversion in PV modules more efficient. In addition, in Myanmar, high temperature areas represent regions where PV operates under higher stress.

For development of solar power systems, it also important to consider **other geographical and meteorological factors**, e.g. terrain elevation, terrain shading, wind speed, rainfall, snow cover and land cover. They are also important for development and operation of solar power systems:

- **Terrain**: maps of elevation, slope inclination and terrain shading show limitations of installation and operating the meteorological stations but also PV power systems.

  Terrain shading blocks direct sunlight and it reduces power generation. Therefore, if possible a PV system and a solar meteorological station should be located in places with no or limited shading.

  Higher elevation above sea level (Map 3.2) reduces atmospheric load by aerosols and thickness of atmosphere and this way it increases solar radiation under clear sky conditions. On the other hand, high elevation may pose increased risk of degradation of components due to low temperature and higher UV radiation.

  High slope inclination (Map 3.3) is challenging for logistics and operation, and poses various geo-hazards, such as landslides, floods and avalanches.
- **Wind speed**: Low and medium speed winds, close to the ground, have cooling effect on PV modules, which in turn increases their conversion efficiency and increases power production. However, occurrence of stronger winds poses a risk of damaging the modules and construction components. Wind speed map is not supplied in this report.
- **Rainfall** (Map 3.8): amount and periodicity of rainfall determine cleaning efficiency of surface of the PV modules. Manual cleaning of PV modules requires special attention in dry and dusty seasons.
- **Water bodies** (Map 3.6): areas close to water bodies may be affected by microclimate features such as local fog, humidity or increased condensation.
- **Industrial and highly urbanised areas** (Map 3.5 and 3.7): these areas typically pose a higher risk of air pollution that triggers higher intensity of soiling of PV modules. PV modules that are covered by dust or atmospheric pollution may show substantial reduction of power production and require more frequent cleaning of surface of the PV modules. The proximity of PV power plant to heavy industry or traffic should be avoided.

Note: map of rainfall provides only indicative information at a regional level. It does not respect the detailed and complex orography, and thus it does not represent local climate.

Below, the geographical diversity of Myanmar is described by several climate zones relevant to PV power production. These climate zones are identified by combining maps of yearly GHI and TEMP (Tables 3.10 and 3.11).

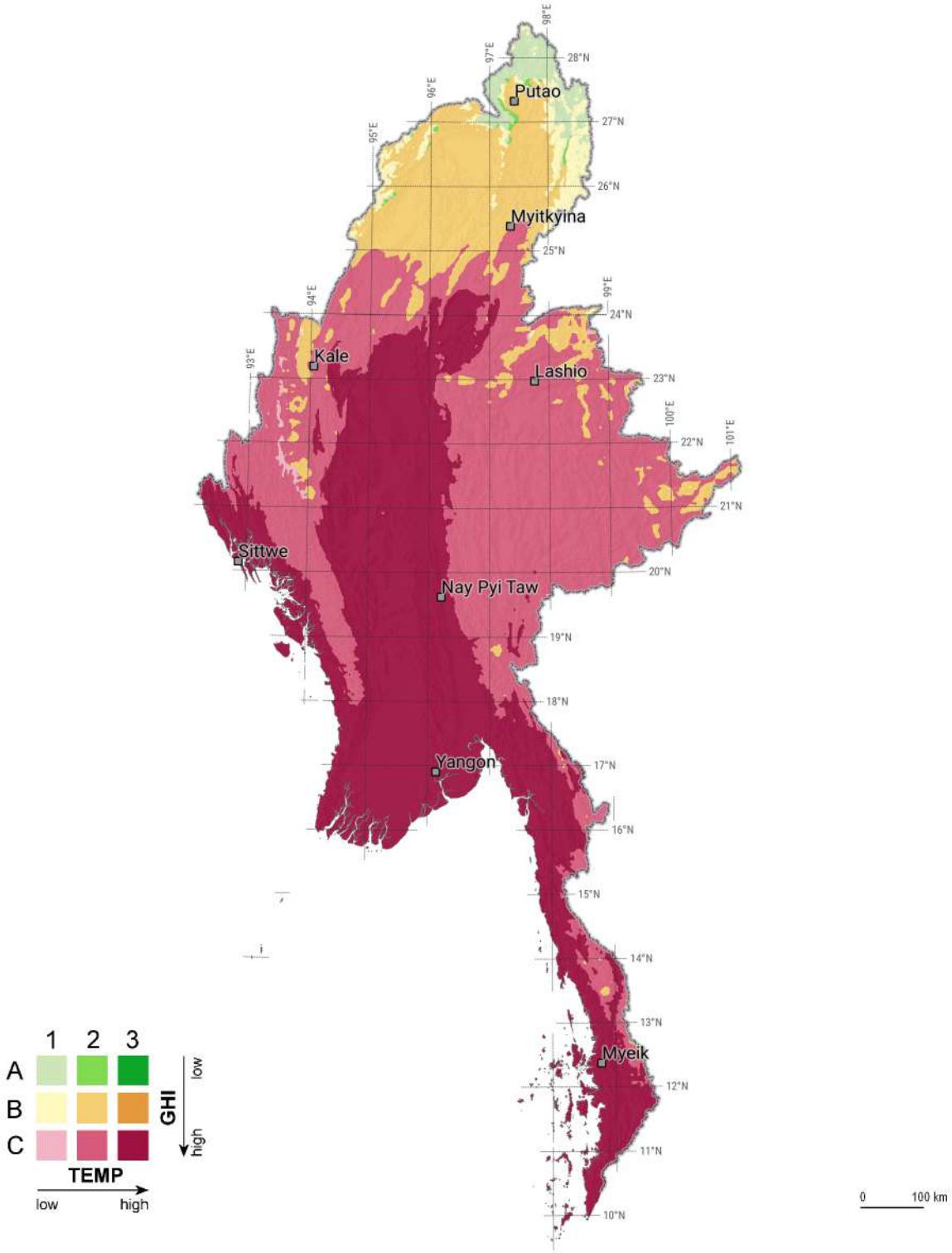

Map 3.18: Solar climate zones of Myanmar – indicative classification based on a combination of GHI and TEMP. Source: Solargis

Table 3.10: Categories of long-term yearly average of global horizontal irradiation

Category	Yearly average of daily global horizontal irradiation (GHI)	
A	Low	< 4.0 kWh/m^2
B	Middle range	From 4.0 to 4.8 kWh/m^2
C	High	> 4.8 kWh/m^2

Table 3.11: Categories of long-term yearly average of air temperature

Category	Yearly average of air temperature (TEMP)	
1	Low	< 4°C
2	Middle range	From 4°C to < 20°C
3	High	> 20°C

We recognize several climate regions that have some relevancy from the perspective of solar power generation and performance efficiency of PV systems (Map 3.18, Tables 3.10 and 3.11, see also Maps 3.9 and 3.10):

- **Solar climate zone A** shows low solar radiation areas (GHI longterm yearly average below 4.0 kWh/m^2 per day).

  This zone represents very small area at the North of the country; it is mostly represented by *ridges and slopes of high mountains* with high occurrence of clouds and air temperature in the middle and low range (A1 and A2). In many areas, the solar resource is reduced by terrain shading. This climate zone is less populated with dominating forests. The main challenge here is accessibility and lower solar resource for PV power systems.

- **Solar climate zone B** in Kachin state and the north part of Sagaing region, with GHI yearly average between 4.0 and 4.8 kWh/m^2 per day.

  The low (B1) and middle range of air temperature (B2) in *middle-elevation mountains,* the land cover consists mainly of croplands and forests in the sparsely populated territory. This region offers opportunities for installing smaller sized PV power systems. The limitation factors are terrain (slope and shading), accessibility (proximity to roads or airports) and presence of natural protected areas.

- **Solar climate zone C** the mostly dominating in Myanmar and indicates areas with high solar radiation (average above 4.8 kWh/m^2 per day).

  The high solar resource zone combined with low temperature (C1) is almost non-present in Myanmar.

  The middle temperature zone (C2) is spread in *highland and mosaic of cultivated land* in western part of the country (south of Sagaing region, Chin state and part of Rakhine states) and eastern Shan state. Population in most of the zone lacks reliable access to electric energy. However, this zone has very good potential for installation of middle or large scale power plants.

  From the perspective of deployment of PV power plants, very perspective is also zone C3 with higher air temperature. This zone spreads in the delta and coastal lowlands, Tanintharyi and Mon region, and lowland of Central Dry Zone. The deployment of solar energy systems is favourable here as it coincides with the most populated part of the country with the highest energy demand for industry and transport. The limiting factor in this zone is mostly air pollution.

3.8 Evaluation

The Chapters above describe various aspects of PV power generation potential in Myanmar, and its relevance for development and operation of photovoltaic systems. A large extent of the country has specific PV electricity output in the range between 1400 kWh/kWp and 1600 kWh/kWp (equals to average daily totals between 3.8 and 4.2 kWh/kWp). **This positions Myanmar among the regions with very feasible potential for PV power generation** (Map 3.19).

In addition, the seasonal variability in the country is very low, compared to other regions further away from the equator. The ratio between months with maximum and minimum GHI is about 1.47, while in Upington, South Africa, it is 2.29 and in Sevilla, Spain, 3.54 (Figure 3.13).

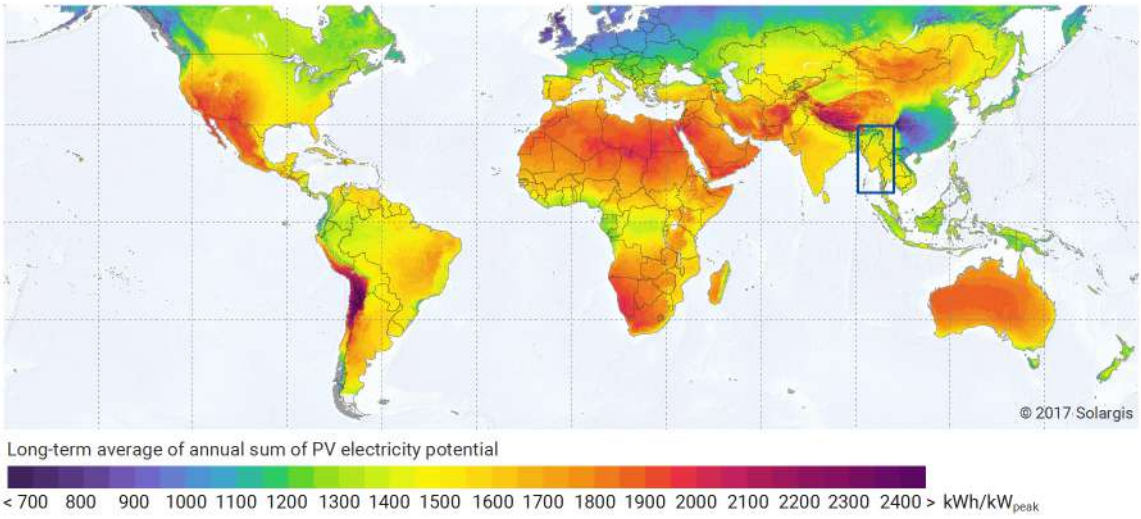

Map 3.19: PV power potential of Myanmar in the global context.
Fixed mounted modules at optimum tilt are considered

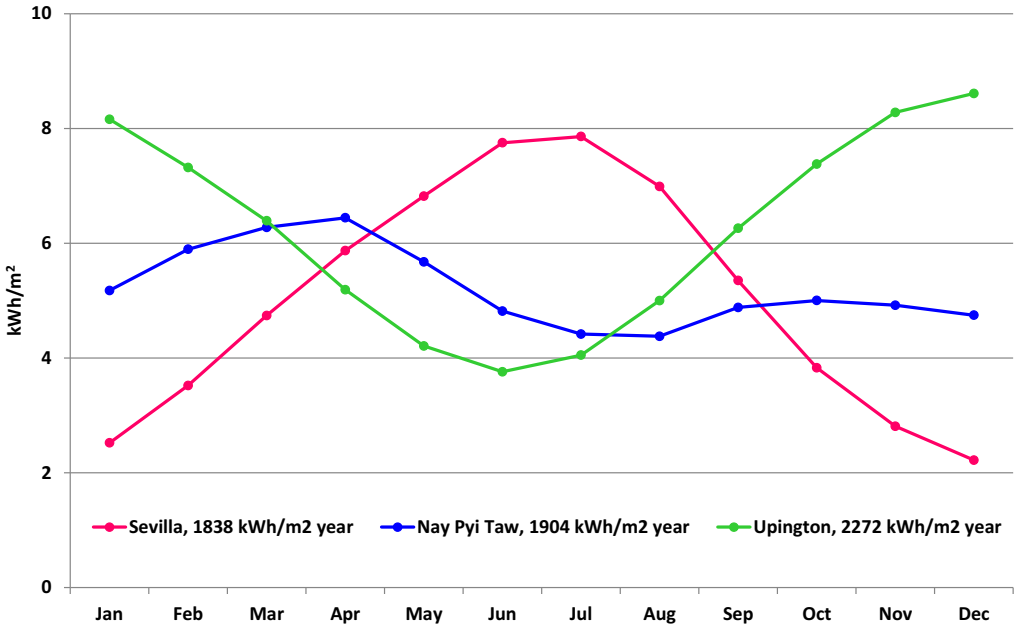

Figure 3.13: Comparing seasonal variability in three locations

Figure 3.14 demonstrates how PV power production depends on solar resource and air temperature in non-linear way. Even that the PV power production is feasible everywhere, for the case of large-scale PV power plants there might be some geographical preferences.

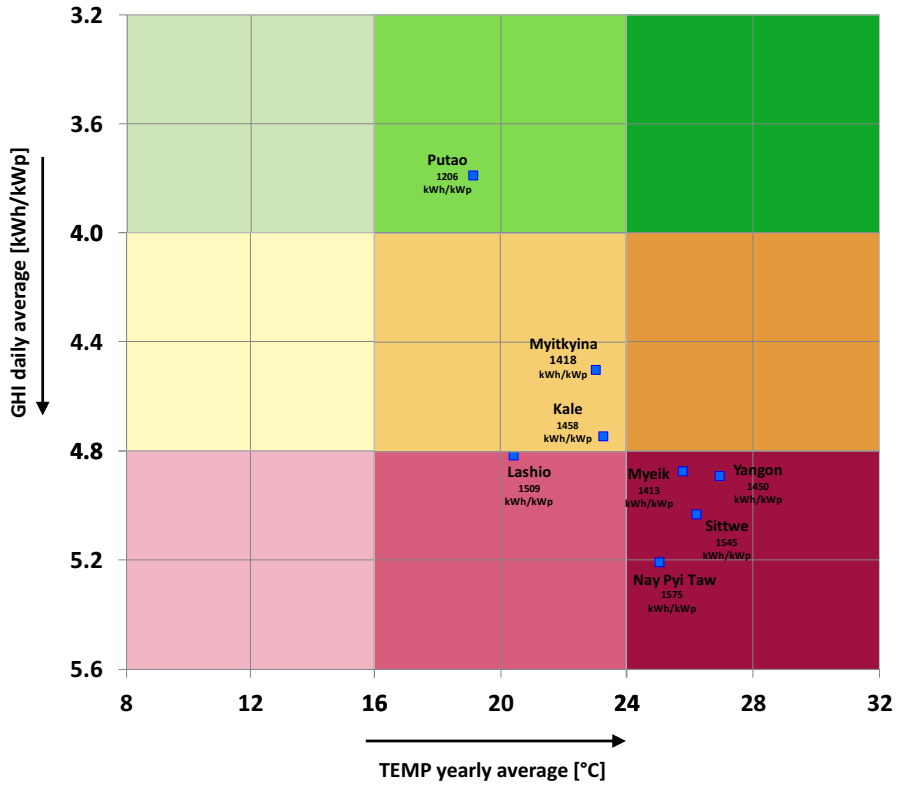

Figure 3.14: Comparing yearly GHI and TEMP with potential PV power output at selected sites

Vast part of Myanmar has very good potential for development of solar power generation, predominantly in lowlands of central part of the country, where also demand is the highest. As majority of the country lacks access to electricity, which is at present mostly used in the residential sector, medium or small installations are feasible in small and even remote communities (off-grids, mini-grids) across the country.

Monsoon season reduces of solar radiation mainly in southern and coastal regions from June to August. The microclimate factors should be considered as well (see Chapter 3.7).

Based on the outcomes of this study, Table 3.12 provides indicative SWOT analysis relative to the exploitation of solar resource in Myanmar.

Table 3.12: SWOT analysis relative to the solar resource and photovoltaic potential in Myanmar

Strengths • Good solar resource and PV power potential • Flat terrain (or low slopes) is available and gives prospect for development of medium to large scale PV power plants • Existing off-grid and mini-grids technology for remote communities is feasible • Most of the Myanmar population (75-85%) lives within 25-50 km buffer of existing high voltage infrastructure [35], which gives prospects for development of medium size and large scale PV power plants	**Weaknesses** • Large areas of dispersed settlements • Underdeveloped transport infrastructure in many regions of the country • High costs of grid connection, long time of connection into high voltage lines for remote areas [25] • Terrain constrains: high elevation and slope, shading, accessibility • Air pollution in urbanized areas • Low penetration of solar installations [36]
Opportunities • Growing demand for electricity • International support programs • Positive attitude to renewable energy • Reduced cost of PV • Combination with other renewable energy sources (mainly hydro) helps dealing with variability of solar resource • Estimated solar potential in central regions is near 52 PWh [25]	**Threats** • Geographical risks: extreme weather events, floods, landslides • Short term variability of resource should be analyzed for more effective PV integration

4 Priority areas for meteorological stations

4.1 Localisation criteria

Based on the analysis of maps presented in this report, and set of criteria we propose areas suitable for deployment of solar meteorological stations. We have in mind the need for the validation of models and reduction of the data uncertainty for development of photovoltaic power systems. The methodology includes two steps:

- Identification of climate regions in Myanmar relevant to photovoltaic power production,
- Identification of areas preferred for deployment of solar meteorological stations.

From the **regional perspective**, *suitable areas* for deployment of solar meteorological stations should be geographically representative, i.e. they should represent in a wider territory, certain type of climate where solar resource, terrain, air temperature and land use are similar, and where they do not change abruptly. We also identify *exclusion areas*, where installation of stations is not recommended, for reasons such as fast changing terrain and landscape, in industrial zones, but also in remote and difficult-to-access areas.

From the **local perspective**, there are several additional localisation criteria for deployment of solar meteorological stations, such as accessibility, availability of personnel for maintenance and cleaning, security, sustainability of running the measurement campaign in a long term, acceptance/interest of the land owner, and other economical and logistical criteria.

This report focuses on the *regional selection criteria*. The local criteria are not considered in this report.

4.2 Areas suitable for solar meteorological stations

Based on the analysis in Chapter 3.7, we propose location of solar measuring stations by excluding areas that are not suitable. One of requirements of the solar measurement campaign is to receive high quality, continuous data sets that can be used for *satellite data validation* and *regional adaptation of the solar model*. Three viewpoints are considered in identification of areas that are suitable for deployment of solar measuring stations.

Map 5.1 is based on the overlay of the following factors:

Exclusion areas:

- Areas with slope inclination higher than 20 degrees; these are areas with rapidly changing terrain and landscape.
- In the low populated zones: areas at a distance more than 5 km from the nearest main road or airport
- Areas affected by excessive terrain shading (Map 3.12)
- Proximity to water bodies
- Industrial areas and areas with high air pollution
- Remote areas

Suitable (preferred) areas for solar meteorological stations:

- Close to the transport means and populated areas, due to requirements for regular maintenance and likelihood that the meteo station will serve the data needs for local power systems,
- Airports, as they offer open space, with good level of security. Typically, there is also personnel, who is experienced in meteorological measurements,

- Close to the electricity grid and power infrastructure. Close position has relevance especially for utility scale PV projects.

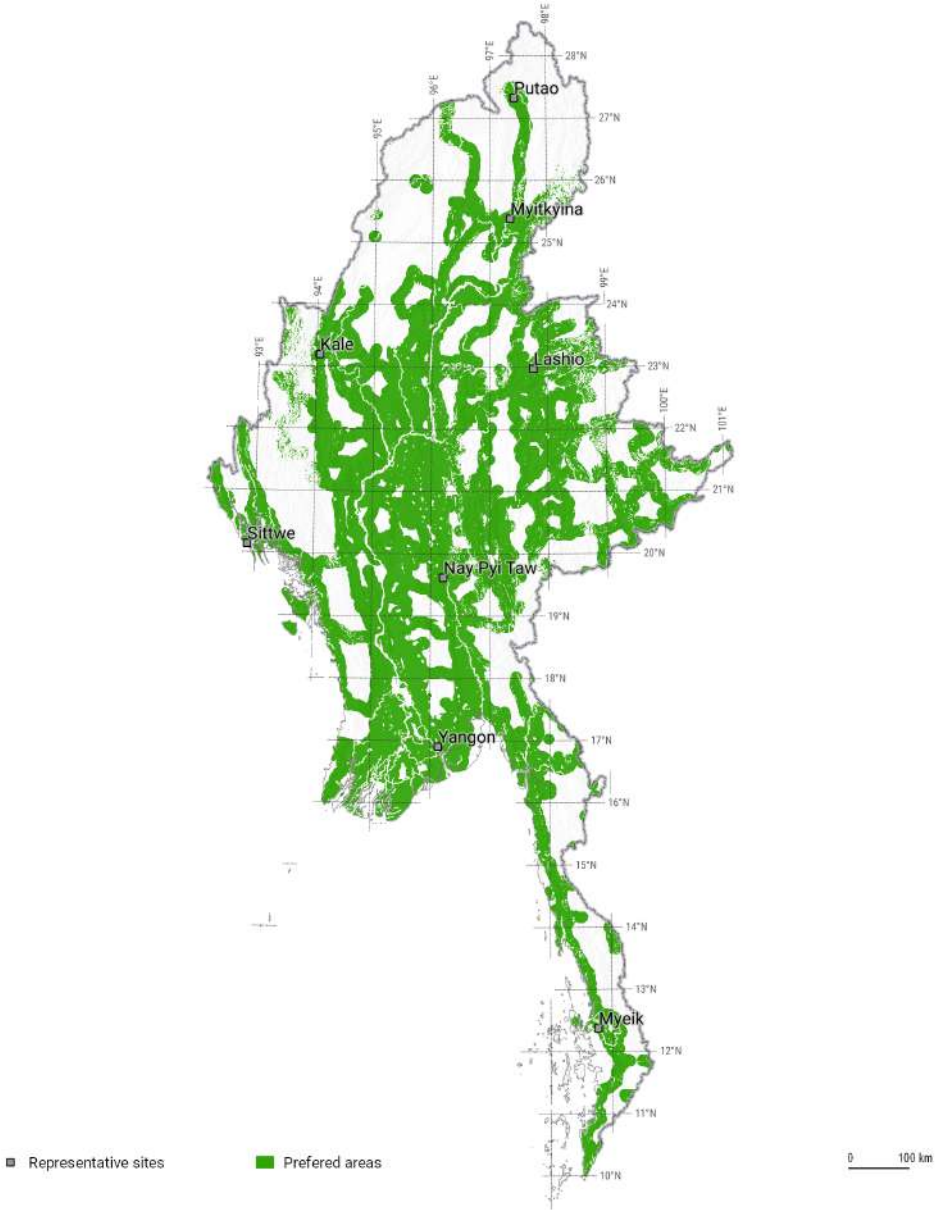

Map 4.1: Preferred areas for deployment of solar meteorological stations (green colour)
Note: areas with high air pollution are not shown in this map

Map 4.1 presents areas *excluded* (white colour on the map) and *prioritized* (green colour on the map) from the point of view of deploying the solar measuring stations. Consulting also Map 3.18, we propose that the meteorological stations are located in solar climate regions B and C, with medium and higher levels of GHI. The sites should be located in the green-indicated areas (see Map 4.1); a good option are airports:

- **Dry lowland region** (Mandalay, Magwe region, south-east of Sagaing region): good candidate will be location accessible by transport infrastructure, distant from industrial, agricultural or transport pollution, not close to the river or water bodies

- **Monsoon lowland region:** any location in the southern Tanintharyi region, Yangon region or Mon state. The primary localization limitation is distance from coast and water bodies, as there is likely occurrence of microclimate features, such as local fog, humidity or increased creation of due.
- **Highland region**: good candidate sites could be possibly located in Shan or Chin state. Micro climate conditions must be considered carefully.

Quality and reliability of the measuring campaign is also of the highest importance. Implementation of the best measurement practices is necessary precondition for achieving reliable data sets required for calibration and validation of solar models. The meteorological instruments must be regularly maintained, cleaned and calibrated. Measurement sites should be in the areas, which are not affected by excessive dust and pollution. Locally shaded areas, caused by surrounding buildings, structures and vegetation, should be also avoided. If shading takes place, the affected solar radiation values should be identified and flagged.

5 Solargis data delivery for Myanmar

The key features of the delivered data and maps for Myanmar are:

- Harmonized solar, meteorological and geographical data based on the best available methods and input data sources.
- Historical long-term averages representing 17 years at high spatial and temporal resolution, available for any location.
- The Solargis database and energy simulation software is extensively validated by company Solargis, and by independent organizations. They are also verified within monitoring of commercial PV power plants and solar measuring stations worldwide.
- Additional data can be accessed online at http://solargis.com.

The delivered data and maps offer a good basis for knowledge-based decision-making and project development. These data are updated in real time can be further used for solar monitoring, performance assessment and forecasting.

5.1 Spatial data products

High-resolution Solargis data have been delivered in the format suitable for common GIS software. The *Primary data* represent solar radiation, meteorological data and PV power potential. The *Supporting data* include various vector data, such administrative divisions, etc.

Tables 5.1 and 5.2 show information about the data layers, and the technical specification is summarized in Tables 5.3 and 5.4. File name convention, used for the individual data sets, is described in Table 5.5.

Table 5.1: General information about GIS data layers

Geographical extent	Federal Democratic Republic of Myanmar with buffer 10 km along the borders (approx. 165 000 km^2)
Map projection	Geographic (Latitude/Longitude), datum WGS84 (also known as *GCS_WGS84*; *EPSG: 4326*)
Data formats	ESRI ASCII raster data format (*asc*) GeoTIFF raster data format (*tif*)

Notes:

- Data layers of both formats (asc and tif) contain the same information, the operator is free to choose the preferential data format. Data layers can be also converted to other standard raster formats.
- More information about ESRI ASCII grid format can be found at http://help.arcgis.com/en/arcgisdesktop/10.0/help/index.html#/ESRI_ASCII_raster_format/009t0000000z000000/
- More information about GeoTIFF format can be found at https://trac.osgeo.org/geotiff/

Table 5.2: Description of primary GIS data layers

Acronym	Full name	Unit	Type of use	Type of data layers
GHI	Global Horizontal Irradiation	kWh/m^2	Reference information for the assessment of flat-plate PV (photovoltaic) and solar heating technologies (e.g. hot water)	Long-term yearly and monthly average of daily totals
DNI	Direct Normal Irradiation	kWh/m^2	Assessment of Concentrated PV (CPV) and Concentrated Solar Power (CSP) technologies, but also calculation of GTI for fixed mounting and sun-tracking flat plate PV	Long-term yearly and monthly average of daily totals
DIF	Diffuse Horizontal Irradiation	kWh/m^2	Complementary parameter to GHI and DNI	Long-term yearly and monthly average of daily totals
GTI	Global Irradiation at optimum tilt	kWh/m^2	Assessment of solar resource for PV technologies	Long-term yearly and monthly average of daily totals
OPTA	Optimum angle	°	Optimum tilt to maximize yearly PV production	-
PVOUT	Photovoltaic power potential	kWh/kWp	Assessment of power production potential for a PV power plant with free-standing fixed-mounted c-Si modules, mounted at optimum tilt to maximize yearly PV production	Long-term yearly and monthly average of daily totals
TEMP	Air Temperature at 2 m above ground level	°C	Defines operating environment of solar power plants	Long-term (diurnal) annual and monthly averages

Table 5.3: Technical specification of primary GIS data layers

Acronym	Full name	Data format	Spatial resolution	Time representation	No. of data layers
GHI	Global Horizontal Irradiation	Raster	30 arc-sec. (approx. 825x925 m)	1999 - 2015	12+1
DNI	Direct Normal Irradiation	Raster	30 arc-sec. (approx. 825x925 m)	1999 - 2015	12+1
DIF	Diffuse Horizontal Irradiation	Raster	30 arc-sec. (approx. 825x925 m)	1999 - 2015	12+1
GTI	Global Irradiation at optimum tilt	Raster	30 arc-sec. (approx. 825x925 m)	1999 - 2015	12+1
OPTA	Optimum angle	Raster	2 arc-min (approx. 3300x3700 m)	-	1
PVOUT	Photovoltaic power potential	Raster	30 arc-sec. (approx. 825x925 m)	1999 - 2015	12+1
TEMP	Air Temperature at 2 m above ground level	Raster	30 arc-sec. (approx. 825x925 m)	1999 - 2015	12+1

Table 5.4: Characteristics of the raster output data files

Characteristics	Range of values
West – East	79:00:00E – 89:00:00E
North – South	31:00:00S – 29:00:00S
Resolution (GHI, DNI, GTI, DIF, PVOUT, TEMP)	00:00:30 (1200 columns x 600 rows)
Resolution (OPTA)	00:02 (300 columns x 150 rows)
Data type	Float
No data value	-9999, NaN

Table 5.5: File name convention for GIS data

Acronym	Full name	Filename pattern	Number of files	Size (approx.)
GHI	Global Horizontal Irradiation; long-term yearly average of daily totals	GHI.*ext*	1+1	5 MB
GHI	Global Horizontal Irradiation; long-term monthly averages of daily totals	GHI_*MM.ext*	12+12	60 MB
DNI	Direct Normal Irradiation; long-term yearly average of daily totals	DNI.*ext*	1+1	5 MB
DNI	Direct Normal Irradiation; long-term monthly averages of daily totals	DNI_*MM.ext*	12+12	60 MB
DIF	Diffuse Horizontal Irradiation; long-term yearly average of daily totals	DIF.*ext*	1+1	5 MB
DIF	Diffuse Horizontal Irradiation; long-term monthly averages of daily totals	DIF_*MM.ext*	12+12	60 MB
GTI	Global Irradiation at optimum tilt; long-term yearly average of daily totals	GTI.*ext*	1+1	5 MB
GTI	Global Irradiation at optimum tilt, long-term monthly averages of daily totals	GTI_*MM.ext*	12+12	60 MB
OPTA	Optimum angle	OPTA.*ext*	1+1	0.2 MB
PVOUT	Photovoltaic power potential; long-term yearly average of daily totals	PVOUT.*ext*	1+1	5 MB
PVOUT	Photovoltaic power potential; long-term monthly averages of daily totals	PVOUT_MM.*ext*	12+12	60 MB
TEMP	Air Temperature at 2 m above ground; long-term yearly average	TEMP.*ext*	1+1	5 MB
TEMP	Air Temperature at 2 m above ground; long-term monthly averages	TEMP_*MM.ext*	12+12	60 MB

Table 5.6: Support GIS data

Data type	Source	Data format
	OpenStreetMap.org contributors, GeoNames.org, adapted by Solargis	Point shapefile
Airports	Wikipedia.org, adapted by Solargis	Point shapefile
Administrative boundaries	Cartography Unit, GSDPM, World Bank Group	Polyline shapefile
Roads	OpenStreetMap.org contributors	Polyline shapefile
Water bodies	OpenStreetMap.org contributors	Polygon shapefile

Explanation:

- MM: month of data – from 01 to 12
- ext: file extension (*asc* or *tif*)

Data layers are provided as separate files in a tree structure, organized according to

- File format (ASCII or GEOTIF)
- Time summarization (*yearly* and *monthly*)

Complementary files:

- Project files (*.prj) complement ESRI ASCII grid files (*.asc)
- World files (*.*tfw*) complement GeoTIFF files (*.*tif*)

The support GIS data are provided in a vector format (ESRI shapefile, Table 5.6).

5.2 Project in QGIS format

For easy manipulation with GIS data files, selected vector and raster data files are integrated into ready-to-open Quantum GIS (QGIS) project file with colour schemes and annotation (see Figure 5.1). QGIS is state-of-art open-source GIS software allowing visualization, query and analysis on the provided data. QGIS includes a rich toolbox to manipulate with data. More information about the software and download packages can be found at http://qgis.org.

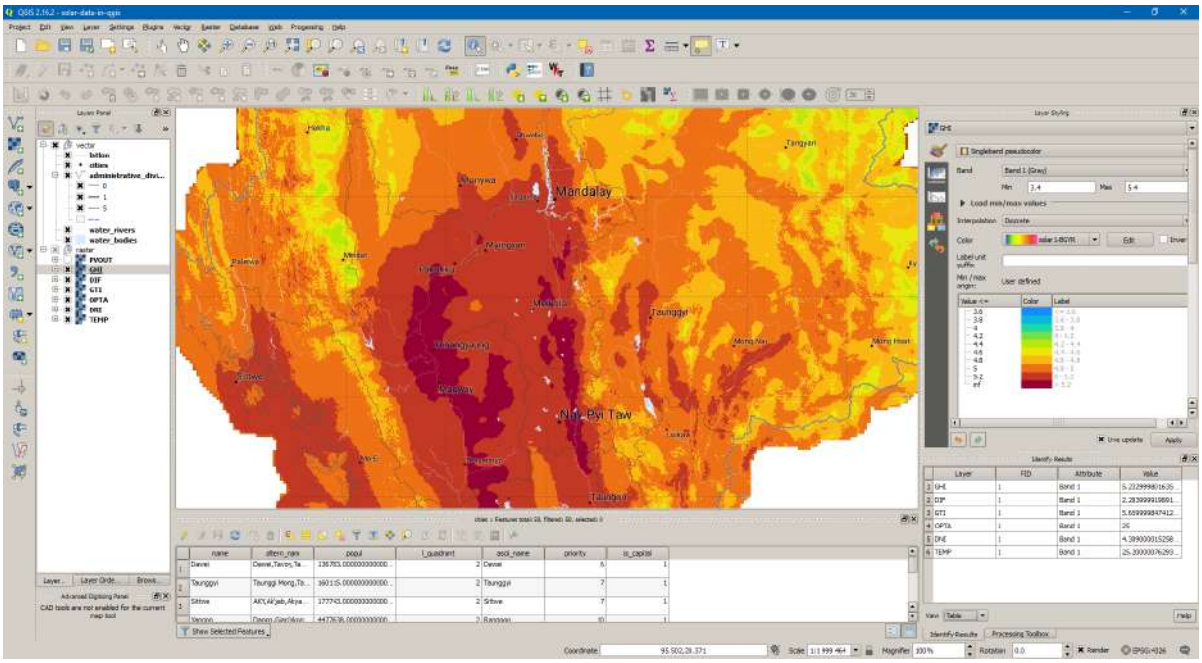

Figure 5.1: Screenshot of the map and data in the QGIS environment

5.3 Digital maps

Besides GIS data layers, digital maps are also delivered for selected data layers for presentation purposes. Digital maps are prepared in three types; each suitable for different purpose:

- High-resolution poster maps
- Medium-resolution maps for presentations

Digital images for high-resolution poster printing (size 120 x 80 cm). The colour-coded maps are prepared in a TIFF format at 300 dpi density and lossless compression.

Following four map files are delivered for high-resolution poster printing:

- Global Horizontal Irradiation; yearly average of the daily totals
- Direct Normal Irradiation; yearly average of the daily totals
- Air temperature at 2 metres; long term yearly average
- Photovoltaic electricity production from a free-standing power plant with optimally tilted c-Si modules; yearly average of the daily totals.

Digital images prepared in a resolution suitable for A4-size (or letter-size) printing or on-screen presentation. The colour-coded maps are prepared in PNG format at 300 dpi density and lossless compression.

Following map files are delivered:

- Annual and monthly long-term averages of Global Horizontal Irradiation
- Annual and monthly long-term averages of ratio Diffuse/Global Horizontal Irradiation
- Annual and monthly long-term averages of Global Tilted Irradiation (for optimum tilt)
- Annual and monthly long-term averages of Direct Normal Irradiation
- Annual and monthly long-term averages of Air Temperature
- Annual and monthly long-term averages of Photovoltaic (PV) Electricity Potential
- High resolution Terrain Elevation
- Myanmar in the world context of Global Horizontal Irradiation map

The maps also include visualization of the following layers:

- Main cities, location and names
- Administrative borders
- Water bodies

5.4 Metainformation related to delivered GIS data layers

The following mete information files are delivered together with GIS data files:

- Global Horizontal Irradiation; long-term yearly and monthly average of daily totals
- Direct Normal Irradiation; long-term yearly and monthly average of daily totals
- Diffuse Horizontal Irradiation; long-term yearly and monthly average of daily totals
- Global Tilted Irradiation; long-term yearly and monthly average of daily totals
- Photovoltaic electricity output for c-Si fixed-mounted modules, optimally tilted Northwards; long-term yearly and monthly average of daily totals
- Air Temperature, long-term (diurnal) annual and monthly averages

6 List of maps

7 List of figures

8 List of tables

9 References

[1] Thet That Han Yee , Su Su Win, Nyein Nyein Soe, 2008. Solar energy potential and applications in Myanmar. Internatonal Journal of Social Behavioral, Educational, Economic, Business and Industrial Engineering, 2, 6, 667-670.

[2] Wint Wint Kyaw, Sukruedee Sukchai, Nipon Ketjoy, Sahataya Ladpala, 2011. Energy utilization and the status of sustainable energy in the Union of Myanmar, Energy Proceedia, 9, 351-358.

[3] Serm Janjai, Itsara Masiri, Jarungsaeng Laksanaboonsong, 2013. Satellite-derived solar resource maps for Myanmar, Renewable Energy 53, 132-140.

[4] Renewable energy developments and potential in the Greater Mekong Subregion, Asian Development Bank, 2015.

[5] Perez R., Cebecauer T., Suri M., 2014. Semi-Empirical Satellite Models. In Kleissl J. (ed.) Solar Energy Forecasting and Resource Assessment. Academic press.

[6] Cebecauer T., Šúri M., Perez R., High performance MSG satellite model for operational solar energy applications. ASES National Solar Conference, Phoenix, USA, 2010.

[7] Šúri M., Cebecauer T., Perez P., Quality procedures of SolarGIS for provision site-specific solar resource information. Conference SolarPACES 2010, September 2010, Perpignan, France.

[8] Cebecauer T., Suri M., Gueymard C., Uncertainty sources in satellite-derived Direct Normal Irradiance: How can prediction accuracy be improved globally? Proceedings of the SolarPACES Conference, Granada, Spain, 20-23 Sept 2011.

[9] Šúri M., Cebecauer T., Requirements and standards for bankable DNI data products in CSP projects, Proceedings of the SolarPACES 2011 Conference, September 2011, Granada, Spain.

[10] Šúri M., Cebecauer T., 2014. Satellite-based solar resource data: Model validation statistics versus user's uncertainty. ASES SOLAR 2014 Conference, San Francisco, 7-9 July 2014.

[11] Ineichen P., A broadband simplified version of the Solis clear sky model, 2008. Solar Energy, 82, 8, 758-762.

[12] Morcrette J., Boucher O., Jones L., Salmond D., Bechtold P., Beljaars A., Benedetti A., Bonet A., Kaiser J.W., Razinger M., Schulz M., Serrar S., Simmons A.J., Sofiev M., Suttie M., Tompkins A., Uncht A., GEMS-AER team, 2009. Aerosol analysis and forecast in the ECMWF Integrated Forecast System. Part I: Forward modelling. Journal of Geophysical Research, 114.

[13] Benedictow A. et al. 2012. Validation report of the MACC reanalysis of global atmospheric composition: Period 2003-2010, MACC-II Deliverable D_83.1.

[14] Cebecauer T., Perez R., Suri M., Comparing performance of SolarGIS and SUNY satellite models using monthly and daily aerosol data. Proceedings of the ISES Solar World Congress 2011, 28 August – 2 September 2011, Kassel, Germany.

[15] Cebecauer T., Šúri M., Accuracy improvements of satellite-derived solar resource based on GEMS re-analysis aerosols. Conference SolarPACES 2010, September 2010, Perpignan, France.

[16] Molod, A., Takacs, L., Suarez, M., and Bacmeister, J., 2015: Development of the GEOS-5 atmospheric general circulation model: evolution from MERRA to MERRA2, Geosci. Model Dev., 8, 1339-1356, doi:10.5194/gmd-8-1339-2015

[17] GFS model. http://www.nco.ncep.noaa.gov/pmb/products/gfs/

[18] CFSR model. https://climatedataguide.ucar.edu/climate-data/climate-forecast-system-reanalysis-cfsr/

[19] CFSv2 model http://www.cpc.ncep.noaa.gov/products/CFSv2/CFSv2seasonal.shtml

[20] Cano D., Monget J.M., Albuisson M., Guillard H., Regas N., Wald L., 1986. A method for the determination of the global solar radiation from meteorological satellite data. Solar Energy, 37, 1, 31–39.

[21] Perez R., Ineichen P., Maxwell E., Seals R. and Zelenka A., 1992. Dynamic global-to-direct irradiance conversion models. ASHRAE Transactions-Research Series, pp. 354-369.

[22] Perez, R., Seals R., Ineichen P., Stewart R., Menicucci D., 1987. A new simplified version of the Perez diffuse irradiance model for tilted surfaces. Solar Energy, 39, 221-232.

[23] Ruiz-Arias J. A., Cebecauer T., Tovar-Pescador J., Šúri M., Spatial disaggregation of satellite-derived irradiance using a high-resolution digital elevation model. Solar Energy, 84, 1644-1657, 2010.

[24] Ineichen P. Long term satellite hourly, daily and monthly global, beam and diffuse irradiance validation. Interannual variability analysis. University of Geneva/IEA SHC Task 46, 2013. http://www.unige.ch/energie/forel/energie/equipe/ineichen/annexes-iae.html

[25] Dobermann T., Energy in Myanmar, International Growth Centre Myanmar, June 2016, https://www.theigc.org/wp-content/uploads/2016/04/Dobermann-2016-1.pdf

[26] Turning on the lights: Integrated energy and rural electrification development in Myanmar, The critical importance of power development, KWR International (Asia) Pte Ltd, 2015 http://kwrintl.com/library/2015/1KWRERIASummary-MyanmarElectrification.pdf

[27] King D.L., Boyson W.E. and Kratochvil J.A., Photovoltaic array performance model, SAND2004-3535, Sandia National Laboratories, 2004.

[28] Huld T., Šúri M., Dunlop E.D., Geographical variation of the conversion efficiency of crystalline silicon photovoltaic modules in Europe. Progress in Photovoltaics: Research and Applications, 16, 595-607, 2008.

[29] Huld T., Gottschalg R., Beyer H. G., Topic M., Mapping the performance of PV modules, effects of module type and data averaging, Solar Energy, 84, 2, 324-338, 2010.

[30] Huld T., Friesen G., Skoczek A., Kenny R.P., Sample T., Field M., Dunlop E.D., 2011. A power-rating model for crystalline silicon PV modules. Solar Energy Materials and Solar Cells, 95, 12, 3359-3369.

[31] Skoczek A., Sample T., Dunlop E. D., The results of performance measurements of field-aged crystalline silicon photovoltaic modules, Progress in Photovoltaics: Research and Applications, 17, 227-240, 2009.

[32] Martin N., Ruiz J.M. Calculation of the PV modules angular losses under field conditions by means of an analytical model. Solar Energy Material and Solar Cells, 70, 25–38, 2001.

[33] The German Energy Society, 2008: Planning and Installing Photovoltaic Systems. A guide for installers, architects and engineers. Second edition. Earthscan, London, Sterling VA.

[34] Šúri M., Cebecauer T., Skoczek A., 2011. Solargis: Solar Data And Online Applications For PV Planning And Performance Assessment. 26th European Photovoltaics Solar Energy Conference, September 2011, Hamburg, Germany.

[35] Myanmar National Electrification Plan (NEP): Least-Cost Geospatial Electrification Planning Results, Earth Institute, Sustainable Engineering Lab, Columbia University, August 2014 https://energypedia.info/images/5/50/MMR-NEP-Geospatial_Least_Cost_Planning_Draft_FinalReport-2014-08-28.pdf

[36] Nam K., Cham M. R., Halili P. R., Power sector development in Myanmar, ADB Economics Working Papers Series, No. 460, Asian Development Bank, October 2015 https://www.adb.org/sites/default/files/publication/175801/ewp-460.pdf


SOLARGIS